

Universal algorithm for transforming Hamiltonian eigenvalues

Tatsuki Odake  ^{1,*} Hlér Kristjánsson  ^{2,3,1} Philip Taranto  ¹ and Mio Murao  ^{1,†}

¹Department of Physics, Graduate School of Science, The University of Tokyo, Hongo 7-3-1, Bunkyo-ku, Tokyo, 113-0033, Japan

²Perimeter Institute for Theoretical Physics, 31 Caroline Street North, Waterloo, Ontario, N2L 2Y5, Canada

³Institute for Quantum Computing, University of Waterloo, 200 University Avenue West, Waterloo, Ontario, N2L 3G1, Canada

Manipulating Hamiltonians governing physical systems has found a broad range of applications, from quantum chemistry to semiconductor design. In this work, we provide a new way of manipulating Hamiltonians, by transforming their eigenvalues while keeping their eigenstates unchanged. We develop a universal algorithm that deterministically implements any desired (suitably differentiable) function on the eigenvalues of any unknown Hamiltonian, whose positive-time and negative-time dynamics are given as a black box. Our algorithm uses correlated randomness to efficiently combine two subroutines—namely controlization and Fourier series simulation—exemplifying a general compilation procedure that we develop. The time complexity of our algorithm is significantly reduced using compilation compared to a naïve concatenation of the subroutines and outperforms similar methods based on the quantum singular value transformation. Finally, to circumvent the need for the negative-time dynamics, we present a universal algorithm to transform positive-time to negative-time dynamics without adding an auxiliary qubit, which could also be of standalone interest.

I. INTRODUCTION

The physical properties of any given system are determined by its Hamiltonian. As such, realizing a Hamiltonian which exhibits properties that are desirable in a given context is an important task in fields ranging from condensed matter physics and materials science to quantum chemistry. For example, an important problem in materials science is the discovery of new materials for specific tasks [1–3].

In many cases, such properties depend on the eigenvalues or eigenstates of the Hamiltonian. The eigenstates of a given Hamiltonian can be straightforwardly transformed through a unitary evolution, however, tuning the eigenvalues of a Hamiltonian while keeping the eigenstates fixed, as discussed in tasks addressed by the Quantum Singular Value Transformation (QSVT) [4, 5], is a much more involved problem. The ability to transform Hamiltonian eigenvalues in an efficient manner would open up a new way of manipulating the physical properties of a system, leading to increased flexibility in the simulation, control, and design of quantum systems.

In this work, we propose a new type of quantum algorithm to transform the eigenvalues of a Hamiltonian by any given (suitably differentiable) function, while keeping the eigenstates unchanged, when the positive-time and negative-time Hamiltonian dynamics are given. In the standard setting of Hamiltonian simulation, a classical description of the Hamiltonian to be transformed is typically known in advance [4, 6–11]. However, in many cases of interest, the description of the Hamiltonian of the system is not given but rather only its dynamics is accessible, especially for many-body or complex systems.

Our algorithm is an alternative *universal* Hamiltonian simulation method which does not require knowledge

of the Hamiltonian, whose *dynamics* can be given as a black box [12]. Although several recent works including algorithms based on QSVT are compatible with this black-box setting, they assume access to controlled versions of the Hamiltonian dynamics [13–17] or access to an oracle encoding information of the Hamiltonian, such as block encoding [4] or a quantum walk oracle [18, 19]. Crucially, our approach returns to the more natural setting where only the *uncontrolled* Hamiltonian dynamics is accessible. Possible applications of our method include constructing oracles for Grover’s algorithm [20], and we envisage that further developments in this direction could find applications more broadly in condensed matter physics, chemistry, and material science, for example in tuning energy gaps to enable precise transitions between energy levels [21] and in the design of semiconductors [22].

To achieve our universal Hamiltonian eigenvalue transformation, we employ the framework of higher-order quantum transformations, a research area that has attracted significant attention in recent years [23–33]. The adjective “higher-order” here refers to the fact that such processes take *quantum maps* as input, returning a transformed quantum map as output, e.g., by appropriately applying quantum operations before and after the dynamics. Here, we will consider the situation where the input and output quantum maps correspond to Hamiltonian dynamics parameterized by a time t (see Fig. 1). In this case, the ability to divide the map in time and intersperse with gate operations provides one with extra power for implementing desired transformations [12]. Leveraging this framework, here we construct a method to implement functions of unknown Hamiltonian dynamics by first controlizing the black-box dynamics [25] and then applying a novel algorithm for Fourier series simulation on the controlled black-box dynamics, which implements the desired function on the eigenvalues.

Our methodology shows how component subroutines can be compiled to build complex and efficient algorithms from simpler ones. Concatenating subroutines—as we

* tatsuki.odake@phys.s.u-tokyo.ac.jp

† murao@phys.s.u-tokyo.ac.jp

do with controlization and Fourier series simulation—provides an instance of quantum functional programming [30, 34, 35], which endows quantum algorithms with a modular flexibility similar to their classical counterparts. Yet, whenever two subroutines relying on random sampling are concatenated directly, the overall time complexity scales poorly due to the independence of the two sampling distributions. To overcome this issue, we develop a general *compilation* procedure for the concatenation of randomised algorithms, which makes use of correlated randomness as a key resource to optimize the algorithm at a global level.

We highlight the power of this method by demonstrating a compiled algorithm that outperforms the naïve concatenation of controlization and Fourier series simulation; moreover, it outperforms other methods based upon combining controlization and QSFT-based algorithms. As such, our compilation technique goes beyond the existing techniques of quantum functional programming, leading to more efficient compiled algorithms. By introducing the notion of compilation to functional programming in the context of quantum information processing, we align it with classical software design principles that allow code to be compiled and executed at various levels of abstraction, opening the possibilities for computations to be deployed across many different applications.

In the main algorithm, we assume that both the positive-time and negative-time Hamiltonian dynamics are given as a black box. If the negative-time Hamiltonian dynamics is not easily applicable and only the positive-time Hamiltonian dynamics is available, we can use the recent higher-order algorithm for universally implementing linear transformations of Hamiltonian dynamics to simulate negative-time evolution from positive-time evolution [12]. However, this algorithm requires adding an auxiliary qubit and performing controlled Pauli operations on the auxiliary qubit and the Hamiltonian system.

Here, we discover a simplified higher-order algorithm that only requires the application of correlated random Pauli operations on the Hamiltonian system to universally simulate negative-time evolution from the positive-time evolution, without using an auxiliary qubit. When the connectivity structure of the interaction is given (but the strength of interactions remains unknown), the time complexity does not depend on the number of qubits for a wide range of Hamiltonians, including low-interaction Hamiltonians [36]. This algorithm can be used as a subroutine to the main algorithm to expand its applicability to scenarios where the negative-time dynamics is not directly available. Due to its simplicity, it can also be used as a subroutine in other quantum algorithms requiring the use of negative-time Hamiltonian dynamics.

The remainder of the paper is structured as follows. First, we present a summary of our main results in Sec. II. In Sec. III, we formalize the task of universal Hamiltonian eigenvalue transformation and the envisaged scenario. The subsequent three sections each pertain to our key results. In Sec. IV, we combine two subroutines, control-

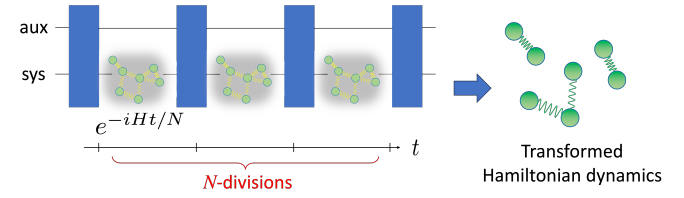


FIG. 1. *Higher-order quantum transformation*.—By appropriately interspersing fixed quantum operations involving an auxiliary system (blue) throughout a Hamiltonian dynamics e^{-iHt} that has been divided into N smaller portions $e^{-iHt/N}$, the physical properties of a system can be transformed as desired.

ization and Fourier series simulation, to achieve the said task. Then, in Sec. V, we use the intuition gained in order to construct a more efficient “compiled” algorithm. In Sec. VI, we compare our new methods with a protocol based upon QSFT [5, 37]. Finally, in Sec. VII, we present a simplified algorithm to universally simulate negative-time evolution using positive-time evolution. We finish with a concluding discussion in Sec. VIII.

II. SUMMARY OF MAIN RESULTS

The main results of our work are schematically depicted in Fig. 2 and summarised as follows.

1. In Sec. IV, we develop an algorithm that performs a universal Hamiltonian eigenvalue transformation by concatenating two subroutines, namely controlization [25] and Fourier series simulation. The controlization subroutine adds control to an unknown Hamiltonian dynamics H ; by approximating the Fourier series of a desired function f , one can then use this controlled dynamics to simulate the dynamics of the transformed Hamiltonian $f(H)$. Both subroutines are implemented efficiently using a randomized Hamiltonian simulation technique.
2. In Sec. V, we present a method, hereby dubbed “compilation”, which provides a framework for constructing a more efficient circuit of any quantum algorithm constructed by concatenating subroutines that make use of randomized Hamiltonian simulation. We achieve this by employing the resource of temporally correlated randomness in order to optimize the overall task at hand rather than the individual modules as per the “uncompiled” algorithm. In our case of UHET, we show that this leads to a more efficient algorithm.
3. In Sec. VI, we compare the performance of our two new algorithms for transforming eigenvalues of an unknown Hamiltonian with a method based upon the Quantum Singular Value Transformation (QSFT). We show that our compiled algorithm has a better time complexity than the QSFT-based algorithm, which in turn outperforms our uncompiled algorithm in this regard.

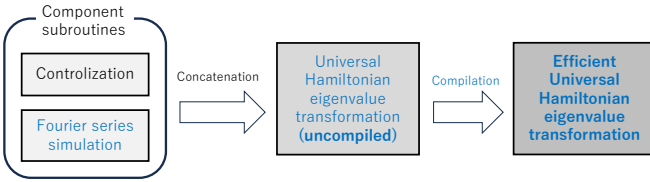


FIG. 2. *Description of our work.*—Tasks written in blue denote our contributions. We first develop an “uncompiled” algorithm for UHET by concatenating two subroutines, controlization and Fourier series simulation. We then present a “compiled” version of the UHET algorithm, which improves upon the efficiency.

4. In Sec. VII, we show how to simulate negative-time evolution of a Hamiltonian when only access to the positive-time evolution is given. Importantly, this algorithm does not make use of an auxiliary qubit, in contrast to the previous work [12], and only requires applications of correlated random Pauli operations on the Hamiltonian system. In many physical situations of interest, the time complexity of this algorithm is independent of the number of qubits n .

We begin by formalizing the task and our envisaged framework.

III. TASK: UNIVERSAL HAMILTONIAN EIGENVALUE TRANSFORMATION (UHET)

The goal of *universal Hamiltonian eigenvalue transformation (UHET)* is to simulate the dynamics of a desired function of an unknown input Hamiltonian H . Here, the term “simulate” refers to implementing the corresponding Hamiltonian dynamics for an arbitrary evolution time up to an acceptable approximation error. More precisely, given a function $f : [-1, 1] \rightarrow \mathbb{R}$, time $t > 0$, and precision $\epsilon > 0$, a universal Hamiltonian eigenvalue transformation uses an *unknown* input dynamics $e^{\pm iH\tau}$ ($\tau > 0$) to approximate a desired transformed dynamics $e^{-i f(H_0)t}$ up to precision ϵ and for all t .

Here, H is associated to an n -qubit Hilbert space \mathcal{H} and $H_0 := H - (\text{tr}(H)/2^n)I$ is its traceless part, which we assume to be upper bounded $\|H_0\|_{\text{op}} \leq 1$. Note that taking only the traceless part of the Hamiltonian leads to no loss of generality, since for $H_1 = H_2 + \alpha I$ where H_1, H_2 are Hamiltonians and $\alpha \in \mathbb{R}$, $e^{-iH_1 t} = e^{-i\alpha t} e^{-iH_2 t}$, thus the dynamics corresponding to H_1 and H_2 are equivalent (up to a global phase). Furthermore, as long as an upper bound Δ_H of the difference between the maximum and the minimum energy eigenvalues of the Hamiltonian is known, then one can always rescale the Hamiltonian as $H \rightarrow H/\Delta_H$ and change the definition of the function f as $f \rightarrow f_H$ such that $f_H(x) := f(\Delta_H x)$, justifying the assumption $\|H_0\|_{\text{op}} \leq 1$. We note that $f(H_0)$ is defined in the usual way, i.e., by applying f to the spectrum of H_0 . Lastly, we assume access to both the positive and negative-time dynamics; if only the positive-time

dynamics is accessible, then the negative time one can be constructed with a small overhead using an algorithm presented in Sec. VII, which does not require an auxiliary system.

As mentioned previously, transforming Hamiltonians has applications ranging from condensed matter physics to quantum information processing. In many situations considered, at least a classical description of the initial seed Hamiltonian is known, e.g., in algorithms based upon QSVD. However, from a physics perspective, this scenario is not always the case; for instance, one may have access to a time-evolving many-body system without knowing any description of the dynamics *a priori*. Our setting of *universal* Hamiltonian transformations allows such scenarios: the classical description of the input Hamiltonian H can be completely unknown, as long as its (positive- and negative-time) dynamics $e^{\pm iH\tau}$ is accessible.

Throughout the remainder of this article, we will present various methods to achieve UHET. At their core, all such methods make use of classical randomness to simulate the desired dynamics by sampling many rounds of evolution; being approximate, one must therefore take the iteration number N sufficiently large to ensure a desired accuracy $\epsilon > 0$. In order to assess the performance of these algorithms, we will employ two related figures of merit. The first we denote *time complexity*, which is defined in terms of the gate depth of the circuit that implements the algorithm when decomposed into single qubit and CNOT gates, *not* counting the calls to unknown dynamics $e^{\pm iHt}$ used as oracles. The second quantifier is the *total evolution time*, which refers to the sum of the absolute values $|\tau|$ of the evolution times τ of the Hamiltonian dynamics $e^{-iH\tau}$ used throughout the algorithm.

To quantify said error in any such scheme, we make use of the following distance measures. First, note that simulating any Hamiltonian dynamics for a specified amount of time (ideally) leads to a unitary operation. Thus, we consider the situation where one attempts to simulate such a unitary operation $\mathcal{U} : \mathcal{L}(\mathcal{H}) \rightarrow \mathcal{L}(\mathcal{H})$ by a random protocol $\sum_j p_j \mathcal{F}_j$ where the index j is chosen with a probability p_j and $\mathcal{F}_j : \mathcal{L}(\mathcal{H}) \rightarrow \mathcal{L}(\mathcal{H})$ is the corresponding quantum operation. If the input state to said dynamics is not fixed (i.e., remains arbitrary), then we use the following error measure for the quantum operation:

$$\sup_{\substack{\dim(\mathcal{H}') \\ |\psi\rangle \in \mathcal{H} \otimes \mathcal{H}' \\ \|\psi\| = 1}} \|\mathcal{U} \otimes \mathcal{I}_{\mathcal{H}'}(|\psi\rangle\langle\psi|) - \sum_j p_j \mathcal{F}_j \otimes \mathcal{I}_{\mathcal{H}'}(|\psi\rangle\langle\psi|)\|_1. \quad (1)$$

Here, \mathcal{I} represents the identity channel, \mathcal{H}' is an auxiliary Hilbert space of arbitrary dimension and $\|\cdot\|_1$ denotes the 1-norm. If, on the other hand, the input state is specified to be some known $|\psi\rangle \in \mathcal{H}$, then the accuracy of any protocol can be determined by comparing the post-transformation state with the ideal case, and hence we

use the following error measure for quantum states:

$$\|\mathcal{U}(|\psi\rangle\langle\psi|) - \sum_j p_j \mathcal{F}_j(|\psi\rangle\langle\psi|)\|_1. \quad (2)$$

When the average state $\sum_j p_j \mathcal{F}_j(|\psi\rangle\langle\psi|)$ approximates the target state $\mathcal{U}(|\psi\rangle\langle\psi|)$ [in terms of Eq. (2)] with an error that is upper bounded by a fixed constant ϵ for *any* input state $|\psi\rangle$, then the mean square of the approximation is upper bounded by 2ϵ for any input, i.e.,

$$\sum_j p_j \|\mathcal{U}(|\psi\rangle\langle\psi|) - \mathcal{F}_j(|\psi\rangle\langle\psi|)\|_1^2 \leq 2\epsilon \quad (3)$$

(see App. B 1 for technical details).

IV. UNCOMPILED UHET ALGORITHM

We now move to present our first algorithm that performs the task of UHET. This algorithm is based upon a random protocol for simulating Hamiltonian dynamics. Our method can be seen as an extension of a Hamiltonian simulation technique called **qDRIFT** [8] to the case where the Hamiltonian is unknown. Using this technique as a basis, we concatenate two subroutines, namely controlization and Fourier series simulation, to develop our overall UHET algorithm. Finally, we present a resource analysis of the time complexity and total evolution time of the protocol. Additional technical details are provided throughout App. C.

A. Efficient Hamiltonian Simulation (qDRIFT)

Suppose one has access to a set of Hamiltonian dynamics, i.e., the ability to perform $e^{-iH_j\tau}$ ($\tau > 0$) for a set of Hamiltonians $\{H_j\}$. Assuming w.l.o.g. that the Hamiltonians are normalized $\|H_j\|_{\text{op}} = 1$, any dynamics of the form $e^{-i(\sum_j h_j H_j)t}$ ($t > 0$) for a set of positive coefficients $h_j > 0$ can be approximated by the following protocol (see Fig. 3):

1. Define $\lambda := \sum_k h_k$ and the probability distribution $p_j := h_j/\lambda$, from which an index j is randomly sampled.
2. Apply the dynamics $e^{-iH_j t \lambda / N}$.
3. Repeat steps (1)–(2) N times.

This method is based on the Hamiltonian simulation technique qDRIFT [8], which makes use of the Trotter-Suzuki decomposition [7] of $e^{-i(\sum_j h_j H_j)t}$ to approximate $e^{-i(\sum_j p_j H_j)\delta t}$ for a small time interval $\delta t := t\lambda/N$ up to the first order of δt via a probabilistic mixture of dynamics $e^{-iH_j\delta t}$ with probability p_j . In order to suppress the approximation error below ϵ , taking the iteration number

$$N(\lambda, t, \epsilon) := \text{ceil}[\max(10\lambda^2 t^2 / \epsilon, 5\lambda t / 2)] \quad (4)$$

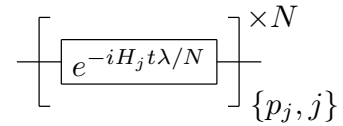


FIG. 3. *qDRIFT primitive.*—Circuit representation of the qDRIFT protocol for approximating $e^{-i(\sum_j h_j H_j)t}$ by randomly implementing $e^{-iH_j\tau}$ with probability p_j for each j for a number N times.

is sufficient (see App. C 1). In this work, we employ a probabilistic Trotter-Suzuki technique in all algorithms and subroutines (except Algorithm 5) since such methods typically exhibit reduced time complexity when compared to deterministic counterparts due to their independence of the number of terms in $\sum_j h_j H_j$.

We now describe the two subroutines that leverage this qDRIFT primitive for *unknown* Hamiltonians, namely controlization [25] and Fourier series simulation, to perform UHET upon their concatenation. We refer to such a straightforward concatenation as *uncompiled*, in contrast to a later algorithm which we dub *compiled* that optimizes UHET globally (see Sec. V).

B. Controlization

Subroutine 1 Controlization

Input:

- A finite number of queries to a black-box Hamiltonian dynamics $e^{-iH\tau}$ of a seed Hamiltonian H normalized as $\|H_0\|_{\text{op}} \leq 1$, where H_0 is the traceless part of H , i.e., $H_0 := H - (1/2^n)\text{tr}(H)I$, with $\tau > 0$
- Allowed error $\epsilon > 0$
- Time $t > 0$

Output:

 A random unitary operator approximating

$$\begin{pmatrix} e^{-iH_0 t} & 0 \\ 0 & I \end{pmatrix} = \text{ctrl}_0(e^{-iH_0 t}) \in \mathcal{L}(\mathcal{H}_c \otimes \mathcal{H}) \quad (5)$$

with an error according to Eq. (1) upper bounded by ϵ

Time complexity: $\Theta(t^2 n / \epsilon)$

Total evolution time: t

Used Resources:

System: n -qubit system \mathcal{H} and one auxiliary qubit \mathcal{H}_c
Gates: $e^{-iH\tau}$ and Clifford gates on $\mathcal{H}_c \otimes \mathcal{H}$

Procedure:

Pre-processing:

1: Compute $N := N(1, t, \epsilon)$ using $N(\lambda, t, \epsilon)$ from Eq. (4)

Main Process:

2: Initialize $U_{\text{current}} \leftarrow I$

3: **for** $m = 1, \dots, N$ **do**

4: Uniformly randomly choose $\vec{v} \in \{0, 1, 2, 3\}^n$

5: $U_{\text{current}} \leftarrow \text{ctrl}(\sigma_{\vec{v}})(I \otimes e^{-iHt/N})\text{ctrl}(\sigma_{\vec{v}})U_{\text{current}}$

6: **end for**

7: **Return** U_{current}

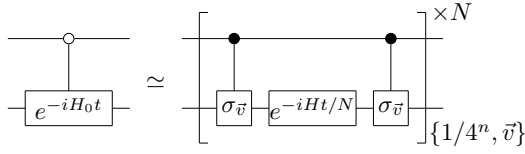


FIG. 4. *Controlization circuit*.—By randomly applying controlled Pauli gates $\text{ctrl}(\sigma_{\vec{v}})$ before and after portions of unknown Hamiltonian dynamics $e^{-iHt/N}$ a sufficient number of times, said dynamics can be controlled, i.e., simulate $\text{ctrl}_0(e^{-iH_0 t})$, where H_0 represents the traceless part of H .

Controlization is a method that adds control to an unknown Hamiltonian dynamics [25]. It takes a finite number of queries to the dynamics $e^{-iH\tau}$ as a resource and outputs a random unitary operator approximating $\text{ctrl}(e^{-iH_0 t}) \in \mathcal{L}(\mathcal{H}_c \otimes \mathcal{H})$, where H_0 represents the traceless part of H , \mathcal{H}_c is the Hilbert space associated to the control qubit, and $\text{ctrl}(e^{-iH_0 t}) := |0\rangle\langle 0| \otimes I + |1\rangle\langle 1| \otimes e^{-iH_0 t}$ represents controlled- $e^{-iH_0 t}$. Our following *uncompiled algorithm* for UHET first makes use of a variant of controlization which simulates $\text{ctrl}_0(e^{-iH_0 t}) := |0\rangle\langle 0| \otimes e^{-iH_0 t} + |1\rangle\langle 1| \otimes I$ by reversing the roles of $|0\rangle$ and $|1\rangle$ of the control qubit, as presented in Subroutine 1 and the circuit in Fig. 4.

Intuitively, controlization makes use of a randomized algorithm to approximately implement a unitary dynamics (in a similar manner to the qDRIFT procedure) to simulate the Hamiltonian

$$\begin{aligned} & \sum_{\vec{v} \in \{0,1,2,3\}^n} \frac{1}{4^n} \begin{pmatrix} I & 0 \\ 0 & \sigma_{\vec{v}} \end{pmatrix} \begin{pmatrix} H & 0 \\ 0 & H \end{pmatrix} \begin{pmatrix} I & 0 \\ 0 & \sigma_{\vec{v}} \end{pmatrix} \\ &= \begin{pmatrix} H_0 & 0 \\ 0 & 0 \end{pmatrix} + \frac{\text{tr}(H)}{2^n} I, \end{aligned} \quad (6)$$

where $\vec{v} := (v_1, \dots, v_n) \in \{0,1,2,3\}^n$ and $\sigma_{\vec{v}} := \sigma_{v_1} \otimes \dots \otimes \sigma_{v_n}$. Equation (6) follows from the identity $\frac{1}{4^n} \sum_{\vec{v}} \sigma_{\vec{v}} H \sigma_{\vec{v}} = \frac{\text{tr}(H)}{2^n} I$. Each term $\text{ctrl}(\sigma_{\vec{v}})(I \otimes H)\text{ctrl}(\sigma_{\vec{v}})$ in the sum on the l.h.s. of Eq. (6) can be implemented by applying the dynamics $e^{-iH\tau}$ in between the gate $\text{ctrl}(\sigma_{\vec{v}})$, which follows from the identity $U e^{-iHt} U^\dagger = e^{-i(UHU^\dagger)t}$ for a general Hamiltonian H and unitary U . When exponentiated, the r.h.s. of Eq. (6) yields the desired controlled Hamiltonian dynamics (up to a global phase contribution from the second term, which is irrelevant).

The time complexity $\Theta(t^2 n / \epsilon)$ follows from the fact that $N := N(1, t, \epsilon)$ is $\Theta(t^2 / \epsilon)$ and that implementing $\text{ctrl}(\sigma_{\vec{v}})$ takes $\Theta(n)$ time. The total evolution time is simply $(t/N) \times N = t$.

Note finally that the time complexity for the case where a deterministic Trotter-Suzuki technique is used instead of the randomized one is lower bounded by the number of terms 4^n in the sum, which grows exponentially with the number of qubits n .

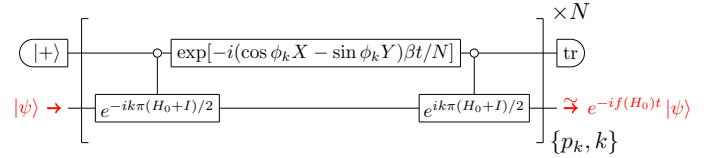


FIG. 5. *Fourier series simulation circuit*.—By randomly applying $\text{ctrl}_0(e^{\pm i k \pi (H_0 + I)/2})$ before and after the dynamics $e^{-i(\cos \phi_k X - \sin \phi_k Y) \beta t/N}$, the circuit simulates the Fourier series of the desired transformation function $\tilde{f}[(H_0 + I)/2] = f(H_0)$.

C. Fourier Series Simulation

We now move to describe the second subroutine that comprises our uncompiled UHET algorithm, namely *Fourier series simulation*. This algorithm serves to transform eigenvalues of an unknown Hamiltonian using the theory of Fourier series at its core. A Fourier expansion of a function $f : [-1, 1] \rightarrow \mathbb{R}$ is given by $\sum_{k=-\infty}^{\infty} c_k e^{i\pi kx}$ for $c_k := (1/2) \int_{-1}^1 dx f(x) e^{-i\pi kx}$, which converges to $f(x)$ for a wide range of functions (see, e.g., [38]). The procedure of Fourier series simulation is described in Subroutine 2, with a circuit representation presented in Fig. 5.

Fourier series simulation makes use of a controlled dynamics $\text{ctrl}_0(e^{\pm i H_0 \tau})$ ($\tau > 0$) (which can be constructed using Subroutine 1) to implement the target Hamiltonian dynamics $e^{-i f(H_0)t}$ ($t > 0$). First, the desired function f is deformed to a periodically smooth function \tilde{f} as

$$\tilde{f}(x) := \begin{cases} g_f(x) & x \in [-1, 0] \\ f(2x - 1) & x \in [0, 1] \end{cases}, \quad (7)$$

with g_f defined in App. C2 (see Fig. 6). Due to its periodic smoothness, the absolute value of the Fourier coefficients of \tilde{f} converges rapidly to 0, which avoids rapid growth of the cutoff number K in terms of the error ϵ .

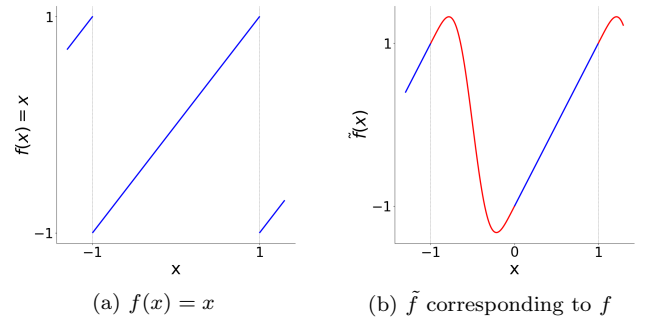


FIG. 6. *Comparison between the function f and its corresponding \tilde{f}* .—The function \tilde{f} is defined by merging f (blue) and an additional function g_f (red, see App. C2). Defined appropriately, \tilde{f} has a faster convergence of the absolute value of its Fourier coefficients $|\tilde{c}_k|$ than f .

Subroutine 2 Fourier Series Simulation

Input:

- A finite number of queries to $\text{ctrl}_0(e^{\pm iH_0\tau}) \in \mathcal{L}(\mathcal{H}_c \otimes \mathcal{H})$ ($\tau > 0$) where $H_0 \in \mathcal{L}(\mathcal{H})$ is a traceless Hamiltonian normalized as $\|H_0\|_{\text{op}} \leq 1$
- A class C^3 (3 times continuously differentiable) function $f : [-1, 1] \rightarrow \mathbb{R}$, such that $f^{(4)}$ is piecewise C^2 (see App. A 1)
- Input state $|\psi\rangle \in \mathcal{H}$
- Allowed error $\epsilon > 0$
- Time $t > 0$

Output: A state approximating $e^{-if(H_0)t} |\psi\rangle$ ($t > 0$) with an error according to Eq. (2) upper bounded by ϵ , and mean squared error according to Eq. (3) upper bounded by 2ϵ

Rime complexity $\Theta(\beta^2 t^2 / \epsilon)$

Total evolution time: $\Theta(C_{2,f} t^2 / \epsilon)$ for an f -dependent constant $C_{2,f}$ which is independent of n , t , and ϵ

Used Resources:

System: n -qubit system \mathcal{H} and one auxiliary qubit \mathcal{H}_c
Gates: $\text{ctrl}(e^{\pm iH_0\tau})$ and single-qubit gates on \mathcal{H}_c

Procedure:
Pre-processing:

- 1: Define modified version \tilde{f} of f as in Eq. (7)
- 2: Compute Fourier coefficients $\tilde{c}_k := (1/2) \int_{-1}^1 dx e^{-ik\pi x} \tilde{f}(x)$ for $k \in \{-K, -K+1, \dots, K\}$ where the cutoff number K satisfies

$$\left| \tilde{f}(x) - \sum_{k=-K}^K \tilde{c}_k e^{ik\pi x} \right| < \frac{\epsilon}{4t} \quad \forall x \in [-1, 1]$$

- 3: Compute $N := N(\beta, t, \epsilon/2)$ using $N(\lambda, t, \epsilon)$ from Eq. (4), for $\beta := \sum_{k=-K}^K |\tilde{c}_k|$

Main Process:

- 4: Initialize $|\text{current}\rangle \leftarrow |+\rangle \otimes |\psi\rangle$
- 5: **for** $m = 1, \dots, N$ **do**
- 6: Randomly choose $k \in \{-K, \dots, K\}$ with probability $p_k := |\tilde{c}_k|/\beta$
- 7: Define $Q := \text{ctrl}_0(e^{-ik\pi H_0/2})$ and $R := \text{ctrl}_0(e^{ik\pi H_0/2})$
- 8: $|\text{current}\rangle \leftarrow (e^{ik\pi Z/4} \otimes I) R (e^{-i[\cos \phi_k X - \sin \phi_k Y] \beta t / N} \otimes I) Q (e^{-ik\pi Z/4} \otimes I) |\text{current}\rangle$ for ϕ_k defined by $\tilde{c}_k = |\tilde{c}_k| e^{i\phi_k}$
- 9: **end for**
- 10: Trace out \mathcal{H}_c of $|\text{current}\rangle$
- 11: **Return** $|\text{current}\rangle$

We then compute the Fourier coefficients $\tilde{c}_k := (1/2) \int_{-1}^1 dx e^{-ik\pi x} \tilde{f}(x)$ for $k \in \{-K, -K+1, \dots, K\}$, where the cutoff number K satisfies

$$\left| \tilde{f}(x) - \sum_{k=-K}^K \tilde{c}_k e^{ik\pi x} \right| < \frac{\epsilon}{4t} \quad \forall x \in [-1, 1], \quad (8)$$

and the iteration number $N := N(\beta, t, \epsilon/2)$ [using Eq. (4)] for $\beta := \sum_{k=-K}^K |\tilde{c}_k|$.

The remainder of Subroutine 2 simulates the Fourier-transformed Hamiltonian of H_0 , which can be understood

from the following analysis. The unitary applied in step 8, for a random k chosen with probability $p_k = |\tilde{c}_k|/\beta$, can be written as a Hamiltonian evolution given by

$$\begin{aligned} & (e^{ik\pi Z/4} \otimes I) \begin{pmatrix} e^{ik\pi H_0/2} & 0 \\ 0 & I \end{pmatrix} (e^{-i(\cos \phi_k X - \sin \phi_k Y) \beta t / N} \otimes I) \cdot \\ & \quad \begin{pmatrix} e^{-ik\pi H_0/2} & 0 \\ 0 & I \end{pmatrix} (e^{-ik\pi Z/4} \otimes I) \\ & = \exp \left[-i \begin{pmatrix} 0 & e^{i\phi_k} e^{ik\pi(H_0+I)/2} \\ e^{-i\phi_k} e^{-ik\pi(H_0+I)/2} & 0 \end{pmatrix} \beta t / N \right]. \end{aligned} \quad (9)$$

As such, steps 5 to 9 of Subroutine 2 correspond to simulating $e^{-i\tilde{H}'t}$ for the following Hamiltonian H'

$$\begin{aligned} H' &:= \sum_{k=-K}^K |\tilde{c}_k| \begin{pmatrix} 0 & e^{i\phi_k} e^{ik\pi(H_0+I)/2} \\ e^{-i\phi_k} e^{-ik\pi(H_0+I)/2} & 0 \end{pmatrix} \\ &\simeq \sum_{k=-\infty}^{\infty} |\tilde{c}_k| \begin{pmatrix} 0 & e^{i\phi_k} e^{ik\pi(H_0+I)/2} \\ e^{-i\phi_k} e^{-ik\pi(H_0+I)/2} & 0 \end{pmatrix} \\ &= \begin{pmatrix} 0 & f(H_0) \\ f(H_0) & 0 \end{pmatrix} = X \otimes f(H_0), \end{aligned} \quad (10)$$

which follows from the fact that

$$\begin{aligned} & \sum_{k=-\infty}^{\infty} |\tilde{c}_k| e^{i\phi_k} e^{ik\pi(H_0+I)/2} \\ &= \sum_{k=-\infty}^{\infty} \sum_m \tilde{c}_k e^{ik\pi(E_m+1)/2} |E_m\rangle \langle E_m| \\ &= \sum_m \tilde{f}((E_m+1)/2) |E_m\rangle \langle E_m| = f(H_0), \end{aligned} \quad (11)$$

where H_0 is diagonalized as $H_0 := \sum_m E_m |E_m\rangle \langle E_m|$. By taking the initial state as $|+\rangle \otimes |\psi\rangle$ in step 4 and tracing out the \mathcal{H}_c subsystem in step 10, the dynamics $e^{-if(H_0)t}$ is applied to the input state $|\psi\rangle$.

We provide a full error analysis of Subroutine 2 in App. C 3. The time complexity, which is equal to the iteration number N , is evaluated as $\Theta(\beta^2 t^2 / \epsilon)$. The total evolution time [of the controlled Hamiltonian dynamics $\text{ctrl}(e^{\pm iH\tau})$] is evaluated as (Number of iterations N) \times (Average evolution time of each iteration). Given that N is $\Theta(\beta^2 t^2 / \epsilon)$ and that each iteration has evolution time $\sum_k p_k \cdot \Theta(|k|)$ on average, the total evolution time is

$$\begin{aligned} & \Theta\left(\frac{\beta^2 t^2}{\epsilon}\right) \times \sum_k p_k \cdot \Theta(|k|) = \\ & \Theta\left(\left(\sum_{k=-\infty}^{\infty} |\tilde{c}_k|\right) \left(\sum_{k=-\infty}^{\infty} |\tilde{c}_k| |k|\right) \frac{t^2}{\epsilon}\right) =: \Theta\left(C_{2,f} \frac{t^2}{\epsilon}\right), \end{aligned} \quad (12)$$

where $C_{2,f}$ is a parameter that depends on f but is independent of n, t, ϵ . Note that the sum $\sum_{k=-\infty}^{\infty} |\tilde{c}_k| |k|$ is guaranteed to converge due to the periodic smoothness of f (see App. C 4 for details).

D. Uncompiled UHET Algorithm

We now present the uncompiled UHET Algorithm 3, which results from concatenating the previous two subroutines and is depicted in Fig. 7. We first construct $\text{ctr1}_0(e^{\pm ik\pi(H_0+I)/2})$ from the input dynamics $e^{\pm iH\tau}$ via controlization and then perform the Fourier series simulation to simulate the desired dynamics $e^{-if(H_0)t}$. Thus, Algorithm 3 is a direct concatenation of Subroutines 1 and 2, and we therefore dub it *uncompiled*.

As a consequence of its concatenated structure, two layers of iterations are used in Algorithm 3: $N_k^{(C)}$ for the controlization part and $N^{(F)}$ for the Fourier series simulation. We choose these numbers such that the total error of each subroutine is bounded from above by $\epsilon/2$ (so that overall error is upper bounded by ϵ). We begin by fixing the allowed error of the Fourier series simulation to be $\epsilon/2$. Then, fixing that for controlization to be $\epsilon/(4N^{(F)})$, it follows that iterating the outer layer of the procedure (see Fig. 7a) $N^{(F)}$ times implies that the error due to controlization is upper bounded by $[\epsilon/(4N^{(F)})] \cdot 2N^{(F)} = \epsilon/2$.

We now analyze the time complexity of Algorithm 3. We split this cost into two parts. First, there is the *pre-processing step*, which refers to the processes that only need to be run once for a given set of inputs. In our case, this corresponds to the time complexity for computing the Fourier coefficients \tilde{c}_k and cutoff number K until Eq. (8) is satisfied, plus the time complexity for computing $N^{(F)}$. We define the sum of these two time complexities as T_3 . The *main process* takes $N^{(F)} \times$ (average time complexity of each iteration), the latter of which in turn depends upon $N_k^{(C)}$.

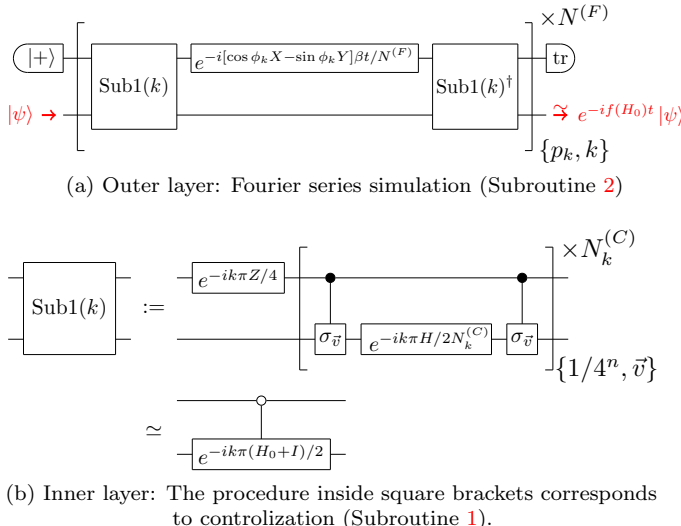


FIG. 7. *Circuit representation of Algorithm 3.*—The uncompiled UHET algorithm comprises an “outer” layer (a) that implements the Fourier series simulation Subroutine 2 upon the output of the “inner” layer (b), which itself controlizes the seed Hamiltonian dynamics via Subroutine 1.

Algorithm 3 Universal Hamiltonian eigenvalue transformation (uncompiled)

Input:

- A finite number of queries to a black-box Hamiltonian dynamics $e^{\pm iH\tau}$ of a seed Hamiltonian H normalized as $\|H_0\|_{\text{op}} \leq 1$ where H_0 is the traceless part of H , i.e., $H_0 := H - (1/2^n)\text{tr}(H)I$, with $\tau > 0$
- A class C^3 (3 times continuously differentiable) function $f : [-1, 1] \rightarrow \mathbb{R}$, such that $f^{(4)}$ is piecewise C^2 (see App. A 1)
- Input state $|\psi\rangle \in \mathcal{H}$
- Allowed error $\epsilon > 0$
- Time $t > 0$

Output: A state approximating $e^{-if(H_0)t} |\psi\rangle$ ($t > 0$) with an error according to Eq. (2) upper bounded by ϵ ; additionally, the mean squared error according to Eq. (3) is upper bounded by 2ϵ

Time complexity

Pre-processing (only once): T_3

Main Process: $\Theta(C_{3,f} t^4 n / \epsilon^3)$ for an f -dependent constant $C_{3,f}$ which is independent of n , t , and ϵ

Total evolution time (main process): $\Theta(C_{2,f} t^2 / \epsilon)$

Used Resources:

System: n -qubit system \mathcal{H} and one auxiliary qubit \mathcal{H}_c

Gates: $e^{\pm iH\tau}$, single-qubit gate on \mathcal{H}_c , and Clifford gates on $\mathcal{H}_c \otimes \mathcal{H}$

Procedure:

Pre-processing:

- 1: Run Pre-processing of Subroutine 2 for allowed error $\epsilon/2$ to obtain iteration number $N^{(F)} := N(\beta, t, \epsilon/4)$, cutoff number K and Fourier coefficients \tilde{c}_k

Main Process:

- 2: Run Main Process of Subroutine 2 with $N^{(F)}$ iterations using K and \tilde{c}_k obtained before, with step 7 modified to:

7.1: Run Pre-processing of Subroutine 1 for allowed error $\epsilon/4N^{(F)}$ to obtain iteration number $N_k^{(C)} := N(1, k\pi/2, \epsilon/4N^{(F)})$

7.2: Run Main Process of Subroutine 1 with $N_k^{(C)}$ iterations and time $k\pi/2$ for H to obtain unitary Q'

7.3: Run Main Process of Subroutine 1 with $N_k^{(C)}$ iterations and time $k\pi/2$ for $-H$ to obtain unitary R'

7.4: Define $Q := Q'$ and $R := R'$

The iteration number $N^{(F)} = N(\beta, t, \epsilon/4)$ scales as $\Theta[(\sum_{k=-\infty}^{\infty} |\tilde{c}_k|^2 t^2 / \epsilon)]$ (note that $\sum_{k=-\infty}^{\infty} |\tilde{c}_k|$ is an upper bound of β which is independent of ϵ). Furthermore, the average time complexity of each iteration is $\sum_{k=-K}^K p_k \times$ (time complexity of circuit inside Fig. 7a for each k), which scales as

$$\begin{aligned} \sum_{k=-K}^K p_k \Theta(n N_k^{(C)}) &= \sum_{k=-K}^K p_k \Theta\left(\frac{\beta^2 t^2 k^2 n}{\epsilon^2}\right) \\ &\leq \Theta\left(\left(\sum_{k=-\infty}^{\infty} |\tilde{c}_k| k^2\right) \left(\sum_{k=-\infty}^{\infty} |\tilde{c}_k|\right) \frac{t^2 n}{\epsilon^2}\right). \end{aligned}$$

The inequality is obtained by replacing K with ∞ in order to remove the ϵ dependence. Taking the product of the scaling of the two iteration layers, the overall time complexity scaling of the main process of Algorithm 3 is bounded from above by

$$\Theta\left(\left(\sum_{k=-\infty}^{\infty} |\tilde{c}_k|\right)^3 \left(\sum_{k=-\infty}^{\infty} |\tilde{c}_k|k^2\right) \frac{t^4 n}{\epsilon^3}\right) =: \Theta\left(C_{3,f} \frac{t^4 n}{\epsilon^3}\right).$$

Lastly, the total evolution time is evaluated in the same manner as in Subroutine 2 to be $\Theta(C_{2,f} t^2/\epsilon)$.

V. COMPILED UHET ALGORITHM

We now move to introduce a more efficient algorithm that implements UHET. At its core, this algorithm is inspired by the components that make up Algorithm 3, but rather than optimizing the subroutines independently, here we *compile* the algorithm at the level of the overall task by making use of *correlated classical randomness* to provide a more efficient implementation. We begin by describing a general framework of this novel notion of compilation, which can be used in many situations in which random Hamiltonian simulation subroutines are concatenated to perform a particular task. We subsequently apply this technique specifically to the task of UHET, compiling Algorithm 3 in order to construct the better Algorithm 4. Finally, we provide a resource analysis. Details are provided throughout App. D.

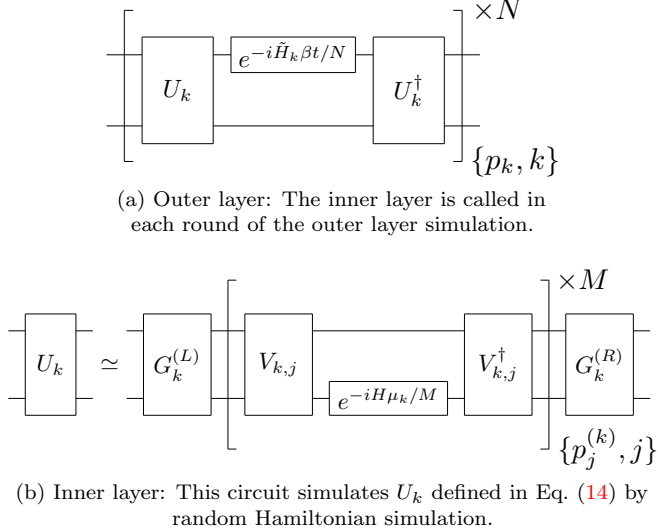


FIG. 8. *Circuit representation of a general algorithm involving two layers of Hamiltonian simulation.*—Our method of compilation can be applied to any general two-layer protocol in which each subroutine uses the method of random Hamiltonian simulation.

A. General Method of Compilation

We begin by abstracting the key structural components of the uncompiled algorithm above. Notably, the algorithm consists of two independent layers, namely those depicted in Figs. 7a and 7b. These circuits are a special case of the more general form depicted in Figs. 8a and 8b respectively. The *outer layer* comprises portions of the input dynamics sandwiched between a unitary $U_k(H)$ that depends on the input Hamiltonian H and is iterated some $N \in \mathbb{Z}_{>0}$ times; for the sake of conciseness, we will simply write U_k instead of explicitly writing $U_k(H)$. Since

$$U_k^\dagger e^{-i\frac{\beta t}{N} \tilde{H}_k} U_k = e^{-i\frac{\beta t}{N} U_k^\dagger \tilde{H}_k U_k}, \quad (13)$$

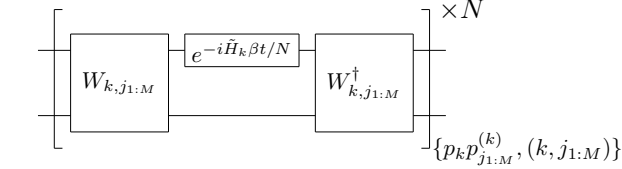
this process corresponds to the simulation of the randomized dynamics $e^{-i(\sum_k p_k \beta U_k^\dagger \tilde{H}_k U_k)t}$. In this simulation, U_k is itself approximated using the *inner layer* procedure depicted in Fig. 8b. Here, j is a random index (depending on the choice of k) sampled from the probability distribution $\{p_j^{(k)}\}_j$, $\mu_k \in \mathbb{R}$, iteration number $M \in \mathbb{Z}_{>0}$ (which also depends on k , but we omit the subscript k for simplicity), and $V_{k,j}$, $G_k^{(L)}$, and $G_k^{(R)}$ are unitaries such that

$$U_k = G_k^{(R)} e^{-i(\sum_j p_j^{(k)} \mu_k V_{k,j}^\dagger H V_{k,j})} G_k^{(L)}. \quad (14)$$

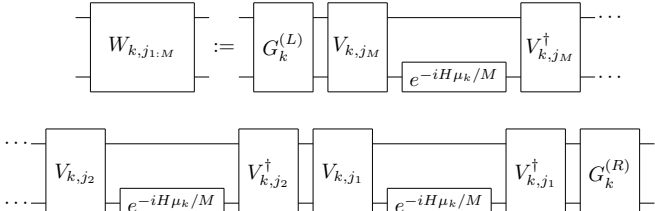
Evidently, Algorithm 3 corresponds to the special case where $\tilde{H}_k = \cos \phi_k X - \sin \phi_k Y$, $\beta = \sum_{k=-K}^K |\tilde{c}_k|$, $p_k = |\tilde{c}_k|/\beta$, $U_k = \text{ctrl}_0(e^{-ik\pi(H_0+I)/2})$, $M = N_k^{(C)}$, $j = \vec{v}$, $\mu_k = k\pi/2$, $p_{\vec{v}}^{(k)} = 1/4^n$, $V_{k,j} = \text{ctrl}(\sigma_{\vec{v}})$, $G_k^{(L)} = e^{-ik\pi Z/4} \otimes I$, and $G_k^{(R)} = I \otimes I$.

Having abstracted the key features of our previous algorithm, we are now in a position to introduce the general notion of *compilation*. The structure described above evidently consists of two *independent* layers of random Hamiltonian simulation; the method of compilation makes use of *correlated randomness* in order to correlate said layers in such a way that the error accumulation is reduced. In general, in order to reduce the approximation error of this overall procedure below ϵ , we must ensure that both errors introduced due to the simulations depicted in Figs. 8a and 8b are at most of $O(\epsilon)$. Subsequently, both iteration numbers N and M must have a $1/\epsilon$ dependence, which leads to an accumulation of $1/\epsilon$ dependence for each round of concatenated subroutines.

We do this by first modifying the circuit in Fig. 8a to an *intermediate circuit* in Fig. 9a, where $W_{k,j_{1:M}}(H) := W_{k,j_{1:M}}$ is written with its dependence on H implicit and defined as in Fig. 9b; similarly, we compress the labels $j_{1:M} := \{j_1, \dots, j_M\}$ and $p_{j_{1:M}}^{(k)} := p_{j_1}^{(k)} \dots p_{j_M}^{(k)}$ for ease of notation. Finally, an additional modification—which depends upon the specific task at hand—can then be applied to said intermediate circuit in order to compensate for error accumulation, leading to the *compiled algorithm*, as we will show for the case of UHET in the coming section.



(a) Instead of taking the two layers independently, here we correlate the outer (Fig. 8a) and inner layer (Fig. 8b) and run the overall scheme N times.



(b) The subroutine constructs the unitary $W_{k,j_{1:M}}$ from M uses of the seed Hamiltonian dynamics.

FIG. 9. *Intermediate stage of compilation.*—By correlating the layers, an additional error is introduced due to the finite iteration of the previously inner layer. However, we next show how this error can be compensated for by choosing $W_{k,j_{1:M}}$ appropriately, therefore constructing an efficient compiled algorithm.

In the intermediate circuit, the random indices $j_{1:M}$ are correlated in such a way that the components before and after the dynamics $e^{-i\tilde{H}_k\beta t/N}$ are inverse to each other. Therefore, the circuit of Fig. 9 corresponds to the simulation of $e^{-iH_{\text{new}}t}$, where

$$H_{\text{new}} := \beta \sum_{k,j_{1:M}} p_k p_{j_{1:M}}^{(k)} W_{k,j_{1:M}}^\dagger \tilde{H}_k W_{k,j_{1:M}}. \quad (15)$$

It can be shown using analysis of qDRIFT [8] that

$$\sum_{j_{1:M}} p_{j_{1:M}}^{(k)} W_{k,j_{1:M}}^\dagger \tilde{H}_k W_{k,j_{1:M}} = U_k^\dagger \tilde{H}_k U_k + O\left(\frac{\mu_k^2}{M}\right), \quad (16)$$

since the error analysis for the qDRIFT procedure remains valid when replacing the simulation of a density operator with that of a Hamiltonian.

In order to suppress the inner layer error $O(\mu_k^2/M)$ due to the random sampling of j in each of the N iterations of the outer layer below $O(\epsilon/N)$, the iteration number M must be chosen as $\Omega(\mu_k^2 N/\epsilon)$. Consequently, since N itself must have $1/\epsilon$ dependence (in order to suppress the overall error below ϵ , as explained previously) the overall time complexity of the intermediate circuit $N \cdot M$ scales according to $1/\epsilon^3$. Next, by compiling the subroutines of the algorithm, one can reduce this resource scaling to $1/\epsilon$. This compilation procedure can be achieved by setting M as $O(\mu_k^2)$ —removing the dependence on ϵ here comes at a cost of increasing the error. However, said $O(\mu_k^2/M) = O(1)$ inner layer error can be compensated for by introducing an additional modification to the procedure shown in Fig. 9, as we will discuss in the coming section. The total time complexity will be proportional to $N \cdot M$ which scales in terms of ϵ in the same way as N . Therefore, the total time complexity scales as $O(1/\epsilon)$ in terms of ϵ .

B. Compiled UHET Algorithm

We now move to apply this general method of compilation to the task of UHET, thereby providing a more efficient procedure than Algorithm 3. The compiled algorithm is presented in full in Algorithm 4, with details regarding the error and time complexity provided throughout App. D.

With respect to the circuit depicted in Fig. 9a, here we choose each iteration of the circuit to correspond to a short time-evolution by the following Hamiltonian:

$$\begin{aligned} & \left(\frac{1}{4}\right)^{nM} \sum_{\vec{v}_{1:M}} W_{k,\vec{v}_{1:M}}^\dagger ([\cos \phi_k X - \sin \phi_k Y] \otimes I) W_{k,\vec{v}_{1:M}} \\ &= A_{k,M} (e^{i\theta_{k,M} Z/2} \otimes I) \begin{pmatrix} 0 & e^{i\phi_k} e^{ik\pi(H_0+I)/2} \\ e^{-i\phi_k} e^{-ik\pi(H_0+I)/2} & 0 \end{pmatrix} (e^{-i\theta_{k,M} Z/2} \otimes I) \end{aligned} \quad (17)$$

where the iteration number M can depend upon k , $A_{k,M} = 1 - O(k^2/M) > 0$, $\theta_{k,M} = O(k^3/M^2) \in \mathbb{R}$ and

$$\begin{aligned} W_{k,\vec{v}_{1:M}}^{(M)} := & \left[\prod_{l=1}^M \mathbf{ctrl}(\sigma_{\vec{v}_l})(I \otimes e^{-i(k\pi H)/(2M)}) \mathbf{ctrl}(\sigma_{\vec{v}_l}) \right] \\ & \times (e^{-ik\pi Z/4} \otimes I). \end{aligned} \quad (18)$$

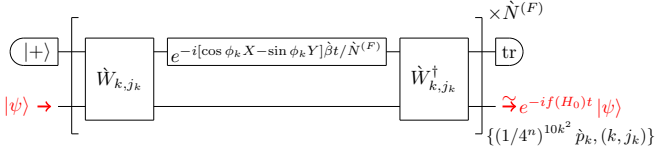


FIG. 10. *Compiled version of outer layer (Fig. 7a).*—By using modified values \hat{p}_k , $\hat{\beta}$, $\hat{N}^{(F)}$, and a modified operator \hat{W}_{k,j_k} (see Algorithm 4 for details), the iteration number $N_k^{(C)} = \Theta(\beta^2 t^2 k^2 / \epsilon^2)$ for controlization in Algorithm 3 is reduced to $10k^2 = \Theta(k^2)$ independent of f, n, t and ϵ , thereby leading to a more efficient algorithm for UHET.

For simplicity, we will sometimes suppress the superscript (M) and just write $W_{k,\vec{v}_{1:M}}$. We prove the validity of Eq. (17) in App. D 1.

As mentioned earlier, in order to improve the scaling behavior with respect to the uncompiled algorithm, we seek to modify the circuit to correct for the error introduced by the finite iteration number M of the inner layer. The factor $A_{k,M}$ can be compensated for by modifying the probability distribution p_k and the iteration number of the outer layer N ; the rotation errors of the form $e^{\pm i\theta_{k,M} Z/2} \otimes I$ can be corrected via an inverse rotation. Thus, the general compilation procedure can be applied to UHET in order to reduce the time complexity. In particular, we take M as $10k^2$ such that $A_{k,M} = 1 - O(k^2/M) > 1/2$ independently of k , which follows from a lower bound of $A_{k,M}$ [see Eq. (D3) in App. D 1].

If a classical description of the dynamics were given, then the compensation parameters $A_{k,M}$ and $\theta_{k,M}$ could be explicitly calculated via Eq. (17); however, since we only have access to the black-box dynamics $e^{\pm iH\tau}$, we must now construct a circuit that efficiently estimates them without relying on explicit knowledge of H . We present such a method that makes use of robust phase estimation [39] to obtain estimates $(\hat{A}_k, \hat{\theta}_k)$ of the error parameters $(A_{k,10k^2}, \theta_{k,10k^2})$ for $k \in \{-K, \dots, K\}$ (where K is a cutoff number) in App. D 2. This completes the pre-processing step of Algorithm 4.

The main part of Algorithm 4 then makes use of these estimates to compensate the error in simulating the desired transformed dynamics $e^{-if(H_0)t}$; we provide a complete error and time complexity analysis in App. D 3. The circuit representation of Algorithm 4 is depicted in Fig. 10, in which we choose a new cutoff number \hat{K} satisfying

$$\left| \tilde{f}(x) - \sum_{k=-\hat{K}}^{\hat{K}} \tilde{c}_k e^{ik\pi x} \right| < \frac{\epsilon}{6t} \quad \forall x \in [-1, 1], \quad (19)$$

Algorithm 4 Efficient universal Hamiltonian eigenvalue transformation (Compiled)

Input:

- A finite number of queries to a black-box Hamiltonian dynamics $e^{\pm iH\tau}$ of a seed Hamiltonian H normalized as $\|H_0\|_{\text{op}} \leq 1$, where H_0 is the traceless part of H , i.e., $H_0 := H - (1/2^n) \text{tr}(H)I$, with $\tau > 0$
- A class C^3 (3 times continuously differentiable) function $f : [-1, 1] \rightarrow \mathbb{R}$, such that $f^{(4)}$ is piecewise C^2 (see App. A 1)
- Input state $|\psi\rangle \in \mathcal{H}$
- Allowed error $\epsilon > 0$
- Time $t > 0$

Output: A state approximating $e^{-if(H_0)t} |\psi\rangle$ ($t > 0$) with an error in terms Eq. (2) upper-bounded by ϵ (also, the mean square of error in terms of Eq. (3) upper-bounded by 2ϵ)

Time complexity:

Pre-processing (only once): $\Theta(\hat{K}^3 t^3 n / \epsilon^3) + T_4$, $\hat{K} = O((t/\epsilon)^{1/3})$

Main Process: $\Theta(C_{4,f} t^2 n / \epsilon)$ for an f -dependent constant $C_{4,f}$ which is independent of n , t , and ϵ

Total evolution time (main process): $\Theta(C_{2,f} t^2 / \epsilon)$

Used Resources:

System: n -qubit system \mathcal{H} and one auxiliary qubit \mathcal{H}_c

Gates: $e^{\pm iH\tau}$, single-qubit gate on \mathcal{H}_c , and Clifford gates on $\mathcal{H}_c \otimes \mathcal{H}$

Procedure:
Pre-processing:

- 1: Define \tilde{f} as shown in Eq. (7) and compute Fourier coefficients $\tilde{c}_k := (1/2) \int_{-1}^1 dx e^{-ik\pi x} \tilde{f}(x)$ for $k \in \{-\hat{K}, -\hat{K} + 1, \dots, \hat{K}\}$ for a $\hat{K} > 0$ satisfying Eq. (19)
- 2: **for** $k \in \{1, \dots, \hat{K}\}$ **do**
- 3: Generate $(\hat{A}_k, \hat{\theta}_k)$ by Subroutine D6 of App. D 2 with allowed error set as $\sqrt{3\epsilon}/(12\pi(\sum_{k=-\infty}^{\infty} |\tilde{c}_k| |k|))$
- 4: $(\hat{A}_{-k}, \hat{\theta}_{-k}) \leftarrow (\hat{A}_k, -\hat{\theta}_k)$
- 5: **end for**
- 6: $(\hat{A}_0, \hat{\theta}_0) \leftarrow (1, 0)$
- 7: Compute $\hat{N} := N(\hat{\beta}, t, \epsilon/3)$ for $\hat{\beta} := \sum_{k=-\hat{K}}^{\hat{K}} (|\tilde{c}_k| / \hat{A}_k)$

Main Process:

- 8: Initialize $|\text{current}\rangle \leftarrow |+\rangle \otimes |\psi\rangle$
- 9: **for** $m \in \{1, \dots, \hat{N}\}$ **do**
- 10: Randomly choose k with probability $\hat{p}_k := |\tilde{c}_k| / (\hat{A}_k \hat{\beta})$
- 11: Randomly choose $j_k := (\vec{v}_{1:10k^2}) \in (\{0, 1, 2, 3\}^n)^{10k^2}$
- 12: $|\text{current}\rangle \leftarrow \hat{W}_{k,j_k}^{\dagger} (e^{-i[\cos \phi_k X - \sin \phi_k Y] \hat{\beta} t / \hat{N}^{(F)}} \otimes I) \hat{W}_{k,j_k} |\text{current}\rangle$
- 13: **end for**
- 14: Trace out \mathcal{H}_c of $|\text{current}\rangle$
- 15: **Return** $|\text{current}\rangle$

and set $j_k := (\vec{v}_{1:10k^2}) \in (\{0, 1, 2, 3\}^n)^{10k^2}$, $\hat{\beta} := \sum_{k=-\hat{K}}^{\hat{K}} (|\tilde{c}_k| / \hat{A}_k)$, $\hat{N} := N(\hat{\beta}, t, \epsilon/3)$, $\hat{p}_k := |\tilde{c}_k| / (\hat{A}_k \hat{\beta})$, and

$$\hat{W}_{k,j_k} := W_{k,j_k}^{(10k^2)} (e^{i\hat{\theta}_k Z/2} \otimes I). \quad (20)$$

The average number of times that the unknown dynamics $e^{-iH\tau}$ ($\tau > 0$) is called in any one sampling of k is reduced via compilation from $\sum_k p_k \Theta(\beta^2 t^2 k^2 / \epsilon^2)$ (Algorithm 3) to $\sum_k \hat{p}_k \Theta(k^2)$ (Algorithm 4) and the average depth of the overall circuit is subsequently reduced accordingly.

The time complexity of Algorithm 4 is $\Theta(\hat{K}^3 t^3 n / \epsilon^3) + T_4$ for pre-processing, where $\hat{K} = O((t/\epsilon)^{1/3})$ is the cutoff number defined in step 1 and T_4 refers to the sum of the classical computation time complexity for steps 1 (computation of the Fourier coefficients \tilde{c}_k until Eq. (19) is satisfied) and step 7 (computation of \hat{N}). The main process has time complexity $\Theta(C_{4,f} t^2 n / \epsilon)$ (see App. D 3 for the proof). The scaling of the time complexity of the main process in the $t \rightarrow \infty$ and $\epsilon \rightarrow 0$ limits are reduced in Algorithm 4 compared to Algorithm 3. Lastly, the total evolution time for the main process is evaluated in the same way as in Subroutine 2 as $\Theta(C_{2,f} t^2 / \epsilon)$.

VI. COMPARISON WITH A QSVT-BASED UHET ALGORITHM

Algorithms 3 and 4 above provide two novel methods to implement the task of UHET; we now move to compare these algorithms with another one that achieves the same task via a modified QSVT procedure. In principle, one can combine standard QSVT methods with the ability to simulate Hamiltonian dynamics to achieve the said task. Given a classical description of the Hamiltonian, this can be achieved by performing a block-encoding of H into a unitary, using QSVT to approximate $e^{-if(H_0)t}$ (up to a proportionality constant), and then amplifying the block via *robust oblivious amplitude amplification* [5, 37]. However, such a procedure requires a classical description of the Hamiltonian to be known *a priori*, in contradistinction to the UHET task we have so far considered. Here, instead of a classical description of H , one is only given access to a black-box Hamiltonian dynamics $e^{\pm iHt}$. In App. E, we provide a method that modifies the standard QSVT procedure by essentially applying control to a modified version of the unknown Hamiltonian and then applying appropriate gates to simulate the desired function.

This allows us to fairly compare the performance of Algorithm 3 (uncompiled), Algorithm 4 (compiled) and the QSVT-based Algorithm 8 presented in full in App. E 1. Note that in all three algorithms compared here, the scaling of the time complexity dominates that of the total evolution time; as such, the overall runtime behavior is determined by the time complexity. Thus, in this section, we only compare the algorithms in terms of their time complexities. We show that the scaling of the time complexity of the main process (i.e., the part that must be run each time) of these algorithms behaves in the limit of $\epsilon \rightarrow 0$ as:

$$\begin{aligned} & \text{time complexity of Algorithm 4 (compiled)} \\ & \leq \text{time complexity of QSVT-based Algorithm 8} \\ & \leq \text{time complexity of Algorithm 3 (uncompiled).} \quad (21) \end{aligned}$$

In other words, Algorithm 3, which is slower than the QSVT-based Algorithm 8 when uncompiled, becomes faster than it via compilation into Algorithm 4. In App. E 1, we first describe how QSVT techniques can be applied to the task of UHET and present an algorithm that leverages ideas from Hamiltonian singular value transformation [40] and the QSVT-based Hamiltonian simulation [5, 37] (see also Ref. [16] for related approaches). In App. E 2, we subsequently calculate the ϵ dependence of the three studied algorithms, demonstrating the relation (21), and explain the technical reasons for the differences in scaling. Put briefly, the resource advantage of Algorithm 4 stems from the fact that we can remove the ϵ -dependence of the controlization part via compilation and the algorithm efficiently treats high frequency terms due to the fact that low-weight terms in the Fourier series are sampled infrequently.

VII. IMPLEMENTING NEGATIVE-TIME HAMILTONIAN DYNAMICS

Algorithm 5 Simulating negative-time evolution

Input:

- A finite number of queries to a black-box Hamiltonian dynamics $e^{-iH\tau}$ of a seed Hamiltonian H normalized as $\|H_0\|_{\text{op}} \leq 1$, where H_0 is the traceless part of H , i.e., $H_0 := H - (1/2^n)\text{tr}(H)I$, with $\tau > 0$
- A subset $J \subseteq \{0, 1, 2, 3\}^n$ such that $H \in \text{span}(\{\sigma_{\vec{v}}\}_{\vec{v} \in J})$
- Allowed error $\epsilon > 0$
- Time $t > 0$

Output: A random unitary operator approximating e^{+iHt} with an error according to Eq. (1) upper bounded by ϵ

Time complexity: $\Theta(L^2 t^2 / \epsilon)$ where L is an integer that depends on J

Total evolution time: $(L - 1)t$

Used Resources:

System: n -qubit system \mathcal{H} (no auxiliary system)
Gates: $e^{-iH\tau}$ and Pauli gates on \mathcal{H}

Procedure:

Pre-processing:

- 1: Obtain a subgroup G of $\{\pm\sigma_{\vec{v}}, \pm i\sigma_{\vec{v}}\}_{\vec{v} \in \{0,1,2,3\}^n}$ such that for all $\vec{v} \in J \setminus \{\vec{0}\}$ there exists a $g \in G$ such that g and $\sigma_{\vec{v}}$ anti-commutes.
- 2: Define $G' := \{\sigma \in \{\sigma_{\vec{v}}\}_{\vec{v} \in \{0,1,2,3\}^n} \mid \exists g \in G, g \propto \sigma\}$ and $L := |G'|$ to compute $N := N(L - 1, t, \epsilon)$, using $N(\lambda, t, \epsilon)$ from Eq. (4)

Main Process:

- 3: Initialize $U_{\text{current}} \leftarrow I$
- 4: **for** $m = 1, \dots, N$ **do**
- 5: Uniformly randomly choose $\sigma \in G' \setminus \{I\}$.
- 6: $U_{\text{current}} \leftarrow (\sigma e^{-iH(L-1)t/N} \sigma) U_{\text{current}}$
- 7: **end for**
- 8: **Return** U_{current}

The algorithms presented above all require access to both the positive e^{-iHt} ($t > 0$) and negative-time Hamiltonian dynamics e^{+iHt} ($t > 0$). However, in many situations, one might only have access to the positive-time dynamics. In such situations, the negative-time evolution can nonetheless be simulated without using auxiliary qubits, as we demonstrate in the following algorithm.

Even in situations where H is unknown, one can often reasonably assume some form of its structure, e.g., that it has at most two-body interactions or that it is based on qubit connectivities. In Algorithm 5, we present a random algorithm to simulate the negative-time evolution in any situation where the seed Hamiltonian H is assumed to belong to a subspace of $\mathcal{L}(\mathcal{H})$ spanned by the set $\{\sigma_{\vec{v}}\}_{\vec{v} \in J}$ for some $J \subseteq \{0, 1, 2, 3\}^n$. This random algorithm approximates the dynamics of the following Hamiltonian,

$$\sum_{\sigma \in G' \setminus \{I\}} \sigma H \sigma = -H + \frac{\text{Ltr}(H)}{2^n} I, \quad (22)$$

which is equal to $-H$ up to a term proportional to I . Here G' is constructed as follows: first take a subgroup G of $\{\pm \sigma_{\vec{v}}, \pm i\sigma_{\vec{v}}\}_{\vec{v} \in \{0, 1, 2, 3\}^n}$ such that for all $\vec{v} \in J \setminus \{\vec{0}\}$ there exists a $g \in G$ such that g and $\sigma_{\vec{v}}$ anti-commutes; then define $G' = \{\sigma \in \{\sigma_{\vec{v}}\}_{\vec{v} \in \{0, 1, 2, 3\}^n} \mid \exists g \in G, g \propto \sigma\}$ as a set of Pauli operators in G ignoring prefactors. Moreover, $L := |G'|$ is defined as the number of terms in G' . Eq. (22) can be derived from the equality

$$\sum_{\sigma \in G'} \sigma H \sigma = \frac{\text{Ltr}(H)}{2^n} I, \quad (23)$$

by noting that

$$\sum_{\sigma \in G' \setminus \{I\}} \sigma H \sigma = \sum_{\sigma \in G'} \sigma H \sigma - H. \quad (24)$$

The proof of Eq. (23) is given in App. F.

Since the sum of all Hamiltonian coefficients used in the qDRIFT simulation $\lambda = \sum_j h_j$ is calculated here as $\lambda = \sum_{\sigma \in G' \setminus \{I\}} 1 = L - 1$, the error [in terms of Eq. (1)] can be upper-bounded by ϵ by taking the iteration number $N = N(L - 1, t, \epsilon)$. This algorithm makes use of n -qubit Pauli gates, which can be run in $O(1)$ depth, therefore, the overall time complexity will be $\Theta(N) = \Theta(L^2 t^2 / \epsilon)$. For a given Hamiltonian structure, there are many possible choices of G ; choosing the smallest G leads to the smallest time complexity. For example, if $J = \{(3, \dots, 3)\}$, corresponding to the Hamiltonian $H \propto Z^{\otimes n}$, both $G_1 = \{\pm \sigma_{\vec{v}}, \pm i\sigma_{\vec{v}}\}_{\vec{v} \in \{0, 1, 2, 3\}^n}$ and $G_2 = \{I, X \otimes I^{\otimes n-1}\}$ satisfy the condition of step 1 of Algorithm 5; however G_2 gives a smaller time complexity since it has fewer distinct Pauli operators. Moreover, since the size of the subset J determines the number of conditions on G , J should also be taken as small as possible.

While finding a subgroup G for a complicated subset J might seem difficult in general, a canonical construction

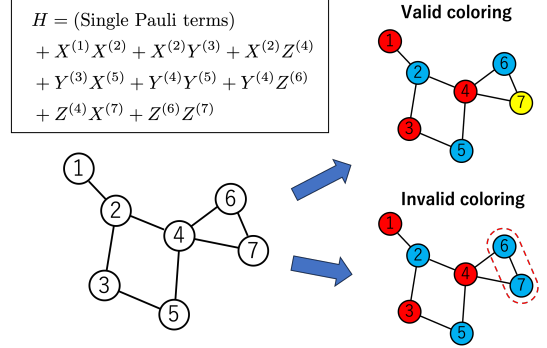


FIG. 11. *Intuition behind the definition of G .*—When the set J corresponds to the bottom-left graph, defining G as per Eq. (25) with a valid coloring leads to Eq. (23) because every term in the Hamiltonian anti-commutes with at least one element of G . On the other hand, if an invalid coloring is used, then Eq. (23) is not satisfied, since there could be a term in the Hamiltonian that commutes with all elements of G , e.g., $I^{\otimes 5} \otimes Z^{(6)} Z^{(7)}$ in the depiction above.

of G exists and often gives a reasonably small L . Suppose that the Hamiltonian H is 2-local and is defined on an n -qubit system whose connectivity is represented by an undirected graph (V, E) . Here, vertices V correspond to qubits, and edges E correspond to pairs of qubits that interact via H . This corresponds to the case where for all $\vec{v} = (v_1, \dots, v_n) \in J \setminus \{\vec{0}\}$, either $|\{j \in \{1, \dots, n\} \mid v_j \neq 0\}| = 1$ or $|\{j \in \{1, \dots, n\} \mid v_j \neq 0\}| = 2$.

For a given connectivity graph, we first assign colors to all vertices in such a way that two different vertices connected by an edge must have different colors. Once a *valid coloring* $\{(c_i, V_i)\}_{i=1}^k$, where $\{c_i\}_i$ is a set of colors and V_i is the set of vertices colored in c_i , is obtained, we can define G as follows:

$$G = \left\{ \pm \bigotimes_{i=1}^k \sigma_{v_i}^{(V_i)}, \pm i \bigotimes_{i=1}^k \sigma_{v_i}^{(V_i)} \right\}_{(v_1, \dots, v_k) \in \{0, 1, 2, 3\}^k}, \quad (25)$$

where $\sigma_v^{(V)} := \bigotimes_{q \in V} \sigma_v^{(q)}$, where $\sigma_v^{(q)}$ refers to the Pauli operator σ_v applied on q -th qubit. Since the integer L corresponding to this G is 4^k , the number of colors k should be taken as small as possible in order to reduce L . The minimum number of colors necessary to color a graph in such a way is called the *chromatic number*.

In many cases, the chromatic number of a graph does not scale with the number of qubits n . For example, when the connectivity of qubits is given by a 2D square lattice, the chromatic number is 2, thus the time complexity $\Theta(L^2 t^2 / \epsilon)$ is constant in n . More generally the chromatic number is upper-bounded by the maximum vertex degree plus one (see, e.g., Refs. [41, 42]), thus as long as the number of neighbors of qubits is upper-bounded by a constant, the time complexity will not depend on n . Although the above construction only applies to 2-local Hamiltonians, in App. F we show a generalization that holds for many-body Hamiltonians. As a consequence, it follows that the time complexity of our negative-time evolution algorithm does not depend on n for a low-intersection Hamiltonian

as defined in Ref. [36]. The proof that G in Eq. (25) satisfies the condition in step 1 of Algorithm 5 is presented in App. F, as well as and an extension of Eq. (25) to general Hamiltonians.

Finally, note that in cases where the time complexity is independent of the number of qubits n —e.g., finite-range interaction Hamiltonian on a lattice—a deterministic second-order Trotter-Suzuki simulation can outperform the randomized qDRIFT approach to behave like $O(N) = O(t^{3/2}/\epsilon^{1/2})$ in the limits $\epsilon \rightarrow 0, t \rightarrow \infty$, and $n \rightarrow \infty$. However, determining the necessary and sufficient conditions for when a deterministic Hamiltonian simulation method outperforms its counterpart probabilistic one remains an open question. Moreover, such an enhancement is only possible when considering a *second-order* Trotter-Suzuki decomposition, since higher-order decompositions require negative-time Hamiltonian dynamics to be accessible [43].

VIII. CONCLUSION

In this work, we developed universal quantum algorithms for transforming the eigenvalues of any Hamiltonian by any (suitably differentiable) function, while keeping the eigenstates unchanged. Our algorithms are universal in the sense that they do not rely on knowledge of the input Hamiltonian, whose dynamics can be given as a black box. The uncompiled algorithm is constructed by concatenating two subroutines, namely controlization and Fourier series simulation. We furthermore introduced a general framework for compilation, which uses correlated randomness to perform multiple layers of random sampling in a more efficient way. For our algorithm, we showed that the compilation step significantly reduces the time complexity, making it even more efficient than simulation methods based on QSFT.

To broaden the realm of applicability of our method, we further proposed a novel algorithm for simulating the negative time-evolution of an unknown Hamiltonian without using an auxiliary system. This algorithm reduces the resource requirements compared to previous ones and exhibits favorable properties that enable its physical implementation in many physical systems. Thus, by combining our UHET algorithms with that for simulating negative time evolution, one can transform an unknown Hamiltonian dynamics by interspersing gate operations throughout the unknown Hamiltonian evolution. However, a practical limitation may arise from the difficulty

of implementing such procedures in experimental setups. Nonetheless, given the ability to apply the interspersed gates on a much shorter timescale than the evolution times of the unknown Hamiltonian dynamics, then the entire situation can be approximated as a short pulse sequence of gates applied on top of a continuously-running Hamiltonian dynamics, circumventing the problem.

Our results have implications broadly across the realm of quantum information and beyond. First, the notion of compilation reconciles quantum computing practices with a key notion implemented in classical computing, where subroutines are compiled into larger functions in order to be implemented more efficiently. Extending this approach to different tasks could significantly improve our ability to develop complex and efficient quantum algorithms in a modular fashion, similar to that of classical software. Second, we expand the class of universal Hamiltonian transformations that can be efficiently performed to all suitably differential functions on the space of Hamiltonians, extending previously known results for linear functions of Hamiltonians [12].

In the future, developing a general theoretical framework for higher-order transformation of Hamiltonian dynamics will provide more insight into the possible manipulation of Hamiltonian dynamics for information processing tasks. As fault-tolerant quantum computers become more readily available, we envisage that our methods will apply to practical use cases in the simulation and manipulation of quantum systems, such as in quantum chemistry or materials discovery.

ACKNOWLEDGMENTS

We would like to thank Anirban Chowdhury, Toshinori Itoko, Antonio Mezzacapo, Kunal Sharma, Satoshi Yoshida, Alexander Zlokapa and Lei Zhang for helpful discussions. This work was supported by MEXT Quantum Leap Flagship Program (MEXT QLEAP) JP-MXS0118069605, JPMXS0120351339, Japan Society for the Promotion of Science (JSPS) KAKENHI Grant No. 21H03394, and the IBM-UTokyo Laboratory. Research at Perimeter Institute is supported in part by the Government of Canada through the Department of Innovation, Science and Economic Development and by the Province of Ontario through the Ministry of Colleges and Universities. P. T. acknowledges support from the Japan Society for the Promotion of Science (JSPS) Postdoctoral Fellowship for Research in Japan.

[1] A. Jain, S. P. Ong, G. Hautier, W. Chen, W. D. Richards, S. Dacek, S. Cholia, D. Gunter, D. Skinner, G. Ceder, *et al.*, Commentary: The Materials Project: A materials genome approach to accelerating materials innovation, *APL Mater.* **1**, 011002 (2013).

[2] F. Tang, H. C. Po, A. Vishwanath, and X. Wan, Efficient topological materials discovery using symmetry indicators, *Nat. Phys.* **15**, 470 (2019), [arXiv:1805.07314](https://arxiv.org/abs/1805.07314).

[3] Y. Alexeev, M. Amsler, P. Baity, M. A. Barroca, S. Bassini, T. Battelle, D. Campsn, D. Casanova, Y. J. Choi, F. T. Chong, *et al.*, Quantum-centric Supercomputing for Materials Science: A Perspective on Challenges

and Future Directions (2023), [arXiv:2312.09733](https://arxiv.org/abs/2312.09733).

- [4] G. H. Low and I. L. Chuang, Hamiltonian simulation by qubitization, *Quantum* **3**, 163 (2019), [arXiv:1610.06546](https://arxiv.org/abs/1610.06546).
- [5] A. Gilyén, Y. Su, G. H. Low, and N. Wiebe, Quantum singular value transformation and beyond: exponential improvements for quantum matrix arithmetics, in *Proceedings of the 51st Annual ACM SIGACT Symposium on Theory of Computing* (2019) pp. 193–204, [arXiv:1806.01838](https://arxiv.org/abs/1806.01838).
- [6] M. Suzuki, Fractal decomposition of exponential operators with applications to many-body theories and Monte Carlo simulations, *Phys. Lett. A* **146**, 319 (1990).
- [7] M. Suzuki, General theory of fractal path integrals with applications to many-body theories and statistical physics, *J. Math. Phys.* **32**, 400 (1991).
- [8] E. Campbell, Random compiler for fast Hamiltonian simulation, *Phys. Rev. Lett.* **123**, 070503 (2019), [arXiv:1811.08017](https://arxiv.org/abs/1811.08017).
- [9] D. W. Berry, A. M. Childs, R. Cleve, R. Kothari, and R. D. Somma, Simulating Hamiltonian dynamics with a truncated Taylor series, *Phys. Rev. Lett.* **114**, 090502 (2015), [arXiv:1412.4687](https://arxiv.org/abs/1412.4687).
- [10] G. H. Low and I. L. Chuang, Optimal Hamiltonian simulation by quantum signal processing, *Phys. Rev. Lett.* **118**, 010501 (2017), [arXiv:1606.02685](https://arxiv.org/abs/1606.02685).
- [11] A. M. Childs, D. Maslov, Y. Nam, N. J. Ross, and Y. Su, Toward the first quantum simulation with quantum speedup, *Proc. Natl. Acad. Sci. U.S.A.* **115**, 9456 (2018), [arXiv:1711.10980](https://arxiv.org/abs/1711.10980).
- [12] T. Odake, H. Kristjánsson, A. Soeda, and M. Murao, Higher-order quantum transformations of Hamiltonian dynamics (2023), [arXiv:2303.09788](https://arxiv.org/abs/2303.09788).
- [13] D. Poulin and P. Wocjan, Sampling from the thermal quantum gibbs state and evaluating partition functions with a quantum computer, *Phys. Rev. Lett.* **103**, 220502 (2009), [arXiv:0905.2199](https://arxiv.org/abs/0905.2199).
- [14] C. Zhang, Randomized algorithms for Hamiltonian simulation, in *Monte Carlo and Quasi-Monte Carlo Methods 2010* (Springer, 2012) pp. 709–719.
- [15] X. Zhang, Y. Shen, J. Zhang, J. Casanova, L. Lamata, E. Solano, M.-H. Yung, J.-N. Zhang, and K. Kim, Time reversal and charge conjugation in an embedding quantum simulator, *Nat. Commun.* **6**, 7917 (2015), [arXiv:1409.3681](https://arxiv.org/abs/1409.3681).
- [16] Y. Wang, L. Zhang, Z. Yu, and X. Wang, Quantum Phase Processing and its Applications in Estimating Phase and Entropies (2022), [arXiv:2209.14278](https://arxiv.org/abs/2209.14278).
- [17] T. Kosugi, Y. Nishiya, H. Nishi, and Y.-I. Matsushita, Imaginary-time evolution using forward and backward real-time evolution with a single ancilla: First-quantized eigensolver algorithm for quantum chemistry, *Phys. Rev. Res.* **4**, 033121 (2022), [arXiv:2111.12471](https://arxiv.org/abs/2111.12471).
- [18] D. W. Berry, A. M. Childs, and R. Kothari, Hamiltonian simulation with nearly optimal dependence on all parameters, in *2015 IEEE 56th annual symposium on foundations of computer science* (IEEE, 2015) pp. 792–809, [arXiv:1501.01715](https://arxiv.org/abs/1501.01715).
- [19] A. M. Childs, R. Kothari, and R. D. Somma, Quantum algorithm for systems of linear equations with exponentially improved dependence on precision, *SIAM J. Comput.* **46**, 1920 (2017), [arXiv:1511.02306](https://arxiv.org/abs/1511.02306).
- [20] L. K. Grover, Quantum Mechanics Helps in Searching for a Needle in a Haystack, *Phys. Rev. Lett.* **79**, 325 (1997), [arXiv:quant-ph/9706033](https://arxiv.org/abs/quant-ph/9706033).
- [21] R. N. Zare, Laser control of chemical reactions, *Science* **279**, 1875 (1998).
- [22] M. T. Greiner, M. G. Helander, W.-M. Tang, Z.-B. Wang, J. Qiu, and Z.-H. Lu, Universal energy-level alignment of molecules on metal oxides, *Nat. Mater.* **11**, 76 (2012).
- [23] G. Chiribella, G. M. D’Ariano, and P. Perinotti, Quantum circuit architecture, *Phys. Rev. Lett.* **101**, 060401 (2008), [arXiv:0712.1325](https://arxiv.org/abs/0712.1325).
- [24] J. Miyazaki, A. Soeda, and M. Murao, Complex conjugation supermap of unitary quantum maps and its universal implementation protocol, *Phys. Rev. Res.* **1**, 013007 (2019), [arXiv:1706.03481](https://arxiv.org/abs/1706.03481).
- [25] Q. Dong, S. Nakayama, A. Soeda, and M. Murao, Controlled quantum operations and combs, and their applications to universal controllization of divisible unitary operations (2019), [arXiv:1911.01645](https://arxiv.org/abs/1911.01645).
- [26] M. T. Quintino, Q. Dong, A. Shimbo, A. Soeda, and M. Murao, Probabilistic exact universal quantum circuits for transforming unitary operations, *Phys. Rev. A* **100**, 062339 (2019), [arXiv:1909.01366](https://arxiv.org/abs/1909.01366).
- [27] M. T. Quintino, Q. Dong, A. Shimbo, A. Soeda, and M. Murao, Reversing unknown quantum transformations: Universal quantum circuit for inverting general unitary operations, *Phys. Rev. Lett.* **123**, 210502 (2019), [arXiv:1810.06944](https://arxiv.org/abs/1810.06944).
- [28] S. Yoshida, A. Soeda, and M. Murao, Reversing Unknown Qubit-Unitary Operation, Deterministically and Exactly, *Phys. Rev. Lett.* **131**, 120602 (2023), [arXiv:2209.02907](https://arxiv.org/abs/2209.02907).
- [29] G. Chiribella and H. Kristjánsson, Quantum Shannon theory with superpositions of trajectories, *Proc. R. Soc. A* **475**, 20180903 (2019), [arXiv:1812.05292](https://arxiv.org/abs/1812.05292).
- [30] G. Chiribella, G. M. D’Ariano, P. Perinotti, and B. Valiron, Quantum computations without definite causal structure, *Phys. Rev. A* **88**, 022318 (2013), [arXiv:0912.0195](https://arxiv.org/abs/0912.0195).
- [31] F. A. Pollock, C. Rodríguez-Rosario, T. Frauenheim, M. Paternostro, and K. Modi, Non-Markovian quantum processes: Complete framework and efficient characterization, *Phys. Rev. A* **97**, 012127 (2018), [arXiv:1512.00589](https://arxiv.org/abs/1512.00589).
- [32] O. Oreshkov, F. Costa, and Č. Brukner, Quantum correlations with no causal order, *Nat. Commun.* **3**, 1092 (2012), [arXiv:1105.4464](https://arxiv.org/abs/1105.4464).
- [33] G. Bai, Y.-D. Wu, Y. Zhu, M. Hayashi, and G. Chiribella, Efficient algorithms for causal order discovery in quantum networks (2020), [arXiv:2012.01731](https://arxiv.org/abs/2012.01731).
- [34] P. Selinger, Towards a Quantum Programming Language, *Math. Struct. Comput. Sci.* **14**, 527 (2004).
- [35] P. Selinger and B. Valiron, A Lambda Calculus for Quantum Computation with Classical Control, in *Typed Lambda Calculi and Applications* (2005) pp. 354–368, [arXiv:cs/0404056](https://arxiv.org/abs/cs/0404056).
- [36] H.-Y. Huang, Y. Tong, D. Fang, and Y. Su, Learning many-body Hamiltonians with Heisenberg-limited scaling (2022), [arXiv:2210.03030](https://arxiv.org/abs/2210.03030).
- [37] J. M. Martyn, Z. M. Rossi, A. K. Tan, and I. L. Chuang, Grand Unification of Quantum Algorithms, *PRX Quantum* **2**, 040203 (2021), [arXiv:2105.02859](https://arxiv.org/abs/2105.02859).
- [38] J. S. Walker, Fourier series, in *Encyclopedia of Physical Science and Technology (Third Edition)*, edited by R. A. Meyers (Academic Press, New York, NY, USA, 2003) pp. 167–183.
- [39] S. Kimmel, G. H. Low, and T. J. Yoder, Robust calibration of a universal single-qubit gate set via robust phase estimation, *Phys. Rev. A* **92**, 062315 (2015), [arXiv:1502.02677](https://arxiv.org/abs/1502.02677).
- [40] S. Lloyd, B. T. Kiani, D. R. Arvidsson-Shukur, S. Bosch,

G. De Palma, W. M. Kaminsky, Z.-W. Liu, and M. Marian, Hamiltonian singular value transformation and inverse block encoding (2021), [arXiv:2104.01410](https://arxiv.org/abs/2104.01410).

[41] Ø. Ore, Theory of graphs, in *American Mathematical Society Colloquium Publications*, Vol. 38 (American Mathematical Society, Providence, RI, USA, 1962).

[42] D. J. A. Welsh and M. B. Powell, An upper bound for the chromatic number of a graph and its application to timetabling problems, *Comput. J.* **10**, 85 (1967).

[43] D. W. Berry, G. Ahokas, R. Cleve, and B. C. Sanders, Efficient quantum algorithms for simulating sparse Hamiltonians, *Commun. Math. Phys.* **270**, 359 (2007), [arXiv:quant-ph/0508139](https://arxiv.org/abs/quant-ph/0508139).

[44] J. Watrous, *The theory of quantum information* (Cambridge University Press, Cambridge, UK, 2018).

[45] M. Bocher, Introduction to the Theory of Fourier's Series, *Ann. Math.* **7**, 81 (1906).

[46] J. P. Boyd, *Chebyshev and Fourier spectral methods* (Dover Publications Inc., New York, NY, USA, 2001).

[47] R. Chao, D. Ding, A. Gilyen, C. Huang, and M. Szegedy, Finding angles for quantum signal processing with machine precision (2020), [arXiv:2003.02831](https://arxiv.org/abs/2003.02831).

APPENDICES

Appendix A: Preliminary Definitions

Here, we provide some basic definitions that will prove useful throughout our work.

1. *J*-Smoothness of Functions

Definition 1 (Piecewise C^J). *Let $\mathcal{X} := \{x_0, \dots, x_n\}$, where $-1 = x_0 < x_1 < \dots < x_n = 1$. A function $g : [-1, 1] \setminus \mathcal{X}' \rightarrow \mathbb{R}$, where $\mathcal{X}' \subseteq \mathcal{X}$, is **piecewise C^J** ($J \in \mathbb{N}_+$) $\stackrel{\text{def}}{\Leftrightarrow}$ the derivatives $g^{(m)}$ for $m \in \{0, 1, \dots, J\}$ are well-defined and continuous everywhere in $[-1, 1] \setminus \mathcal{X}$, and additionally, at the exceptional points x_1, \dots, x_{n-1} of g , we have that for all $j \in \{1, \dots, n-1\}$, $\lim_{x \rightarrow x_j^+} g^{(m)}(x)$ and $\lim_{x \rightarrow x_j^-} g^{(m)}(x)$ exist for all $m \in \{0, \dots, J\}$ (although the limits from above and below need not coincide), as well as for $x = \pm 1$, $\lim_{x \rightarrow -1^+} g^{(m)}(x)$ and $\lim_{x \rightarrow 1^-} g^{(m)}(x)$ exist. In particular, when $J = 1$, g is said to be **piecewise smooth***

Definition 2 (*J*-Smoothness). *Here, we extend the notion of piecewise continuity to higher orders of smoothness.*

1. *A function $g : [-1, 1] \rightarrow \mathbb{R}$ is J -smooth $\stackrel{\text{def}}{\Leftrightarrow}$ g is piecewise C^{J-1} and $g^{(J)}$ is piecewise C^2 .*
2. *A function $g : [-1, 1] \rightarrow \mathbb{R}$ is periodically J -smooth $\stackrel{\text{def}}{\Leftrightarrow}$ g is J -smooth and $g^{(m)}(+1) = g^{(m)}(-1) \forall m \in \{0, \dots, J-1\}$.*
3. *A function $g : [-1, 1] \rightarrow \mathbb{R}$ is strictly J -smooth $\stackrel{\text{def}}{\Leftrightarrow}$ g is J -smooth and $g^{(J)}$ does not satisfy*

$$\lim_{x \rightarrow a^+} g^{(J)}(x) = \lim_{x \rightarrow a^-} g^{(J)}(x) \quad \forall a \in (-1, 1). \quad (\text{A1})$$

4. *A function $g : [-1, 1] \rightarrow \mathbb{R}$ is strictly periodically J -smooth $\stackrel{\text{def}}{\Leftrightarrow}$ g is periodically J -smooth and $g^{(J)}$ does not satisfy either or both of the following conditions:*

1. $\lim_{x \rightarrow a^+} g^{(J)}(x) = \lim_{x \rightarrow a^-} g^{(J)}(x) \quad \forall a \in (-1, 1)$
2. $\lim_{x \rightarrow 1^-} g^{(J)}(x) = \lim_{x \rightarrow -1^+} g^{(J)}(x).$

2. Norms for Quantifying Errors

When quantifying the error of a simulated operation, we will often make use of the diamond norm, defined as

$$\|\Phi\|_\diamond := \max_{A \in \mathcal{L}(\mathcal{H} \otimes \mathcal{H}); \|A\|_1=1} \|(\Phi \otimes \mathcal{I})(A)\|_1, \quad (\text{A3})$$

where $\Phi : \mathcal{L}(\mathcal{H}) \rightarrow \mathcal{L}(\mathcal{H})$ is a quantum operation, \mathcal{I} is an identity operation on $\mathcal{L}(\mathcal{H})$, and $\|\cdot\|_1$ denotes the 1-norm defined as $\|A\|_1 := \text{tr}(\sqrt{A^\dagger A})$.

3. Scaling Notation

Throughout this article, we use the symbols $O(\cdot)$, $\Omega(\cdot)$, and $\Theta(\cdot)$, the definitions of which are provided in Table I, to denote the scaling behavior of time complexities of the algorithms presented. Furthermore, we consider various limits depending on the parameter of interest. In particular, we consider the limit $\rightarrow \infty$ for qubit number $n \in \mathbb{Z}_{>0}$, simulation time $t \in \mathbb{R}$, and the limit $\rightarrow 0$ for the allowed error $\epsilon > 0$. For instance $f(t, \epsilon) = O(t^2 \epsilon^{-1})$ means that $\limsup_{t \rightarrow \infty} (f(t, \epsilon)/t^2) < \infty$ for all $\epsilon > 0$ and $\limsup_{\epsilon \rightarrow 0} (f(t, \epsilon)/\epsilon^{-1}) < \infty$ for all $t \in \mathbb{R}$. Intuitively speaking, $f(x) = O(g(x))$ if $g(x)$ grows at least as fast as $f(x)$ in $\lim x \rightarrow \infty$ (i.e., g asymptotically upper bounds f); $f(x) = \Omega(g(x))$ if $f(x)$ grows at least as fast as $g(x)$ in $\lim x \rightarrow \infty$ (i.e., g asymptotically lower bounds f); and $f(x) = \Theta(g(x))$ if g provides both an upper and lower bound of f asymptotically.

Notation	Definition
$f(x) = O(g(x))$	$\limsup_{x \rightarrow \infty} (f(x)/g(x)) < \infty$
$f(x) = \Omega(g(x))$	$\liminf_{x \rightarrow \infty} (f(x)/g(x)) > 0$
$f(x) = \Theta(g(x))$	$f(x) = O(g(x))$ and $f(x) = \Omega(g(x))$

TAB. I. *Scaling symbols.*—For any $g(x)$, we say that a function $f(x)$ is $O(g(x))$, $\Omega(g(x))$, or $\Theta(g(x))$, if the above are satisfied.

Appendix B: Universal Hamiltonian Eigenvalue Transformation (UHET)

1. Mean Squared Error Bound

Here we demonstrate the validity of Eq. (3), which bounds the mean squared error of an average operation in terms of some original error bound. More precisely, we prove:

Lemma 1 (Mean Squared Error Bound). *Consider an arbitrary unitary operation defined by $\mathcal{U}(\rho) := U\rho U^\dagger$ with a unitary operator U and a density operator ρ on a Hilbert space \mathcal{H} . If the error (in terms of the 1-norm) of a set of deterministic quantum operations (completely-positive trace-preserving maps) $\mathcal{F}_j : \mathcal{L}(\mathcal{H}) \rightarrow \mathcal{L}(\mathcal{H})$ and a probability distribution $\{p_j\}$ satisfies*

$$\sup_{|\psi\rangle \in \mathcal{H}} \|\mathcal{U}(|\psi\rangle \langle \psi|) - \sum_j p_j \mathcal{F}_j(|\psi\rangle \langle \psi|)\|_1 \leq \Delta, \quad (\text{B1})$$

for some $\Delta > 0$, then the mean squared error of the average operation $\sum_j p_j \mathcal{F}_j$ is upper bounded by

$$\sup_{|\psi\rangle; \|\psi\|=1} \sum_j p_j \|\mathcal{U}(|\psi\rangle \langle \psi|) - \mathcal{F}_j(|\psi\rangle \langle \psi|)\|_1^2 \leq 2\Delta, \quad (\text{B2})$$

where $|\psi\rangle$ is any pure state on \mathcal{H} .

This lemma is proven in App. B of Ref. [12]. Furthermore, if a modified version of Eq. (B1) is applied to an extended Hilbert space, namely

$$\sup_{\substack{\dim(\mathcal{H}') \\ |\psi\rangle \in \mathcal{H} \otimes \mathcal{H}' \\ \|\psi\|=1}} \|\mathcal{U} \otimes \mathcal{I}_{\mathcal{H}'}(|\psi\rangle \langle \psi|) - \sum_j p_j \mathcal{F}_j \otimes \mathcal{I}_{\mathcal{H}'}(|\psi\rangle \langle \psi|)\|_1 \leq \Delta \quad (\text{B3})$$

holds, then a stronger version of Eq. (B2), i.e.,

$$\sup_{\substack{\dim(\mathcal{H}') \\ |\psi\rangle \in \mathcal{H} \otimes \mathcal{H}' \\ \|\psi\|=1}} \sum_j p_j \|\mathcal{U} \otimes \mathcal{I}_{\mathcal{H}'}(|\psi\rangle \langle \psi|) - \mathcal{F}_j \otimes \mathcal{I}_{\mathcal{H}'}(|\psi\rangle \langle \psi|)\|_1^2 \leq 2\Delta, \quad (\text{B4})$$

follows.

Appendix C: Uncompiled UHET Algorithm

Here we provide details relevant to the uncompiled UHET algorithm presented throughout Sec. IV of the main text.

1. Sufficient Number of qDRIFT Iterations

The qDRIFT procedure is a stochastic method for simulating Hamiltonian dynamics [8]. Here, we determine a sufficient number of iterations to ensure a sufficiently small error ϵ .

Lemma 2. *Suppose one is given access to the dynamics $e^{-iH_j\tau}$ ($\tau > 0$) corresponding to a set of Hamiltonians $\{H_j\}_j$ on $\mathcal{L}(\mathcal{H})$ which normalized as $\|H_j\|_{\text{op}} = 1$. Then, the dynamics e^{-iHt} ($t > 0$) of a Hamiltonian represented as $H = \sum_j h_j H_j$ for a set of positive coefficients $\{h_j\}_j$ can be simulated using qDRIFT with an error of at most $(2\lambda^2 t^2/N)e^{2\lambda t/N}$ where $\lambda := \sum_j h_j$ and N refers to the number of iterations of the random sampling. Here, the error is quantified by*

$$\frac{1}{2} \|\mathcal{F}_{\text{target}} - \mathcal{F}_{\text{approx}}\|_{\diamond}, \quad (\text{C1})$$

where $\mathcal{F}_{\text{target}}(\rho) := e^{-iHt}\rho e^{iHt}$ and $\mathcal{F}_{\text{approx}}$ is the average quantum operation simulated by the qDRIFT protocol.

The proof of this Lemma is provided in Ref. [8]. In particular, if N is chosen as $N(\lambda, t, 2\epsilon)$ (as defined in Eq. (4)), then the error in terms of Eq. (C1) is bounded from above by ϵ , i.e.,

$$\frac{2\lambda^2 t^2}{N(\lambda, t, 2\epsilon)} e^{2\lambda t/N(\lambda, t, 2\epsilon)} \leq 2\lambda^2 t^2 \cdot \left(\frac{5\lambda^2 t^2}{\epsilon} \right)^{-1} e^{2\lambda t \cdot (5\lambda t/2)^{-1}} = \frac{2\epsilon}{5} e^{4/5} < \epsilon. \quad (\text{C2})$$

Moreover, making use of Eqs. (B3) and (B4), it follows that the error in terms of Eq. (1), namely

$$\sup_{\substack{|\psi\rangle \in \mathcal{H} \otimes \mathcal{H}' \\ \|\langle \psi | \|=1 \\ \dim \mathcal{H}'}} \|\mathcal{F}_{\text{target}} \otimes \mathcal{I}_{\mathcal{H}'}(|\psi\rangle \langle \psi|) - \mathcal{F}_{\text{approx}} \otimes \mathcal{I}_{\mathcal{H}'}(|\psi\rangle \langle \psi|)\|_1 \quad (\text{C3})$$

is upper bounded by twice that of Eq. (C1) and can therefore be upper bounded by ϵ by choosing the iteration number as $N(\lambda, t, \epsilon)$.

2. Definition of g_f in Fourier Series Simulation [Subroutine 2, Eq. (7)]

The first step in the Fourier Series Simulation part of our UHET algorithm is to modify the desired transformation function f to a suitable periodically smooth one \tilde{f} , which is in turn defined in terms of the function g below [see Eq. (7)]:

$$g_f(x) := C_1 \cos(\pi x) + S_1 \sin(\pi x) + \frac{1}{2} S_2 \sin(2\pi x) + C_2 \cos(2\pi x) + C_3 \cos(3\pi x) + \frac{1}{3} S_3 \sin(3\pi x) + \frac{1}{4} S_4 \sin(4\pi x) + C_4 \cos(4\pi x), \quad (\text{C4})$$

where the coefficients $C_1, C_2, C_3, C_4, S_1, S_2, S_3, S_4$ are defined succinctly in terms of the coefficient matrix

$$\Phi := \begin{pmatrix} 9/16 & 1/16 & -9/16 & -1/16 \\ 2/3 & 1/24 & 2/3 & 1/24 \\ -1/16 & -1/16 & 1/16 & 1/16 \\ -1/6 & -1/24 & -1/6 & -1/24 \end{pmatrix} \quad (\text{C5})$$

as

$$(C_1, C_2, C_3, C_4)^T := \Phi \cdot \left(f(-1), \frac{4f^{(2)}(-1)}{\pi^2}, f(1), \frac{4f^{(2)}(1)}{\pi} \right)^T, \\ (S_1, S_2, S_3, S_4)^T := \Phi \cdot \left(\frac{2f^{(1)}(-1)}{\pi}, \frac{8f^{(3)}(-1)}{\pi^3}, \frac{2f^{(1)}(1)}{\pi}, \frac{8f^{(3)}(1)}{\pi^3} \right)^T. \quad (\text{C6})$$

3. Error Analysis of Fourier Series Simulation (Subroutine 2)

Here, we rigorously analyze the performance of Subroutine 2. In particular, we prove the following Theorem:

Theorem 1. *Subroutine 2 outputs $e^{-if(H_0)t} |\psi\rangle$ with an error of at most ϵ . Here, the error is defined as:*

$$\sup_{\substack{\dim(\mathcal{H}') \\ |\psi\rangle \in \mathcal{H} \otimes \mathcal{H}' \\ \|\psi\rangle\|=1}} \|\mathcal{G} \otimes \mathcal{I}_{\mathcal{H}'}(|\psi\rangle\langle\psi|) - \sum_j p_j (\mathcal{G}_j \otimes \mathcal{I}_{\mathcal{H}'})(|\psi\rangle\langle\psi|)\|_1, \quad (\text{C7})$$

where $\mathcal{G}(\rho) := e^{-if(H_0)t} \rho e^{if(H_0)t}$, j labels the tuple of all random indices k chosen in N iterations, p_j refers to the probability that j is chosen, which leads to the particular quantum operation \mathcal{G}_j being simulated, and \mathcal{H}' is an auxiliary system of arbitrary dimension.

We prove this theorem as follows. First, we decompose the error into two contributions: that of approximating the function \tilde{f} via its (truncated) Fourier series and that of the qDRIFT protocol itself. We then upper bound each error to derive an upper bound for the total error of the subroutine.

Proof: First, we define three quantum operations $\mathcal{G}_1, \mathcal{G}_2, \mathcal{G}_3 : \mathcal{L}(\mathcal{H}_c \otimes \mathcal{H}) \rightarrow \mathcal{L}(\mathcal{H}_c \otimes \mathcal{H})$:

$$\begin{aligned} \mathcal{G}_1(\rho) &:= e^{-i(X \otimes f(H_0))t} \rho e^{i(X \otimes f(H_0))t} \\ \mathcal{G}_2(\rho) &:= e^{-i(X \otimes \tilde{f}_K(H_0))t} \rho e^{i(X \otimes \tilde{f}_K(H_0))t} \\ \mathcal{G}_3 &:= \sum_j p_j \mathcal{G}'_j. \end{aligned} \quad (\text{C8})$$

where $\tilde{f}_K(x) := \sum_{k=-K}^K \tilde{c}_k e^{ik\pi(x+1)/2}$ is the truncated Fourier representation of f (which is a real function due to $\tilde{c}_{-k} = \tilde{c}_k^*$) and $\mathcal{G}'_j : \mathcal{L}(\mathcal{H}_c \otimes \mathcal{H}) \rightarrow \mathcal{L}(\mathcal{H}_c \otimes \mathcal{H})$ is the quantum operation simulated between steps 5 and 9 of Subroutine 2. By applying \mathcal{G}_1 to the initial state $|+\rangle \otimes |\psi\rangle$ and finally tracing over the control Hilbert space \mathcal{H}_c , one yields the desired transformation, i.e., the ideal dynamics. The expression \mathcal{G}_2 corresponds to the simulated dynamics of a truncated Fourier series in the absence of any Trotterization error (i.e., a perfectly accurate simulation of the finite Fourier series). Lastly, \mathcal{G}_3 denotes the actual dynamics simulated in Subroutine 2, which includes errors due to both finite Fourier series cutoff and Trotterization.

Consider the norm E defined as

$$E(\mathcal{F}) := \sup_{\substack{\dim(\mathcal{H}') \\ |\psi\rangle \in \mathcal{H}_c \otimes \mathcal{H} \otimes \mathcal{H}' \\ \|\psi\rangle\|=1}} \|\mathcal{F} \otimes \mathcal{I}_{\mathcal{H}'}(|\psi\rangle\langle\psi|)\|_1, \quad (\text{C9})$$

for any quantum operation $\mathcal{F} : \mathcal{L}(\mathcal{H}_c \otimes \mathcal{H}) \rightarrow \mathcal{L}(\mathcal{H}_c \otimes \mathcal{H})$. The difference $E(\mathcal{G}_3 - \mathcal{G}_1)$, therefore quantifies the error between the simulated dynamics and the ideal case.

Since \mathcal{G}_3 is a qDRIFT protocol approximating the ideal dynamics by simulating a Hamiltonian $X \otimes \tilde{f}_K(H_0)$ with finite cutoff number K as shown in Eq. (10), it follows from Lemma 2 that $E(\mathcal{G}_3 - \mathcal{G}_2) = \epsilon/2$ (since the precision is chosen as $\epsilon/2$). Furthermore, we can make use of the identity $\|\langle\beta| \langle\beta| - \langle\gamma| \langle\gamma|\|_1 = 2\sqrt{1 - |\langle\beta|\gamma\rangle|^2}$ (see, e.g., Eq. (1.186) of [44]) where $|\beta\rangle, |\gamma\rangle$ are unit vectors in the same Hilbert space, as well as the triangle inequality to yield

$$\begin{aligned} E(\mathcal{G}_3 - \mathcal{G}_1) &\leq E(\mathcal{G}_3 - \mathcal{G}_2) + E(\mathcal{G}_2 - \mathcal{G}_1) \\ &\leq \frac{\epsilon}{2} + \sup_{\substack{\dim(\mathcal{H}') \\ |\psi\rangle \in \mathcal{H}_c \otimes \mathcal{H} \otimes \mathcal{H}' \\ \|\psi\rangle\|=1}} 2 \left[1 - |\langle\psi| e^{-iX \otimes (f(H_0) - \tilde{f}_K(H_0))t} \otimes I |\psi\rangle|^2 \right]^{1/2}. \end{aligned} \quad (\text{C10})$$

We now lower bound the r.h.s. by decomposing $|\psi\rangle =: \sum_{s,m} a_{s,m} |s\rangle |E_m\rangle |\psi_{s,m}\rangle$ ($\sum_{s,m} |a_{s,m}|^2 = 1$), where E_m and $|E_m\rangle$ are the eigenvalues and eigenvectors of H_0 respectively, $|s\rangle \in \{|+\rangle, |-\rangle\}$ are eigenvectors of the operator X in

\mathcal{H}_c , and $|\psi_{s,m}\rangle$ is a unit vector in \mathcal{H}' . With this, it follows that $|\langle\psi|e^{-iX\otimes(f(H_0)-\tilde{f}_K(H_0))t}\otimes I|\psi\rangle|$ is lower bounded as

$$\begin{aligned}
|\langle\psi|e^{-iX\otimes(f(H_0)-\tilde{f}_K(H_0))t}\otimes I|\psi\rangle| &= \left| \sum_{s,m} |a_{s,m}|^2 e^{-i\langle s|X|s\rangle \cdot (f(E_m)-\tilde{f}_K(E_m))t} \right| \\
&\geq \left| \sum_{s,m} |a_{s,m}|^2 \operatorname{Re}(e^{-i\langle s|X|s\rangle \cdot (f(E_m)-\tilde{f}_K(E_m))t}) \right| \\
&\geq \left| \sum_{s,m} |a_{s,m}|^2 \cos(\tfrac{1}{2}R(f-\tilde{f}_K)t) \right| \\
&= \cos(\tfrac{1}{2}R(f-\tilde{f}_K)t),
\end{aligned} \tag{C11}$$

where $R(g) := 2 \max_{x \in [-1,1]} |g(x)|$ for a function $g : [-1,1] \rightarrow \mathbb{R}$. Substituting Eq. (C11) into Eq. (C10) and invoking Eq. (8), we finally have

$$E(\mathcal{G}_3 - \mathcal{G}_1) \leq \frac{\epsilon}{2} + 2 \sin[R(f-\tilde{f}_K)t/2] \leq \frac{\epsilon}{2} + R(f-\tilde{f}_K)t \leq \frac{\epsilon}{2} + \frac{\epsilon}{2} = \epsilon. \tag{C12}$$

By substituting back to Eq. (C9), we have that

$$\begin{aligned}
\epsilon \geq E(\mathcal{G}_3 - \mathcal{G}_1) &\geq \sup_{\substack{|\psi\rangle \in \mathcal{H}_c \otimes \mathcal{H} \otimes \mathcal{H}' \\ \|\psi\| = 1 \\ \dim \mathcal{H}'}} \|\operatorname{tr}_{\mathcal{H}_c}[(\mathcal{G}_3 - \mathcal{G}_1) \otimes \mathcal{I}_{\mathcal{H}'}](|\psi\rangle\langle\psi|)\|_1 \\
&\geq \sup_{\substack{|\psi\rangle \in \mathcal{H} \otimes \mathcal{H}' \\ \|\psi\| = 1 \\ \dim \mathcal{H}'}} \|\operatorname{tr}_{\mathcal{H}_c}[(\mathcal{G}_3 - \mathcal{G}_1) \otimes \mathcal{I}_{\mathcal{H}'}](|+\rangle\langle+| \otimes |\psi\rangle\langle\psi|)\|_1,
\end{aligned} \tag{C13}$$

which is equal to the expression in Eq. (C7), therefore asserting our claim. \square

4. Fourier Series Convergence

Lemma 3. *For arbitrary $f : [-1,1] \rightarrow \mathbb{R}$ which belongs to class C^3 with $f^{(4)}$ being piecewise C^2 , the function \tilde{f} defined in Eq. (7) is periodically 4-smooth.*

Proof: We will now demonstrate that \tilde{f} belongs to class C^3 , $\tilde{f}^{(j)}(1) = \tilde{f}^{(j)}(-1)$ ($j \in \{0, 1, 2, 3\}$), and $\tilde{f}^{(4)}$ is piecewise C^2 . Let $S \subset [-1,1]$ denote the finite set of points outside of which $f^{(4)}$ is defined and is continuously differentiable. It is straightforward to see that $\tilde{f}^{(4)}$ is piecewise C^2 with exceptional points $x \in \tilde{S} \cup \{0\}$ where $\tilde{S} := \{(x+1)/2 \mid x \in S\}$. Thus it suffices to show that \tilde{f} belongs to class C^3 and $\tilde{f}^{(j)}(1) = \tilde{f}^{(j)}(-1) \forall j \in \{0, 1, 2, 3\}$. This follows directly from the following equations, which in turn follow from the definition of g_f

$$\begin{aligned}
\frac{d^j}{dx^j} g_f(x)|_{x=0} &= \frac{d^j}{dx^j} f(2x-1)|_{x=0} \\
\frac{d^j}{dx^j} g_f(x)|_{x=-1} &= \frac{d^j}{dx^j} f(2x-1)|_{x=1},
\end{aligned} \tag{C14}$$

where $j \in \{0, 1, 2, 3\}$. \square

We now move on to analyze the convergence rate of the Fourier series being simulated, which leads to a relationship between the allowed error ϵ and the truncation number K . Whenever a function $g : [-1,1] \rightarrow \mathbb{R}$ is piecewise smooth, its Fourier series converges (except for at a finite number of discontinuities; see, e.g., Ref. [45]). In general, for a periodically J -smooth function, the rate of convergence can be determined via the following lemma.

Lemma 4. *For any periodically J -smooth function $g : [-1,1] \rightarrow \mathbb{R}$, its Fourier coefficients $c_k := (1/2) \int_{-1}^1 dx g(x) e^{-i\pi kx}$ converge at the rate:*

$$\lim_{|k| \rightarrow \infty} |c_k| |k|^J < \infty. \tag{C15}$$

In particular, if g is strictly periodically J -smooth, then

$$\sum_{k=K}^{\infty} |c_k|^2 = \Omega(K^{-(2J+1)}) \quad \text{and} \quad \sum_{k=\infty}^{-K} |c_k|^2 = \Omega(K^{-(2J+1)}) \quad (\text{C16})$$

hold for $K > 0$.

Proof: If g is periodically J -smooth, then each coefficient c_k can be rewritten using the following Fourier asymptotic coefficient expansion method [46]:

$$\begin{aligned} c_k &= \frac{1}{2} \int_{-1}^1 dx g(x) e^{-i\pi k x} \\ &= \frac{1}{2} \frac{i}{\pi k} \left[(-1)^k \{g(1) - g(-1)\} - \int_{-1}^1 dx g^{(1)}(x) e^{-i\pi k x} \right] \\ &= \dots = \frac{1}{2} \sum_{j=0}^{J-1} (-1)^{k+j} \left(\frac{i}{\pi k} \right)^{j+1} \left\{ g^{(j)}(1) - g^{(j)}(-1) \right\} + \frac{(-1)^J}{2} \left(\frac{i}{\pi k} \right)^J \int_{-1}^1 dx g^{(J)}(x) e^{-i\pi k x}. \end{aligned} \quad (\text{C17})$$

The final line follows by successively applying integration by parts on the relevant integral term; this technique is valid since the interval of integration $[-1, 1]$ can be decomposed into smaller intervals $[x_0, x_1], \dots, [x_{n-1}, x_n]$ (with $x_0 = -1$ and $x_n = 1$) between the exceptional points, upon which all derivatives of g are C^2 by assumption. The rightmost part of Eq. (C17) is $O(1/k^J)$ because all of the terms in the summation vanish due to periodicity and the remaining integral in the second term is bounded. This proves the first part of our claim, i.e., the rate of convergence according to Eq. (C15).

Furthermore, when g is *strictly* periodically J -smooth, then the integral term on the r.h.s. of Eq. (C17) can be rewritten as:

$$\begin{aligned} \int_{-1}^1 dx g^{(J)}(x) e^{-i\pi k x} &= \int_{-1}^{x_1} dx g^{(J)}(x) e^{-i\pi k x} + \dots + \int_{x_{n-1}}^1 dx g^{(J)}(x) e^{-i\pi k x} \\ &= \frac{i}{\pi k} \left[e^{i\pi k} \{g^{(J)}(1^-) - g^{(J)}(-1^+)\} + e^{-i\pi k x_1} \{g^{(J)}(x_1^-) - g^{(J)}(x_1^+)\} + \dots + e^{-i\pi k x_{n-1}} \{g^{(J)}(x_{n-1}^-) - g^{(J)}(x_{n-1}^+)\} \right] - \frac{i}{\pi k} \int_{-1}^1 dx g^{(J+1)}(x) e^{-i\pi k x}. \end{aligned} \quad (\text{C18})$$

By rewriting the final integral similarly, we can show that this expression is of $O(1/k^2)$. Specifically, let us define g_m for $m \in \{0, \dots, n-1\}$ as $g_0 := g^{(J)}(1^-) - g^{(J)}(-1^+)$ and $g_m := g^{(J)}(x_m^-) - g^{(J)}(x_m^+)$ for $m > 1$; with this, Eq. (C18) can be expressed succinctly as $\frac{i}{\pi k} \sum_{m=0}^{n-1} g_m e^{-i\pi k x_m} + O(1/k^2)$. Substituting Eq. (C18) into Eq. (C17) then yields

$$c_k = \frac{(-1)^J}{2} \left(\frac{i}{\pi k} \right)^{J+1} \left(\sum_{m=0}^{n-1} g_m e^{-i\pi k x_m} \right) + O(k^{-(J+2)}). \quad (\text{C19})$$

In order to reach the desired claim, we now seek to lower bound $|c_k|$. For any $k_0 \in \mathbb{Z}$ and $M > 0$, we have that

$$\begin{aligned} \sum_{k=k_0}^{k_0+M-1} \left| \sum_{m=0}^{n-1} g_m e^{-i\pi k x_m} \right|^2 &= \sum_{k=k_0}^{k_0+M-1} \left[\sum_{m=0}^{n-1} |g_m|^2 + \sum_{m_1 \neq m_2} g_{m_1}^* g_{m_2} e^{-i\pi k(x_{m_2} - x_{m_1})} \right] \\ &\geq \sum_{k=k_0}^{k_0+M-1} \sum_{m=0}^{n-1} |g_m|^2 - \left| \sum_{m_1 \neq m_2} g_{m_1}^* g_{m_2} \sum_{k=k_0}^{k_0+M-1} e^{-i\pi k(x_{m_2} - x_{m_1})} \right| \\ &\geq \sum_{k=k_0}^{k_0+M-1} \sum_{m=0}^{n-1} |g_m|^2 - \sum_{m_1 \neq m_2} |g_{m_1}| |g_{m_2}| \left| \sum_{k=k_0}^{k_0+M-1} e^{-i\pi k(x_{m_2} - x_{m_1})} \right| \\ &\geq M \sum_{m=0}^{n-1} |g_m|^2 - \frac{1}{\Delta} \left(\sum_{m=0}^{n-1} |g_m| \right)^2, \end{aligned} \quad (\text{C20})$$

where $\Delta := \sin \left[\frac{\pi}{2} \left\{ \min_{0 \leq m_1 < m_2 \leq n-1} (x_{m_2} - x_{m_1}, 2 - (x_{m_2} - x_{m_1})) \right\} \right] > 0$. The last inequality above follows by evaluating the geometric series and then bounding it appropriately, i.e., $|\sum_{k=k_0}^{k_0+M-1} e^{-i\pi k q}| = |(e^{-i\pi(k_0+M)q} - e^{-i\pi k_0 q})/(e^{-i\pi q} - 1)| \leq 2/|e^{-i\pi q} - 1| = 1/\sin(\pi q/2)$ for $q > 0$. Since $1/\sin(\pi q/2) = 1/\sin(\pi(2-q)/2)$ and $1/\sin(\pi q/2)$ is a decreasing function in $0 < q \leq 1$, it follows that $|\sum_{k=k_0}^{k_0+M-1} e^{-i\pi k(x_{m_2} - x_{m_1})}|$ can be upper bounded by $1/\Delta$ for $m_1 \neq m_2$.

In particular, when M is chosen as $M' := \text{ceil}\{[2(\sum_{m=0}^{n-1} |g_m|^2)]/[\Delta(\sum_{m=0}^{n-1} |g_m|^2)]\}$, the last line of Eq. (C20) yields

$$\begin{aligned} M' \sum_{m=0}^{n-1} |g_m|^2 - \frac{1}{\Delta} \left(\sum_{m=0}^{n-1} |g_m| \right)^2 &= M' \left[\sum_{m=0}^{n-1} |g_m|^2 - \frac{1}{M' \Delta} \left(\sum_{m=0}^{n-1} |g_m| \right)^2 \right] \\ &\geq M' \left[\sum_{m=0}^{n-1} |g_m|^2 - \frac{1}{\Delta} \left(\sum_{m=0}^{n-1} |g_m| \right)^2 \cdot \frac{\Delta(\sum_{m=0}^{n-1} |g_m|^2)}{2(\sum_{m=0}^{n-1} |g_m|)^2} \right] \\ &= M' \cdot \frac{1}{2} \sum_{m=0}^{n-1} |g_m|^2. \end{aligned} \tag{C21}$$

Therefore, the average value of $\left| \sum_{m=0}^{n-1} g_m e^{-i\pi k x_m} \right|^2$ for $k \in \{k_0, \dots, k_0 + M' - 1\}$ is lower bounded by $(\sum_{m=0}^{n-1} |g_m|^2)/2$. Since there exists at least one $k \in \{k_0, \dots, k_0 + M' - 1\}$ such that $|\sum_{m=0}^{n-1} g_m e^{-i\pi k x_m}|^2 \geq (\sum_{m=0}^{n-1} |g_m|^2)/2$ for all $k_0 > 0$ and the $O(k^{-(J+2)})$ term converges to 0 quicker than $1/k^{J+1}$, there exists constants $C > 0$ and $k'_0 > 0$ such that for all $k_0 > k'_0$, there exists at least one $k \in \{k_0, \dots, k_0 + M' - 1\}$ such that $|c_k| > C/k^{J+1} \geq C/(k_0 + M' - 1)^{J+1}$. Since $\sum_{k=K}^{\infty} |c_k|^2 = \sum_{l=1}^{\infty} \sum_{j=0}^{M'-1} |c_{K+(l-1)M'+j}|^2 \geq \sum_{l=1}^{\infty} |C/(K + lM' - 1)^{J+1}|^2 = \Theta(K^{-(2J+1)})$ for sufficiently large K , it follows that $\sum_{k=K}^{\infty} |c_k|^2 = \Omega(K^{-(2J+1)})$ and $\sum_{k=\infty}^{-K} |c_k|^2 = \Omega(K^{-(2J+1)})$ for $K > 0$, asserting the second part of our claim. \square

Appendix D: Compiled UHET Algorithm

1. Proof of Eq. (17) for the Compiled Algorithm (Algorithm 4)

Here, we prove the validity of Eq. (17) of the main text. To be precise with notation, we denote the order of matrix multiplication as $\Pi_{j=1}^n M_j := M_1 \cdots M_n$. Formally, we show:

Lemma 5. *Let $k \in \mathbb{Z}$, $N \in \mathbb{Z}_{\geq 0}$, and $j := (\vec{v}_1, \dots, \vec{v}_N) \in (\{0, 1, 2, 3\}^n)^N$. For any unitary $W_{k,j}^{(N)}$ defined as per Eq. (18), namely*

$$W_{k,j}^{(N)} := \left[\prod_{m=1}^N \mathbf{ctrl}(\sigma_{\vec{v}_m})(I \otimes e^{-i\frac{k\pi}{2N}H}) \mathbf{ctrl}(\sigma_{\vec{v}_m}) \right] (e^{-i\frac{k\pi}{4}Z} \otimes I), \quad (\text{D1})$$

there exist parameters $A_{k,N} > 0$ and $\theta_{k,N} \in [0, 2\pi)$ such that

$$\begin{aligned} & \left(\frac{1}{4} \right)^{nN} \sum_{\vec{v}_1, \dots, \vec{v}_N} (W_{k,j}^{(N)})^\dagger ([\cos \phi_k X - \sin \phi_k Y] \otimes I) W_{k,j}^{(N)} \\ &= A_{k,N} (e^{i\frac{\theta_{k,N}}{2}Z} \otimes I) \begin{pmatrix} 0 & e^{i\phi_k} e^{i\frac{k\pi}{2}(H_0+I)} \\ e^{-i\phi_k} e^{-i\frac{k\pi}{2}(H_0+I)} & 0 \end{pmatrix} (e^{-i\frac{\theta_{k,N}}{2}Z} \otimes I), \end{aligned} \quad (\text{D2})$$

where H_0 is the traceless part of H , i.e., $H_0 := H - (\text{tr}[H]/2^n)I$. Furthermore, $A_{k,N}$ and $\theta_{k,N}$ satisfy

$$1 - \frac{\pi^2 k^2}{8N} \leq A_{k,N} \leq 1 \quad \text{and} \quad |\theta_{k,N}| \leq \frac{\pi^3 k^3}{32N^2} \quad (N \geq 0.625\pi k). \quad (\text{D3})$$

Proof: For the special case $N = 0$ (in which case we employ the convention that for any matrices $\{X_m\}_m$, we have $\Pi_{m=1}^{N=0} X_m = I$), it is straightforward to verify that $(A_{k,N}, \theta_{k,N}) = (1, 0)$ satisfies Eq. (D2); thus, the remainder of the proof concerns $N > 0$.

For convenience, we define

$$\Upsilon_{k,N,j} := \prod_{m=1}^N \mathbf{ctrl}(\sigma_{\vec{v}_m})(I \otimes e^{-i\frac{k\pi}{2N}H}) \mathbf{ctrl}(\sigma_{\vec{v}_m}) = \begin{pmatrix} e^{-i\frac{k\pi}{2}H} & 0 \\ 0 & \prod_{m=1}^N \sigma_{\vec{v}_m} e^{-i\frac{k\pi}{2N}H} \sigma_{\vec{v}_m} \end{pmatrix}. \quad (\text{D4})$$

With this, Eq. (D2) can be rewritten as

$$\begin{aligned} & \left(\frac{1}{4} \right)^{nN} \sum_{\vec{v}_1, \dots, \vec{v}_N} \Upsilon_{k,N,j}^\dagger ([\cos \phi_k X - \sin \phi_k Y] \otimes I) \Upsilon_{k,N,j} \\ &= \left(\frac{1}{4} \right)^{nN} \sum_{\vec{v}_1, \dots, \vec{v}_N} \begin{pmatrix} 0 & e^{i\phi_k} e^{i\frac{k\pi}{2}H} (\prod_{l=1}^N \sigma_{\vec{v}_l} e^{-i\frac{k\pi}{2N}H} \sigma_{\vec{v}_l}) \\ e^{-i\phi_k} (\prod_{l=1}^N \sigma_{\vec{v}_l} e^{-i\frac{k\pi}{2N}H} \sigma_{\vec{v}_l})^\dagger e^{-i\frac{k\pi}{2}H} & 0 \end{pmatrix} \\ &= \begin{pmatrix} 0 & e^{i\phi_k} e^{i\frac{k\pi}{2}H} [\prod_{l=1}^N \{(\frac{1}{4})^n \sum_{\vec{v}_l} \sigma_{\vec{v}_l} e^{-i\frac{k\pi}{2N}H} \sigma_{\vec{v}_l}\}] \\ e^{-i\phi_k} [\prod_{l=1}^N \{(\frac{1}{4})^n \sum_{\vec{v}_l} \sigma_{\vec{v}_l} e^{-i\frac{k\pi}{2N}H} \sigma_{\vec{v}_l\}}]^\dagger e^{-i\frac{k\pi}{2}H} & 0 \end{pmatrix} \\ &= \left(\frac{1}{2} \right)^{nN} \begin{pmatrix} 0 & e^{i\phi_k} \{\text{tr}[e^{-i\frac{k\pi}{2N}H}]\}^N e^{i\frac{k\pi}{2}H} \\ e^{-i\phi_k} \{\text{tr}[e^{-i\frac{k\pi}{2N}H}]\}^N e^{-i\frac{k\pi}{2}H} & 0 \end{pmatrix}, \end{aligned} \quad (\text{D5})$$

where we have made use of the matrix identity $\sum_{\vec{v}_1, \dots, \vec{v}_N} (\prod_{l=1}^N M_{\vec{v}_l}) = \prod_{l=1}^N (\sum_{\vec{v}_l} M_{\vec{v}_l})$. By now invoking $\{\text{tr}(e^{-i\frac{\pi k}{2N}H})\}^N e^{i\frac{\pi k}{2}H} = \{\text{tr}(e^{-i\frac{\pi k\alpha}{2N}} e^{-i\frac{\pi k}{2N}H_0})\}^N e^{i\frac{\pi k\alpha}{2}} e^{i\frac{\pi k}{2}H_0} = \{\text{tr}(e^{-i\frac{\pi k}{2N}H_0})\}^N e^{i\frac{\pi k}{2}H_0}$, where $\alpha := \text{tr}(H)/2^n$, the final line of Eq. (D5) can be rewritten as

$$\begin{aligned} & \left(\frac{1}{2} \right)^{nN} \begin{pmatrix} 0 & e^{i\phi_k} \{\text{tr}(e^{-i\frac{k\pi}{2N}H})\}^N e^{i\frac{k\pi}{2}H} \\ e^{-i\phi_k} \{\text{tr}(e^{-i\frac{k\pi}{2N}H})\}^N e^{-i\frac{k\pi}{2}H} & 0 \end{pmatrix} \\ &= \left(\frac{1}{2} \right)^{nN} \begin{pmatrix} 0 & e^{i\phi_k} \{\text{tr}(e^{-i\frac{\pi k}{2N}H_0})\}^N e^{i\frac{\pi k}{2}H_0} \\ e^{-i\phi_k} \{\text{tr}(e^{-i\frac{\pi k}{2N}H_0})\}^N e^{-i\frac{\pi k}{2}H_0} & 0 \end{pmatrix}. \end{aligned} \quad (\text{D6})$$

Thus, by setting

$$A_{k,N} e^{i\theta_{k,N}} := \left[\frac{\text{tr}(e^{-i\frac{\pi k}{2N} H_0})}{2^n} \right]^N, \quad (\text{D7})$$

where $A_{k,N} \geq 0$ and $\theta_{k,N} \in \mathbb{R}$, we obtain

$$\left(\frac{1}{4} \right)^{nN} \sum_{\vec{v}_1, \dots, \vec{v}_N} \Upsilon_{k,N,j}^\dagger ([\cos \phi_k X - \sin \phi_k Y] \otimes I) \Upsilon_{k,N,j} = A_{k,N} \begin{pmatrix} 0 & e^{i(\phi_k + \theta_{k,N})} e^{i\frac{k\pi}{2} H_0} \\ e^{-i(\phi_k + \theta_{k,N})} e^{-i\frac{k\pi}{2} H_0} & 0 \end{pmatrix}, \quad (\text{D8})$$

which is equivalent to Eq. (D2).

For the second part of the claim, note that when H_0 is diagonalized as $H_0 = \sum_{j=0}^{2^n-1} E_j |j\rangle\langle j|$, then the expression $\{\text{tr}(e^{-i\frac{\pi k}{2N} H_0})/2^n\}^N$ reduces to

$$\{\text{tr}(e^{-i\frac{\pi k}{2N} H_0})/2^n\}^N = \left(\frac{\sum_{j=0}^{2^n-1} e^{-i\frac{\pi k}{2N} E_j}}{2^n} \right)^N = \left(\frac{\sum_{j=0}^{2^n-1} \cos(\frac{\pi k}{2N} E_j) - i \sum_{j=0}^{2^n-1} \sin(\frac{\pi k}{2N} E_j)}{2^n} \right)^N, \quad (\text{D9})$$

from which $A_{k,N} \leq 1$ follows. Further invoking $|E_j| \leq 1$ (which follows from our assumption that $\|H_0\|_{\text{op}} = 1$) and the inequality $\cos(x) \geq 1 - x^2/2$ ($x \in \mathbb{R}$), it follows that $\cos(\frac{\pi k}{2N} E_j) \geq \cos(\frac{\pi k}{2N}) \geq 1 - \frac{1}{2} (\frac{\pi k}{2N})^2$ and subsequently

$$A_{k,N} \geq \left| \frac{\sum_{j=0}^{2^n-1} \cos(\frac{\pi k}{2N} E_j)}{2^n} \right|^N \geq \left[1 - \frac{1}{2} \left(\frac{\pi k}{2N} \right)^2 \right]^N \geq 1 - \frac{\pi^2 k^2}{8N}. \quad (\text{D10})$$

Finally, due to the fact that $\sum_{j=0}^{2^n-1} E_j = 0$ (which follows from $\text{tr}(H_0) = 0$) as well as the inequality $|\sin x - x| \leq (|x|^3/6)$ ($x \in \mathbb{R}$), we have

$$\left| \sum_{j=0}^{2^n-1} \sin \left(\frac{\pi k}{2N} E_j \right) \right| = \left| \sum_{j=0}^{2^n-1} \left[\sin \left(\frac{\pi k}{2N} E_j \right) - \frac{\pi k}{2N} E_j \right] \right| \leq \frac{1}{6} \sum_{j=0}^{2^n-1} \left| \frac{\pi k}{2N} E_j \right|^3 \leq \frac{2^n}{6} \left(\frac{\pi k}{2N} \right)^3. \quad (\text{D11})$$

Then, since $\frac{1}{2^n} \sum_{j=0}^{2^n-1} \cos(\frac{\pi k}{2N} E_j) \geq \frac{1}{2^n} \sum_{j=0}^{2^n-1} \cos(\frac{\pi k}{2N}) = \cos(\frac{\pi k}{2N}) \geq 1 - \frac{1}{2} (\frac{\pi k}{2N})^2$, it follows that $\theta_{k,N}$ is upper bounded by

$$|\theta_{k,N}| \leq N \tan^{-1} \left[\left\{ \frac{1}{6} \left(\frac{\pi k}{2N} \right)^3 \right\} \left\{ 1 - \frac{1}{2} \left(\frac{\pi k}{2N} \right)^2 \right\}^{-1} \right] \leq \frac{\pi^3 k^3}{32N^2} \quad (N \geq 0.625\pi k). \quad (\text{D12})$$

The final inequality follows from $\tan^{-1}[\frac{1}{6}x^3/(1 - \frac{1}{2}x^2)] \leq \frac{1}{4}x^3$ ($0 \leq x \leq 0.8$). \square

2. Parameter Estimation for Compiled Algorithm (Algorithm 4)

The compiled UHET Algorithm 4 makes use of ‘‘correction’’ parameters $(\hat{A}_k, \hat{\theta}_k)$ to compensate the error of the main process and reduce the time complexity from that of Algorithm 3. Here, we will develop two subroutines, namely Subroutine D6 and D7, that allow one to estimate such parameters without any knowledge of the seed Hamiltonian. Subroutine D7 is used in step 2 of Subroutine D6 to generate a state $|\phi(N', l, k\pi/N', 25k, \Phi)\rangle$ that is used for robust phase estimation, from which the parameters of interest can be estimated.

Subroutine D6 Generating parameters $(\hat{A}_l, \hat{\theta}_l)$

Input:

- A finite number of queries to a black-box Hamiltonian dynamics $e^{\pm iH\tau}$ of a seed Hamiltonian H with $\tau > 0$ on an n -qubit system \mathcal{H}
- Parameter $l \in \mathbb{Z}_{>0}$
- Allowed error $\epsilon > 0$
- Time $t > 0$

Output: Estimates $\hat{A}_l > \frac{1}{2}$ and $\hat{\theta}_l \in [0, 2\pi)$ of $A_{l,10l^2}$ and $\theta_{l,10l^2}$, respectively, with root mean square error of $|1 - (A_{l,10l^2} e^{i\theta_{l,10l^2}}) / (\hat{A}_l e^{i\hat{\theta}_l})|$ that is upper bounded by ϵ/t .

Time complexity: $\Theta(l^2 t^3 n / \epsilon^3)$

Procedure:

1: **for** $\Phi \in \{0, \frac{\pi}{2}\}$ **do**

2: Perform robust phase estimation [39] with allowed root mean square of error set as $\epsilon/(\sqrt{2}t)$. Here, success of $|0\rangle$ -measurements and $|+\rangle$ -measurements are defined as obtaining outcomes for $|0\rangle \otimes I$ and $|+\rangle \otimes I$ when performing Z - and X -basis measurements respectively on the first qubit of the state $|\phi(N', l, k\pi/N', 25k, \Phi)\rangle$, where $N' := N(1, k\pi, 1/(4\sqrt{2}))$, generated by Subroutine D7. This provides an estimate \hat{v}_Φ .

3: **end for**

4: **if** $(1/2\pi)\sqrt{\hat{v}_0^2 + \hat{v}_{\pi/2}^2} \leq \frac{1}{2}$ **then**

5: Return to step 1

6: **end if**

7: Compute $\hat{A}_l, \hat{\theta}_l$ by

$$\begin{aligned}\hat{A}_l \cos(\hat{\theta}_l) &= \frac{1}{2\pi} \hat{v}_0 \\ \hat{A}_l \sin(\hat{\theta}_l) &= \frac{1}{2\pi} \hat{v}_{\pi/2}\end{aligned}$$

8: **Return** $(\hat{A}_l, \hat{\theta}_l)$

Step 2 of this routine makes use of the following subroutine to generate an appropriate state.

Subroutine D7 Generating a state used in Subroutine D6

Input:

- A finite number of queries to a black box Hamiltonian dynamics $e^{\pm iH\tau}$ of a seed Hamiltonian H with $\tau > 0$ on an n -qubit system \mathcal{H}
- Parameters $N, l, M \in \mathbb{Z}_{>0}$
- $\gamma \in [0, 1]$
- $\Phi \in [0, 2\pi)$

Output: A random state $|\phi(N, l, \gamma, M, \Phi)\rangle$

Time complexity: $\Theta(Nl^2 n M)$

Procedure:

1: Initialize:

$|\text{current}\rangle \leftarrow |0\rangle \otimes |0\rangle \in \mathcal{H}_c \otimes \mathcal{H}$

2: **for** $m \in \{1, \dots, N\}$ **do**

3: From $j' := \{\vec{u}_1, \dots, \vec{u}_{10l^2}\}$, $j'' := \{\vec{w}_1, \dots, \vec{w}_{l^2 M}\}$ where $\vec{u}_1, \dots, \vec{u}_{10l^2}, \vec{w}_1, \dots, \vec{w}_{l^2 M} \in \{0, 1, 2, 3\}^n$, and $s \in \{+1, -1\}$, uniformly randomly choose $j = (j', j'', s)$

4: $|\text{current}\rangle \leftarrow \widetilde{W}_{l,j,\Phi}(e^{-i\gamma Y} \otimes I) \widetilde{W}_{l,j,\Phi}^\dagger |\text{current}\rangle$ for

$$\widetilde{W}_{l,j,\Phi} := (e^{-i\frac{s\Phi}{2}Z} \otimes I) \left[\prod_{m''=1}^{l^2 M} \text{ctrl}(\sigma_{\vec{w}_{m''}})(I \otimes e^{i\frac{s\pi}{2lM}H}) \text{ctrl}(\sigma_{\vec{w}_{m''}}) \right] \left[\prod_{m'=1}^{10l^2} \text{ctrl}(\sigma_{\vec{u}_{m'}})(I \otimes e^{-i\frac{s\pi}{20l}H}) \text{ctrl}(\sigma_{\vec{u}_{m'}}) \right]$$

5: **end for**

6: **Return** $|\phi(N, l, \gamma, M, \Phi)\rangle := |\text{current}\rangle$

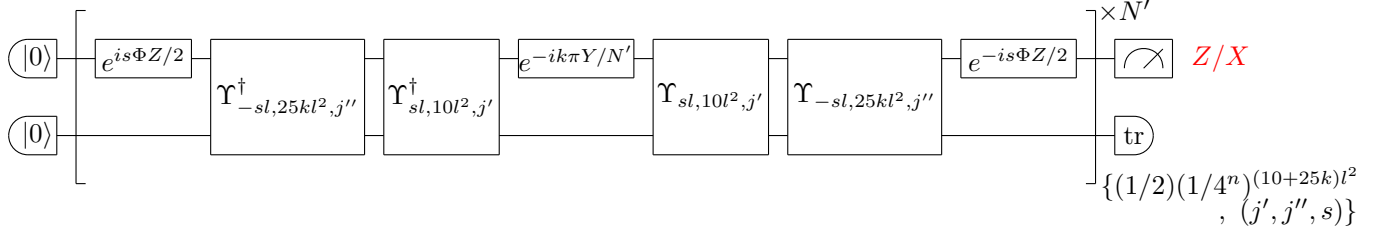


FIG. 12. *Compensation parameter estimation.*—The circuit used to obtain estimates (A_l, θ_l) that are subsequently used in Algorithm 4.

The time complexity of Subroutine D7 scales as (Number of iterations N) \times (The time complexity of $\widetilde{W}_{l,j,\Phi}$) $=N\times\Theta(l^2nM)=\Theta(Nl^2nM)$.

A circuit depiction of the combination of Subroutines D6 and D7 is provided in Fig. 12. In particular, the preparation of the state $|\phi(N', l, k\pi/N', 25k, \Phi)\rangle$ in Subroutine D7 corresponds to the part of Fig. 12 before the measurement, with M, γ set to $25k, k\pi/N'$ respectively. For many values of k , Subroutine D6 implements this circuit and performs appropriate measurements on the state in order to estimate $(\hat{A}_l, \hat{\theta}_l)$ via robust phase estimation [39]. We now formalize the validity of this algorithm and demonstrate its time complexity.

Theorem 2. *Subroutine D6 outputs estimates $(\hat{A}_l, \hat{\theta}_l)$ of the parameters $(A_{l,10l^2}, \theta_{l,10l^2})$ defined in Lemma 5 for $l > 0$ with a root mean square of $|1 - (A_{l,10l^2}e^{i\theta_{l,10l^2}})/(\hat{A}_l e^{i\hat{\theta}_l})|$ upper bounded by ϵ/t with a time complexity $\Theta(l^2t^3n/\epsilon^3)$.*

In order to prove Theorem 2, we combine the results of Lemma 5 with Lemma 6 below, which concerns the robust phase estimation procedure and is proven in Ref. [39]. We first show that steps 2 to 5 of Subroutine D7 generates the state $|\phi(N, l, \gamma, M, \Phi)\rangle$ by simulating a particular Hamiltonian that is proportional to \hat{v}_Φ [which is, in turn, a function of $(A_{l,10l^2}, \theta_{l,10l^2})$ and is defined below] via qDRIFT. We then show that the success probabilities of $|0\rangle$ -measurements and $|+\rangle$ -measurements for each k (respectively, denoted $(0, k)$ -measurements and $(+, k)$ -measurements in Lemma 6) differ from $\frac{1}{2}(1 + \cos(k\hat{v}_\Phi))$ and $\frac{1}{2}(1 + \sin(k\hat{v}_\Phi))$, respectively, at most by $\frac{1}{\sqrt{8}}$, demonstrating that \hat{v}_Φ can be well-estimated by robust phase estimation. Finally, we prove that $A_{l,10l^2}$ and $\theta_{l,10l^2}$ can be obtained with a root mean square of error smaller than or equal to ϵ/t .

Lemma 6 (Robust Phase Estimation [39]). *Let $k \in \mathbb{Z}_{>0}$. Suppose that one can perform two families of measurements, $(0, k)$ -measurements and $(+, k)$ -measurements, whose success probabilities for obtaining outcomes 0 and + respectively are given in terms of $\theta \in (-\pi, \pi]$ as*

$$\begin{aligned} (0, k)\text{-measurement: } p_{0,k}(\theta) &:= \frac{1 + \cos(k\theta)}{2} + \delta_0(k) \\ (+, k)\text{-measurement: } p_{+,k}(\theta) &:= \frac{1 + \sin(k\theta)}{2} + \delta_+(k), \end{aligned}$$

where $\delta_0(k)$ and $\delta_+(k)$ satisfy

$$\sup_k \{|\delta_0(k)|, |\delta_+(k)|\} =: \delta_{\sup} < \frac{1}{\sqrt{8}}.$$

Then for any allowed standard deviation $s > 0$, an estimate $\hat{\theta}$ of θ can be obtained with a root mean squared error smaller than or equal to s by a classical computation with time complexity $O(\text{poly}K)$. This computation is a function of the numbers of successful $(0, 2^{j-1})$ -measurements and $(+, 2^{j-1})$ -measurements ($j \in \{1, \dots, K\}$), with both measurement choices being implemented M_j times. Here, M_j and K are defined as

$$\begin{aligned} K &:= \text{ceil} \left[\log_2 \left(\frac{3\pi}{s} \right) \right] \\ M_j &:= F(\delta_{\sup})(3(K - j) + 1) \\ F(\delta_{\sup}) &:= \text{ceil} \left[\frac{\log \left(\frac{1}{2}(1 - \sqrt{8}\delta_{\sup}) \right)}{\log \left(1 - \frac{1}{2}(1 - \sqrt{8}\delta_{\sup})^2 \right)} \right]. \end{aligned} \tag{D13}$$

This lemma is proven in Ref. [39] (see Theorem 1 therein). We are now in a position to prove Theorem 2.

Proof of Theorem 2: To begin, note that steps 2 to 5 of Subroutine D7 simulates the dynamics $e^{-iH'}$ using qDRIFT for the Hamiltonian H' defined as

$$H' = \frac{N\gamma}{2} \left(\frac{1}{4} \right)^{(10+M)l^2} \sum_{\substack{\vec{u}_1, \dots, \vec{u}_{10l^2} \\ \vec{w}_1, \dots, \vec{w}_{l^2M} \\ s \in \{1, -1\}}} \widetilde{W}_{l,j,\Phi}(Y \otimes I) \widetilde{W}_{l,j,\Phi}^\dagger =: t \sum_j h_j H_j, \quad (\text{D14})$$

where $j := \{(\vec{u}_1, \dots, \vec{u}_{10l^2}), (\vec{w}_1, \dots, \vec{w}_{l^2M}), s\}$, $t := N\gamma$, $h_j := \frac{1}{2}(\frac{1}{4})^{(10+M)l^2}$, and $H_j := \widetilde{W}_{l,j,\Phi}(Y \otimes I) \widetilde{W}_{l,j,\Phi}^\dagger$. With respect to Lemma 2, we can evaluate $\lambda = \sum_j h_j = 1$ and thus the error of simulating this dynamics via qDRIFT in terms of Eq. (C1) is upper bounded by $(2t^2/N)e^{2t^2/N}$.

We can further simplify Eq. (D14) as follows. First, note that $\widetilde{W}_{l,j,\Phi}$ can be rewritten as

$$\widetilde{W}_{l,j,\Phi} = (e^{-i\frac{s\Phi}{2}Z} \otimes I) \Upsilon_{-sl, l^2M, j''} \Upsilon_{sl, 10l^2, j'} \quad (\text{D15})$$

by using $\Upsilon_{k,N,j}$ defined in Eq. (D4). Moreover, according to Eq. (D8), the equality

$$\left(\frac{1}{4} \right)^{nN} \sum_{\vec{v}_1, \dots, \vec{v}_N} \Upsilon_{k,N,j}^\dagger \begin{pmatrix} 0 & e^{-i\phi}I \\ e^{i\phi}I & 0 \end{pmatrix} \Upsilon_{k,N,j} = A_{k,N} \begin{pmatrix} 0 & e^{-i(\phi-\theta_{k,N})}e^{i\frac{k\pi}{2}H_0} \\ e^{i(\phi-\theta_{k,N})}e^{-i\frac{k\pi}{2}H_0} & 0 \end{pmatrix} \quad (\text{D16})$$

holds for $\phi \in [0, 2\pi)$. Thus, Eq. (D14) can be rewritten as

$$\begin{aligned} & \frac{N\gamma}{2} \left(\frac{1}{4} \right)^{(10+M)l^2} \sum_{\substack{\vec{u}_1, \dots, \vec{u}_{10l^2} \\ \vec{w}_1, \dots, \vec{w}_{l^2M} \\ s \in \{1, -1\}}} \widetilde{W}_{l,j,\Phi}(Y \otimes I) \widetilde{W}_{l,j,\Phi}^\dagger \\ &= \frac{t}{2} \left(\frac{1}{4} \right)^{(10+M)l^2} \sum_{\substack{\vec{u}_1, \dots, \vec{u}_{10l^2} \\ \vec{w}_1, \dots, \vec{w}_{l^2M} \\ s \in \{1, -1\}}} (e^{-i\frac{s\Phi}{2}Z} \otimes I) \Upsilon_{-sl, l^2M, j''} \Upsilon_{sl, 10l^2, j'} \begin{pmatrix} 0 & -iI \\ iI & 0 \end{pmatrix} \Upsilon_{sl, 10l^2, j'}^\dagger \Upsilon_{-sl, l^2M, j''}^\dagger (e^{i\frac{s\Phi}{2}Z} \otimes I) \\ &= \frac{t}{2} \left(\frac{1}{4} \right)^{(10+M)l^2} \sum_{\substack{\vec{u}_1, \dots, \vec{u}_{10l^2} \\ \vec{w}_1, \dots, \vec{w}_{l^2M} \\ s \in \{1, -1\}}} (e^{-i\frac{s\Phi}{2}Z} \otimes I) \Upsilon_{sl, l^2M, j''}^\dagger \Upsilon_{-sl, 10l^2, j'}^\dagger \begin{pmatrix} 0 & -iI \\ iI & 0 \end{pmatrix} \Upsilon_{-sl, 10l^2, j'} \Upsilon_{sl, l^2M, j''} (e^{i\frac{s\Phi}{2}Z} \otimes I) \\ &= \frac{t}{2} A_{-sl, 10l^2} \left(\frac{1}{4} \right)^{Ml^2} \sum_{\substack{\vec{w}_1, \dots, \vec{w}_{l^2M} \\ s \in \{1, -1\}}} (e^{-i\frac{s\Phi}{2}Z} \otimes I) \Upsilon_{sl, l^2M, j''}^\dagger \begin{pmatrix} 0 & -ie^{i\theta_{-sl, 10l^2}}I \\ ie^{-i\theta_{-sl, 10l^2}}I & 0 \end{pmatrix} \Upsilon_{sl, l^2M, j''} (e^{i\frac{s\Phi}{2}Z} \otimes I) \\ &= \frac{t}{2} A_{-sl, 10l^2} A_{sl, l^2M} \sum_{s \in \{1, -1\}} (e^{-i\frac{s\Phi}{2}Z} \otimes I) \begin{pmatrix} 0 & -ie^{i(\theta_{-sl, 10l^2} + \theta_{sl, l^2M})}I \\ ie^{-i(\theta_{-sl, 10l^2} + \theta_{sl, l^2M})}I & 0 \end{pmatrix} (e^{i\frac{s\Phi}{2}Z} \otimes I), \end{aligned} \quad (\text{D17})$$

where in the third line we made use of the fact that $\Upsilon_{-k,N,j} = (\Upsilon_{k,N,j'})^\dagger$, where $j' := (\vec{v}_N, \dots, \vec{v}_1)$. By substituting Eq. (D7) into Eq. (D17), we have

$$t \sum_j h_j H_j = \frac{t}{2} \sum_s (e^{-i\frac{s\Phi}{2}Z} \otimes I) \begin{pmatrix} 0 & -ia'_{l,M,s}a'_{l,10,-s}I \\ ia'_{l,M,-s}a'_{l,10,s}I & 0 \end{pmatrix} (e^{i\frac{s\Phi}{2}Z} \otimes I) = ta_{l,M,\Phi} Y \otimes I, \quad (\text{D18})$$

where $a'_{l,m,s} := [\frac{1}{2^m} \text{tr}\{e^{-is(\pi/(2ml))H_0}\}]^{ml^2}$ and $a_{l,M,\Phi} := \frac{1}{2}(e^{i\Phi}a'_{l,M,-s}a'_{l,10,s} + e^{-i\Phi}a'_{l,M,s}a'_{l,10,-s})$ (note that $a_{l,M,\Phi} \in \mathbb{R}$). In terms of the parameters $A_{k,N}$ and $\theta_{k,N}$, it is straightforward to show that $a_{l,M,\Phi}$ can be expressed as

$$a_{l,M,\Phi} = A_{l,ML^2} A_{l,10l^2} \cos(\theta_{l,10l^2} - \theta_{l^2,ML^2} + \Phi). \quad (\text{D19})$$

In Subroutine D6, the input parameters of the state are specifically chosen as $(N, l, \gamma, M, \Phi) = (N', l, k\pi/N', 25k, \Theta)$ where $N' = N(1, k\pi, 1/(4\sqrt{2}))$, with respect to which, $ta_{l,M,\Phi}$ is expressed as

$$ta_{l,M,\Theta} = k\pi A_{l,25kl^2} A_{l,10l^2} \cos(\theta_{l,10l^2} - \theta_{l,25kl^2} + \Phi). \quad (\text{D20})$$

Using the fact that $A_{l,10l^2} \leq 1$, we can upper bound the difference between the above equation and $k\pi A_{l,10l^2} \cos(\theta_{l,10l^2} + \Phi)$ by

$$\begin{aligned} |ta_{l,25k,\Phi} - k\pi A_{l,10l^2} \cos(\theta_{l,10l^2} + \Phi)| &= k\pi |A_{l,25kl^2} A_{l,10l^2} \cos(\theta_{l,10l^2} - \theta_{l,25kl^2} + \Phi) - A_{l,10l^2} \cos(\theta_{l,10l^2} + \Phi)| \\ &\leq k\pi |A_{l,25kl^2} \cos(\theta_{l,10l^2} - \theta_{l,25kl^2} + \Phi) - \cos(\theta_{l,10l^2} + \Phi)| \\ &\leq k\pi \{|A_{l,25kl^2} [\cos(\theta_{l,10l^2} - \theta_{l,25kl^2} + \Phi) - \cos(\theta_{l,10l^2} + \Phi)]| + |(1 - A_{l,25kl^2}) \cos(\theta_{l,10l^2} + \Phi)|\}. \end{aligned} \quad (\text{D21})$$

Invoking the inequality $|\cos(\theta + \theta') - \cos(\theta)| = |-\int_{\theta}^{\theta+\theta'} dx \sin(x)| \leq \theta'$ and Eq. (D3), we then have that

$$\begin{aligned} k\pi \{|A_{l,25kl^2} [\cos(\theta_{l,10l^2} - \theta_{l,25kl^2} + \Phi) - \cos(\theta_{l,10l^2} + \Phi)]| + |(1 - A_{l,25kl^2}) \cos(\theta_{l,10l^2} + \Phi)|\} \\ \leq k\pi (|\theta_{l,25kl^2}| + |1 - A_{l,25kl^2}|) \leq k\pi \left(\left| \frac{\pi^3}{20000k^2l} \right| + \left| \frac{\pi^2}{200k} \right| \right) < 0.16 < \frac{1}{4\sqrt{2}}. \end{aligned} \quad (\text{D22})$$

Now, let us define $\mathcal{F}_1, \mathcal{F}_2, \mathcal{F}_3 : \mathcal{L}(\mathcal{H}_c \otimes \mathcal{H}) \rightarrow \mathcal{L}(\mathcal{H}_c \otimes \mathcal{H})$ as

$$\begin{aligned} \mathcal{F}_1(\rho) &:= e^{-ik\pi A_{l,10l^2} \cos(\theta_{l,10l^2} + \Phi) Y \otimes I} \rho e^{ik\pi A_{l,10l^2} \cos(\theta_{l,10l^2} + \Phi) Y \otimes I} \\ \mathcal{F}_2(\rho) &:= e^{-ik\pi a_{l,25k,\Phi} Y \otimes I} \rho e^{ik\pi a_{l,25k,\Phi} Y \otimes I} \\ \mathcal{F}_3 &:= \text{quantum operation simulated by qDRIFT in steps 2 to 5 of Subroutine D7.} \end{aligned} \quad (\text{D23})$$

With this, the success probability of $|0\rangle$ -measurements and $|+\rangle$ -measurements, which is given by $\langle 0 | \text{tr}_{\mathcal{H}}[\mathcal{F}_3(|0\rangle\langle 0| \otimes |0\rangle\langle 0|)] | 0 \rangle$ and $\langle + | \text{tr}_{\mathcal{H}}[\mathcal{F}_3(|0\rangle\langle 0| \otimes |0\rangle\langle 0|)] | + \rangle$ respectively, satisfies

$$|S(\mathcal{F}_3, |\psi\rangle) - S(\mathcal{F}_1, |\psi\rangle)| \leq |S(\mathcal{F}_3, |\psi\rangle) - S(\mathcal{F}_2, |\psi\rangle)| + |S(\mathcal{F}_2, |\psi\rangle) - S(\mathcal{F}_1, |\psi\rangle)| < \frac{1}{4\sqrt{2}} + \frac{1}{4\sqrt{2}} = \frac{1}{\sqrt{8}}, \quad (\text{D24})$$

where, for any quantum operation $\mathcal{F} : \mathcal{L}(\mathcal{H}_c \otimes \mathcal{H}) \rightarrow \mathcal{L}(\mathcal{H}_c \otimes \mathcal{H})$ and state $|\psi\rangle \in \mathcal{H}_c$, we define $S(\mathcal{F}, |\psi\rangle) := \langle \psi | \text{tr}_{\mathcal{H}}[\mathcal{F}(|0\rangle\langle 0| \otimes |0\rangle\langle 0|)] |\psi\rangle$. Here, the upper bound of $|S(\mathcal{F}_3, |\psi\rangle) - S(\mathcal{F}_2, |\psi\rangle)|$ is obtained using Lemma 2, and that of $|S(\mathcal{F}_2, |\psi\rangle) - S(\mathcal{F}_1, |\psi\rangle)|$ is obtained by noting that $\text{tr}_{\mathcal{H}}[\mathcal{F}_1(|0\rangle\langle 0| \otimes |0\rangle\langle 0|)]$ and $\text{tr}_{\mathcal{H}}[\mathcal{F}_2(|0\rangle\langle 0| \otimes |0\rangle\langle 0|)]$ are pure states, and so we can use the fact that the operator norm of $|\beta\rangle\langle\beta| - |\gamma\rangle\langle\gamma|$ for unit vectors $|\beta\rangle$ and $|\gamma\rangle$ is $\sqrt{1 - |\langle\beta|\gamma\rangle|^2}$ (see Eq. (1.185) of Ref. [44]). In particular, $\langle\beta|\gamma\rangle$ in this case is evaluated as $\langle 0 | e^{-ik\pi(A_{l,10l^2} \cos(\theta_{l,10l^2} + \Phi) - a_{l,25k,\Phi})Y} | 0 \rangle$ and $t = k\pi$. Invoking Eqs. (D21) and (D22), as well as a similar discussion to Eq. (C11), we have $|S(\mathcal{F}_2, |\psi\rangle) - S(\mathcal{F}_1, |\psi\rangle)| \leq 1/4\sqrt{2}$.

Setting the appropriate measurements as $|0\rangle$ and $|+\rangle$, we can express the success probabilities as

$$\begin{aligned} S(\mathcal{F}_1, |0\rangle) &= \frac{1 + \cos(2k\pi A_{l,10l^2} \cos(\theta_{l,10l^2} + \Phi))}{2} \\ S(\mathcal{F}_1, |+\rangle) &= \frac{1 + \sin(2k\pi A_{l,10l^2} \cos(\theta_{l,10l^2} + \Phi))}{2}. \end{aligned} \quad (\text{D25})$$

Thus, an estimate \hat{v}_Φ of $2\pi A_{l,10l^2} \cos(\theta_{l,10l^2} + \Phi)$ can be successfully obtained by robust phase estimation. In particular, by setting K in Eq. (D13) as $K = \text{ceil}[\log_2(3\sqrt{2}t/\epsilon)]$, one can estimate $A_{l,10l^2} \cos(\theta_{l,10l^2} + \Phi)$ with root mean square of error upper bounded by $\epsilon/(2\sqrt{2}t)$ with a time complexity $\Theta(l^2 t^3 n / \epsilon^3)$. This follows from the fact that the time complexity of generating $|\phi(N', l, k\pi/N', 25k, \Phi)\rangle$ is $\Theta(l^2 n k^3)$ and invoking

$$\sum_{j=1}^K (K-j)r^j = \frac{r^{K+1} - Kr^2 + (K-1)r}{(r-1)^2} \quad r > 1. \quad (\text{D26})$$

Thus, the total time complexity of the robust phase estimation procedure is given by $\sum_{j=1}^K M_j \Theta(l^2 n (2^{j-1})^3) = \Theta(l^2 n t^3 / \epsilon^3)$. Finally, by setting $\Phi \in \{0, \frac{\pi}{2}\}$, one can obtain estimates $\hat{v}_0, \hat{v}_{\pi/2}$ of $2\pi A_{l,10l^2} \cos(\theta_{l,10l^2})$ and $2\pi A_{l,10l^2} \sin(\theta_{l,10l^2})$, respectively with the aforementioned error and time complexity. When $A_{l,10l^2} \cos(\theta_{l,10l^2})$ and $A_{l,10l^2} \sin(\theta_{l,10l^2})$ are estimated with an error of δ_1 and δ_2 , respectively, then the quantity $|1 - (A_{l,10l^2} e^{i\theta_{l,10l^2}}) / (\hat{A}_l e^{i\hat{\theta}_l})|$ is upper bounded by

$$\begin{aligned} \left| 1 - \frac{A_{l,10l^2} e^{i\theta_{l,10l^2}}}{\hat{A}_l e^{i\hat{\theta}_l}} \right| &= \frac{1}{|\hat{A}_l e^{i\hat{\theta}_l}|} |A_{l,10l^2} e^{i\theta_{l,10l^2}} - \hat{A}_l e^{i\hat{\theta}_l}| \\ &= \frac{1}{|\hat{A}_l e^{i\hat{\theta}_l}|} \left| \left(A_{l,10l^2} \cos(\theta_{l,10l^2}) - \frac{\hat{v}_0}{2\pi} \right) + i \left(A_{l,10l^2} \sin(\theta_{l,10l^2}) - \frac{\hat{v}_{\pi/2}}{2\pi} \right) \right| \\ &\leq 2\sqrt{\delta_1^2 + \delta_2^2}, \end{aligned} \quad (\text{D27})$$

where the inequality comes from the fact that Subroutine D6 returns values for the estimators only if $\hat{A}_l = \sqrt{\hat{v}_0^2 + \hat{v}_{\pi/2}^2} > 1/2$. Since the root mean square errors of δ_1 and δ_2 are upper bounded by $\epsilon/(2\sqrt{2}t)$, it follows that the root mean square error of $|1 - (A_{l,10l^2}e^{i\theta_{l,10l^2}})/(\hat{A}_le^{i\hat{\theta}_l})|$ is upper bounded by ϵ/t , as claimed in the output of Subroutine D6. Finally, note that including the rejection condition of steps 4 and 5 of Subroutine D6 only increases the average time complexity of generating $\hat{v}_0, \hat{v}_{\pi/2}$ by constant factor. This is because the root mean square of $|1 - (A_{l,10l^2}e^{i\theta_{l,10l^2}})/(\hat{A}_le^{i\hat{\theta}_l})|$ is upper bounded by ϵ/t and according to Eq. (D3), we have that $A_{l,10l^2} \geq 1 - \pi^2/80 > 1/2$, and thus the probability that $\sqrt{\hat{v}_0^2 + \hat{v}_{\pi/2}^2} \leq 1/2$ is smaller than 1/2 for sufficiently small ϵ/t . \square

Above, we have demonstrated the ability to accurately obtain estimates $(\hat{A}_l, \hat{\theta}_l)$ for the case of $l > 0$. We now show how these estimates can be used to provide estimates for cases $l \leq 0$.

Lemma 7. *With respect to estimates $(\hat{A}_l, \hat{\theta}_l)$ with $l > 0$ obtained by Subroutine D6, define $(\hat{A}_l, \hat{\theta}_l)$ for $l \leq 0$ as*

$$(\hat{A}_l, \hat{\theta}_l) := \begin{cases} (\hat{A}_{-l}, -\hat{\theta}_{-l}) & l < 0 \\ (1, 0) & l = 0. \end{cases} \quad (\text{D28})$$

Thus defined, these provide estimates of $(A_{l,10l^2}, \theta_{l,10l^2})$ in Lemma 5 with a root mean squared error of $|1 - (A_{l,10l^2}e^{i\theta_{l,10l^2}})/(\hat{A}_le^{i\hat{\theta}_l})|$ upper bounded by ϵ/t .

Proof: For $l = 0$, it is shown in the proof of Lemma 5 that $(A_{l,10l^2}, \theta_{l,10l^2}) = (1, 0)$, thus Eq. (D28) provides an exact estimate of $(A_{l,10l^2}, \theta_{l,10l^2})$. For $l < 0$, note that by Eq. (D7), we have

$$A_{l,10l^2}e^{i\theta_{l,10l^2}} := \left[\frac{\text{tr}(e^{-i\frac{\pi}{20l}H_0})}{2^n} \right]^{10l^2}, \quad (\text{D29})$$

and so $(A_{l,10l^2}, \theta_{l,10l^2}) = (A_{-l,10(-l)^2}, -\theta_{-l,10(-l)^2})$ holds. We can then write

$$\left| 1 - \frac{A_{l,10l^2}e^{i\theta_{l,10l^2}}}{\hat{A}_le^{i\hat{\theta}_l}} \right| = \left| 1 - \frac{A_{-l,10(-l)^2}e^{-i\theta_{-l,10(-l)^2}}}{\hat{A}_{-l}e^{-i\hat{\theta}_{-l}}} \right| = \left| \left(1 - \frac{A_{-l,10(-l)^2}e^{i\theta_{-l,10(-l)^2}}}{\hat{A}_{-l}e^{i\hat{\theta}_{-l}}} \right)^* \right| = \left| 1 - \frac{A_{-l,10(-l)^2}e^{i\theta_{-l,10(-l)^2}}}{\hat{A}_{-l}e^{i\hat{\theta}_{-l}}} \right|,$$

whose root mean square is upper bounded by ϵ/t , thus asserting our claim. \square

In summary, we have shown that one can estimate the parameters $(\hat{A}_l, \hat{\theta}_l)$, which are necessary to construct appropriate corrections to the ‘‘intermediate circuit’’ in order to build the compiled Algorithm 4, as depicted in Fig. 13.

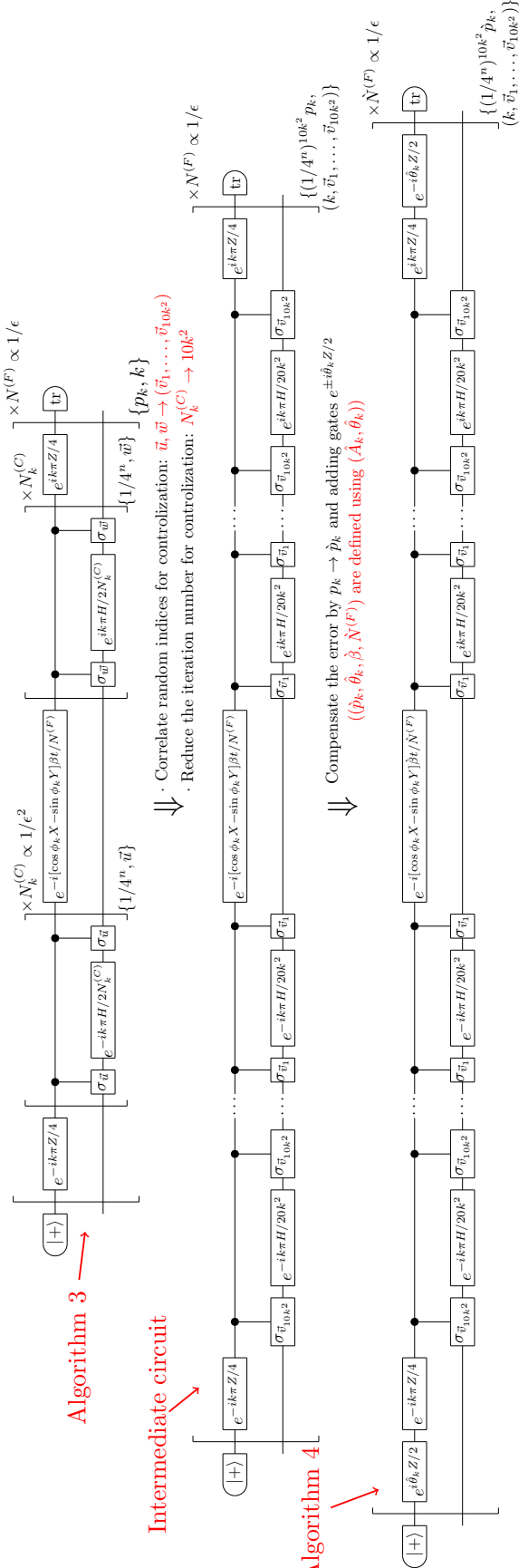


FIG. 13. *Summary of compilation of Algorithm 3.*—First, the random variables $\vec{u}, \vec{w} \in \{0, 1, 2, 3\}^n$ of the controlization become correlated. Since the error of this intermediate circuit for finite iteration number $10k^2$ of the controlization happens as in Eq. (18), this error is compensated in the final step by modifying $N^{(F)} \rightarrow \hat{N}^{(F)}$, and $p_k \rightarrow \hat{p}_k$, and introducing an additional gate $e^{\pm i\theta_k Z/2}$ according to the parameters $(\hat{A}_k, \hat{\theta}_k)$ obtained by Subroutine D6 in App. D 2.

3. Error and Time Complexity Analysis of Compiled Algorithm (Algorithm 4)

Here, we will prove a theorem on the error, the mean square of the error, and the time complexity of Algorithm 4.

Theorem 3.

1. Algorithm 4 outputs $e^{-if(H_0)t} |\psi\rangle$ with an error (in terms of the 1-norm) upper bounded by ϵ , i.e.

$$\sup_{\substack{\dim(\mathcal{H}') \\ |\psi\rangle \in \mathcal{H} \otimes \mathcal{H}' \\ \|\psi\rangle\| = 1}} \|\mathcal{F} \otimes \mathcal{I}_{\mathcal{H}'}(|\psi\rangle\langle\psi|) - \sum_j p_j (\mathcal{F}_j \otimes \mathcal{I}_{\mathcal{H}'})(|\psi\rangle\langle\psi|)\|_1 \leq \epsilon, \quad (\text{D30})$$

where $j \in [\bigcup_{k=-\hat{K}}^{\hat{K}} (\{k\} \times (\{0, 1, 2, 3\}^n)^{10k^2})]^{\hat{N}^{(F)}} \times (\mathbb{R} \times [0, 2\pi])^{\hat{K}}$ is chosen from the set of all random indices, namely (k, j_k) where $k \in \{-\hat{K}, \dots, \hat{K}\}$ and $j_k = (\vec{v}_{1:10k^2}) \in (\{0, 1, 2, 3\}^n)^{10k^2}$ for each of the $\hat{N}^{(F)}$ iterations and parameters $\Phi := [(\hat{A}_1, \hat{\theta}_1), \dots, (\hat{A}_{\hat{K}}, \hat{\theta}_{\hat{K}})]$ where $\hat{A}_l \in \mathbb{R}$ and $\hat{\theta}_l \in [0, 2\pi]$ (which are random due to dependence on measurement outcomes) with $l \in \{1, \dots, \hat{K}\}$, p_j is the probability that j is chosen, $\mathcal{F}(\rho) := e^{-if(H_0)t} \rho e^{if(H_0)t}$, \mathcal{F}_j is the unitary performed when j is chosen, and \mathcal{H}' is an auxiliary system of arbitrary dimension.

2. Algorithm 4 outputs $e^{-if(H_0)t} |\psi\rangle$ with mean squared error upper-bounded by 2ϵ , i.e.

$$\sup_{\substack{\dim(\mathcal{H}') \\ |\psi\rangle \in \mathcal{H} \otimes \mathcal{H}' \\ \|\psi\rangle\| = 1}} \sum_j p_j \|(\mathcal{F} \otimes \mathcal{I}_{\mathcal{H}'})(|\psi\rangle\langle\psi|) - (\mathcal{F}_j \otimes \mathcal{I}_{\mathcal{H}'})(|\psi\rangle\langle\psi|)\|_1^2 \leq 2\epsilon. \quad (\text{D31})$$

3. The time complexity of Algorithm 4 comprises of a pre-processing step and a main process. The pre-processing step has a time complexity of $\Theta(\hat{K}^3 t^3 n / \epsilon^3) + T_4$, where T_4 is the sum of computation time complexities (on a classical computer) for step 1 (calculation of Fourier coefficients \tilde{c}_k until Eq. (19) is satisfied) and step 7 (computation of $\hat{N}^{(F)}$), and $\hat{K} = O[(t/\epsilon)^{1/3}]$. The main process has a time complexity of $\Theta(C_{4,f} t^2 n / \epsilon)$, where $C_{4,f}$ is a (function-dependant) constant.

Part 1 of Theorem 3 implies in particular that for an arbitrary input state $|\psi\rangle \in \mathcal{H}$:

$$\|\mathcal{F}(|\psi\rangle\langle\psi|) - \sum_j p_j \mathcal{F}_j(|\psi\rangle\langle\psi|)\|_1 \leq \epsilon. \quad (\text{D32})$$

In addition, part 2 of Theorem 3 implies in particular that the mean square of the difference between the ideal state and the single-shot output state is bounded above as:

$$\sum_j p_j \|\mathcal{F}(|\psi\rangle\langle\psi|) - \mathcal{F}_j(|\psi\rangle\langle\psi|)\|_1^2 \leq 2\epsilon. \quad (\text{D33})$$

Therefore, we prove the error bounds stated in Algorithm 4.

Proof: We begin with the first statement.

1. Steps 2 to 13 of Algorithm 4 simulate the following quantum operation

$$\mathcal{F}_6 := \sum_{\Phi} p_{\Phi} \mathcal{F}_{\Phi} \quad (\text{D34})$$

applied to the input state $|+\rangle \otimes |\psi\rangle$, where $\Phi := ((\hat{A}_1, \hat{\theta}_1), \dots, (\hat{A}_{\hat{K}}, \hat{\theta}_{\hat{K}}))$, p_{Φ} is the probability Φ is obtained, and \mathcal{F}_{Φ} is the quantum operation simulated by qDRIFT in steps 9 to 13 of Algorithm 4 whenever Φ is chosen. The operation

\mathcal{F}_Φ approximates the dynamics $e^{-iH_\Phi t}$ for the Hamiltonian

$$\begin{aligned}
H_\Phi &:= \sum_{k=-\hat{K}}^{\hat{K}} \frac{|\tilde{c}_k|}{\hat{A}_k} \left(\frac{1}{4}\right)^{10nk^2} \sum_{j_k \in \{\{0,1,2,3\}^n\}^{10k^2}} \hat{W}_{k,j_k}^\dagger ([\cos(\phi_k)X - \sin(\phi_k)Y] \otimes I) \hat{W}_{k,j_k} \\
&= \sum_{k=-\hat{K}}^{\hat{K}} \frac{|\tilde{c}_k|}{\hat{A}_k} (e^{-i\frac{\hat{\theta}_k}{2}Z} \otimes I) \left[\left(\frac{1}{4}\right)^{10nk^2} \sum_{j_k \in \{\{0,1,2,3\}^n\}^{10k^2}} (W_{k,j_k}^{(10k^2)})^\dagger ([\cos(\phi_k)X - \sin(\phi_k)Y] \otimes I) W_{k,j_k}^{(10k^2)} \right] (e^{i\frac{\hat{\theta}_k}{2}Z} \otimes I) \\
&= \sum_{k=-\hat{K}}^{\hat{K}} \frac{|\tilde{c}_k|}{\hat{A}_k} A_{k,10k^2} (e^{i\frac{\theta_{k,10k^2}-\hat{\theta}_k}{2}Z} \otimes I) \begin{pmatrix} 0 & e^{i\phi_k} e^{i\frac{k\pi}{2}(H_0+I)} \\ e^{-i\phi_k} e^{-i\frac{k\pi}{2}(H_0+I)} & 0 \end{pmatrix} (e^{-i\frac{\theta_{k,10k^2}-\hat{\theta}_k}{2}Z} \otimes I). \tag{D35}
\end{aligned}$$

By defining $\Delta_k := \frac{A_{k,10k^2} e^{i\theta_{k,10k^2}}}{\hat{A}_k e^{i\hat{\theta}_k}} - 1$, the last line of Eq. (D35) can be rewritten as

$$\sum_{k=-\hat{K}}^{\hat{K}} |\tilde{c}_k| \begin{pmatrix} 0 & (1 + \Delta_k) e^{i\phi_k} e^{i\frac{k\pi}{2}(H_0+I)} \\ (1 + \Delta_k^*) e^{-i\phi_k} e^{-i\frac{k\pi}{2}(H_0+I)} & 0 \end{pmatrix}. \tag{D36}$$

This expression can be further simplified by defining a function $f_\Phi : [-1, 1] \rightarrow \mathbb{R}$ as

$$f_\Phi(x) := \sum_{k=-\hat{K}}^{\hat{K}} \tilde{c}_k \Delta_k e^{ik\pi x}. \tag{D37}$$

Note that the output is real since $\Delta_{-k} = \Delta_k^*$. With this, we have

$$H_\Phi = X \otimes \left[f_{\hat{K}} \left(\frac{H_0 + I}{2} \right) + f_\Phi \left(\frac{H_0 + I}{2} \right) \right] \tag{D38}$$

where $f_{\hat{K}}(x) := \sum_{k=-\hat{K}}^{\hat{K}} \tilde{c}_k e^{ik\pi x}$.

Now, for any quantum operation $\mathcal{F} : \mathcal{L}(\mathcal{H}_c \otimes \mathcal{H}) \rightarrow \mathcal{L}(\mathcal{H}_c \otimes \mathcal{H})$ we define the following norm

$$E(\mathcal{F}) := \sup_{\substack{|\psi\rangle \in \mathcal{H}_c \otimes \mathcal{H} \otimes \mathcal{H}' \\ \|\psi\| = 1 \\ \dim \mathcal{H}'}} \|\mathcal{F} \otimes \mathcal{I}_{\mathcal{H}'}(|\psi\rangle \langle \psi|)\|_1, \tag{D39}$$

where $\mathcal{I}_{\mathcal{H}'}$ is the identity operation in $\mathcal{L}(\mathcal{H}')$. Moreover, we define

$$\begin{aligned}
\mathcal{F}_4(\rho) &:= e^{-i(X \otimes f(H_0))t} \rho e^{i(X \otimes f(H_0))t} \\
\mathcal{F}_5(\rho) &:= \sum_{\Phi} p_{\Phi} e^{-iH_{\Phi}t} \rho e^{iH_{\Phi}t} =: \sum_{\Phi} p_{\Phi} \mathcal{G}_{\Phi}. \tag{D40}
\end{aligned}$$

With these definitions at hand, we can upper bound the simulation error $E(\mathcal{F}_6 - \mathcal{F}_4)$ using Lemma 2 and similar arguments to those presented in Eqs. (C10) and (C11) as follows.

$$\begin{aligned}
E(\mathcal{F}_6 - \mathcal{F}_4) &\leq E(\mathcal{F}_6 - \mathcal{F}_5) + E(\mathcal{F}_5 - \mathcal{F}_4) \\
&= \sup_{\substack{|\psi\rangle \in \mathcal{H}_c \otimes \mathcal{H} \otimes \mathcal{H}' \\ \|\psi\| = 1 \\ \dim \mathcal{H}'}} \left\| \sum_{\Phi} p_{\Phi} [\mathcal{F}_{\Phi} \otimes \mathcal{I}_{\mathcal{H}'}(|\psi\rangle \langle \psi|) - \mathcal{G}_{\Phi} \otimes \mathcal{I}_{\mathcal{H}'}(|\psi\rangle \langle \psi|)] \right\|_1 \\
&+ \sup_{\substack{|\psi\rangle \in \mathcal{H}_c \otimes \mathcal{H} \otimes \mathcal{H}' \\ \|\psi\| = 1 \\ \dim \mathcal{H}'}} \left\| \sum_{\Phi} p_{\Phi} [(e^{-iH_{\Phi}t} \otimes I) |\psi\rangle \langle \psi| (e^{iH_{\Phi}t} \otimes I) - (e^{-i(X \otimes f(H_0))t} \otimes I) |\psi\rangle \langle \psi| (e^{i(X \otimes f(H_0))t} \otimes I)] \right\|_1 \\
&\leq \sum_{\Phi} p_{\Phi} \|\mathcal{F}_{\Phi} - \mathcal{G}_{\Phi}\|_{\diamond} + \sum_{\Phi} p_{\Phi} \sup_{\substack{|\psi\rangle \in \mathcal{H}_c \otimes \mathcal{H} \otimes \mathcal{H}' \\ \|\psi\| = 1 \\ \dim \mathcal{H}'}} 2[1 - |\langle \psi | (e^{-i\{X \otimes (\tilde{f}((H_0+I)/2) - f_{\hat{K}}((H_0+I)/2) - f_{\Phi}((H_0+I)/2))\}t} \otimes I) |\psi\rangle|^2]^{1/2} \\
&\leq \frac{\epsilon}{3} + \sum_{\Phi} p_{\Phi} 2 \sin(R(\tilde{f} - f_{\hat{K}} - f_{\Phi})t/2) \leq \frac{\epsilon}{3} + \sum_{\Phi} p_{\Phi} [R(\tilde{f} - f_{\hat{K}}) + R(f_{\Phi})]t \leq \frac{\epsilon}{3} + \frac{\epsilon}{3} + \sum_{\Phi} p_{\Phi} R(f_{\Phi})t, \tag{D41}
\end{aligned}$$

where for any function $g : [-1, 1] \rightarrow \mathbb{R}$, we have $R(g) := 2 \max_{x \in [-1, 1]} |g(x)|$.

The final term $\sum_{\Phi} p_{\Phi} R(f_{\Phi})t$ in the above equation can be upper bounded as follows. First note that, for f_{Φ} defined in Eq. (D37), we have

$$R(f_{\Phi}) \leq 2 \sum_{k=-\hat{K}}^{\hat{K}} |\tilde{c}_k| |\Delta_k|. \quad (\text{D42})$$

Now, because the allowed error of Subroutine D6 in step 3 of Algorithm 4 is set as $\sqrt{3}\epsilon/(12\pi(\sum_{k=-\infty}^{\infty} |\tilde{c}_k| |k|))$, one can employ the Chebyshev inequality to show that the probability that $|\Delta_k| \leq |k|(\sqrt{3}\epsilon C)/(12\pi(\sum_{k=-\infty}^{\infty} |\tilde{c}_k| |k|)t)$ for all k and a fixed positive value $C > 0$ is lower bounded by

$$\prod_{k \in \{-\hat{K}, \dots, -1, 1, \dots, \hat{K}\}} \left(1 - \frac{1}{k^2 C^2}\right) \geq 1 - 2 \left(\sum_{k=1}^{\infty} \frac{1}{k^2 C^2}\right) = 1 - \frac{\pi^2}{3C^2}, \quad (\text{D43})$$

where the final equality follows from the identity $\sum_{k=1}^{\infty} (1/k^2) = \pi^2/6$.

Independently, assuming that $|\Delta_k| \leq |k|(\sqrt{3}\epsilon C)/(12\pi(\sum_{k=-\infty}^{\infty} |\tilde{c}_k| |k|)t)$ holds for all k , it follows that the r.h.s. of Eq. (D42) is upper bounded by $(\sqrt{3}C\epsilon)/(6\pi t)$.

Combining these two results, we have that

$$\Pr \left[R(f_{\Phi}) \geq \frac{\sqrt{3}C\epsilon}{6\pi t} \right] \leq \frac{\pi^2}{3C^2}. \quad (\text{D44})$$

Making use of the identity

$$\sum_{\Phi} p_{\Phi} R(f_{\Phi}) = \int_0^{\infty} dx \Pr[R(f_{\Phi}) \geq x], \quad (\text{D45})$$

we can upper bound $\sum_{\Phi} p_{\Phi} R(f_{\Phi})$ via

$$\sum_{\Phi} p_{\Phi} R(f_{\Phi}) \leq \int_0^{\infty} dx \min \left(1, \frac{\epsilon^2}{6^2 t^2 x^2}\right) = \frac{\epsilon}{6t} + \frac{\epsilon}{6t} = \frac{\epsilon}{3t}. \quad (\text{D46})$$

Finally substituting Eq. (D46) into Eq. (D41), we obtain

$$E(\mathcal{F}_6 - \mathcal{F}_4) \leq \epsilon. \quad (\text{D47})$$

Therefore,

$$\begin{aligned} \epsilon &\geq E(\mathcal{F}_6 - \mathcal{F}_4) \geq \sup_{\substack{|\psi\rangle \in \mathcal{H}_c \otimes \mathcal{H} \otimes \mathcal{H}' \\ \||\psi\rangle\|=1 \\ \dim \mathcal{H}'}} \|\text{tr}_{\mathcal{H}_c}[(\mathcal{F}_6 - \mathcal{F}_4) \otimes \mathcal{I}_{\mathcal{H}'}](|\psi\rangle \langle \psi|)\|_1 \\ &\geq \sup_{\substack{|\psi\rangle \in \mathcal{H} \otimes \mathcal{H}' \\ \||\psi\rangle\|=1 \\ \dim \mathcal{H}'}} \|\text{tr}_{\mathcal{H}_c}[(\mathcal{F}_6 - \mathcal{F}_4) \otimes \mathcal{I}_{\mathcal{H}'}](|+\rangle \langle +| \otimes |\psi\rangle \langle \psi|)\|_1 \\ &\quad , \end{aligned} \quad (\text{D48})$$

which is equal to the expression in D30, as required.

2. This statement follows directly by combining the above result with Lemma 1.

3. In order to prove this statement regarding the time complexity, we use Lemma 3, which shows that \tilde{f} defined for any input function f of Algorithm 4 is 4-smooth.

Based on Lemmas 3 and 4, we have that $\sum_{k=-K}^{\infty} |\tilde{c}_k| = O(1/K^3)$ and $\sum_{k=-\infty}^{-K} |\tilde{c}_k| = O(1/K^3)$ for $K > 1$. Thus, the truncation number \hat{K} defined in Eq. (19) is shown to be $O((t/\epsilon)^{1/3})$, as claimed. Furthermore, the time complexity

can be split into one for pre-processing stage and one for the main process as follows.

Pre-processing: For each $k \in \{-\hat{K}, \dots, \hat{K}\}$, the time complexity of generating $(\hat{A}_k, \hat{\theta}_k)$ is shown in Lemma 2 to be $\Theta(k^2 t^3 n / \epsilon^3)$. Thus, by summing this over all k , the total time complexity of steps 2 to 6 in Algorithm 4 is $\Theta(\hat{K}^3 t^3 n / \epsilon^3)$. Thus the total time complexity of the pre-processing step is $\Theta(\hat{K}^3 t^3 n / \epsilon^3) + T_4$.

Main process: The average time complexity of the main process in Algorithm 4 is evaluated as (number of iterations $\hat{N}^{(F)}$) \times (average time complexity of steps 10 to 12) = $\hat{N}(\beta, t, \epsilon/3) \times \Theta(\sum_{k=-\infty}^{\infty} \hat{p}_k n k^2) = \Theta((\sum_{k=-\infty}^{\infty} |\tilde{c}_k|)(\sum_{k=-\infty}^{\infty} |\tilde{c}_k| k^2) t^2 n / \epsilon) =: \Theta(C_{4,f} t^2 n / \epsilon)$ (note that $|\hat{A}_k| \geq 1/2$ due to steps 4 to 5 of Subroutine D6). \square

Appendix E: QSVT-based UHET Algorithm

We will now present and analyze an alternative procedure to achieve UHET based upon a QSVT procedure. We will finally compare this method to Algorithms 3 and 4.

1. QSVT-based UHET Algorithm (Algorithm 8)

Formally, the QSVT-based algorithm is as follows.

Algorithm 8 QSVT-based algorithm

Input:

- A finite number of queries to a black-box Hamiltonian dynamics $e^{\pm iH\tau}$ of a seed Hamiltonian H normalized as $\|H_0\|_{\text{op}} = 1$ where H_0 is the traceless part of H , i.e., $H_0 := H - (1/2^n)\text{tr}(H)I$, with $\tau > 0$
- A class C^3 function $f : [-1, 1] \rightarrow \mathbb{R}$ such that $f^{(4)}$ is piecewise C^2 (see App. A 1)
- Input state $|\psi\rangle \in \mathcal{H}$
- Allowed error $\epsilon > 0$
- Time $t > 0$

Output: A state approximating $e^{-if(H_0)t} |\psi\rangle$ ($t > 0$) with an error in terms Eq. (2) upper bounded by ϵ

Time complexity:

Pre-processing (only once): $O((K_{f,t,\epsilon}^Q)^3)$

Main Process: $\Theta((K_{f,t,\epsilon}^Q)^2/\epsilon)$ for $K_{f,t,\epsilon}^Q$ depending on f , t , and ϵ

Total evolution time (main process): $\Theta(K_{f,t,\epsilon}^Q)$

Used Resources:

System: \mathcal{H} and two auxiliary qubit \mathcal{H}_b , \mathcal{H}_c

Gates: $e^{\pm iH\tau}$ ($\tau > 0$) and controlled-Pauli gates on $\mathcal{L}(\mathcal{H}_b \otimes \mathcal{H}_c \otimes \mathcal{H})$

Procedure:

Pre-processing:

1: Define functions $f_0, f_1 : [-1, 1] \mapsto \mathbb{R}$ as per Eq. (E2)

2: Compute $c_k^{(s)} := \int_{-1}^1 dx 2 \sin(\frac{\pi}{10}) f_s[\cos(\pi x)] \cos(k\pi x)$ and K_s^Q ($s \in \{0, 1\}$) that satisfies

$$\left| 2 \sin(\frac{\pi}{10}) f_s[\cos(\pi x)] - \sum_{k=0}^{K_s^Q} c_k^{(s)} \cos(\pi kx) \right| < \Theta(\epsilon) \quad (\text{E1})$$

for all $x \in [0, 1]$. Note that one can recast the above bound in terms of Chebyshev polynomials T_k as $\left| 2 \sin(\pi/10) f_s(x') - \sum_{k=0}^{K_s^Q} c_k^{(s)} T_k(x') \right| < \Theta(\epsilon)$ for $x =: (1/\pi) \cos^{-1}(x')$ ($x' \in [-1, 1]$), as we will employ in the coming steps.

3: Set $K_{f,t,\epsilon}^Q \leftarrow K_0^Q + K_1^Q$

4: For $s \in \{0, 1\}$, find gate sequence of QSVT for a $(1, 2, 0)$ -block-encoding unitary U_s of $\sum_{k=0}^{K_s^Q} c_k^{(s)} T_k[\cos(H^Q)]$ on $|s0\rangle\langle s0| \in \mathcal{L}(\mathcal{H}_b \otimes \mathcal{H}_c)$ using B_s defined Eq. (E4) (see Fig. 14)

Main Process:

5: Initialize $U_{\text{current}} \leftarrow I$

6: **for** $s \in \{0, 1\}$ **do**

7: Construct unitary U'_s by replacing B_s in the gate sequence for U_s by the random unitary B'_s which approximate B_s up to an error of $\Theta(\epsilon/K_{f,t,\epsilon}^Q)$ (see Fig. 15)

8: $U_{\text{current}} \leftarrow (S^{-s} \otimes I \otimes I) U'_s U_{\text{current}} \quad \triangleright S := |0\rangle\langle 0| + i|1\rangle\langle 1| \text{ is the phase gate}$

9: **end for**

10: Set $U_{\text{current}} \leftarrow (\text{HAD} \otimes I \otimes I) U_{\text{current}} (\text{HAD} \otimes I \otimes I)$

11: Perform robust oblivious amplitude amplification [5] with $n = 5$ on the block of U_{current} specified by $|00\rangle\langle 00| \in \mathcal{L}(\mathcal{H}_b \otimes \mathcal{H}_c)$

12: **Return** $U_{\text{current}}(|0\rangle\langle 0| \otimes |\psi\rangle)$

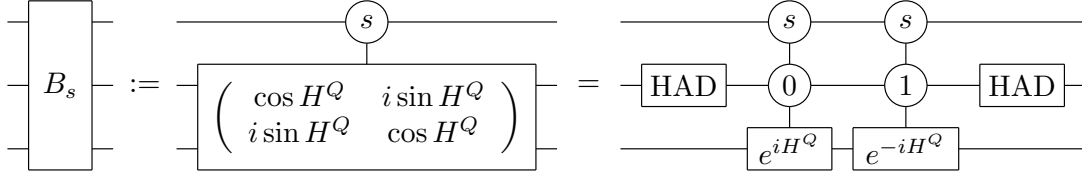


FIG. 14. *Circuit representation of B_s .*—The circled number in the controlled qubits means that the unitary on the target qubit is applied if the control qubit is that state and otherwise identity is applied.

Begin by defining functions f_0 and f_1 as

$$f_0(x) := \begin{cases} f_{0,-}(x) & (0 \leq x \leq \frac{1}{2}) \\ \cos \left[f \left(\frac{12 \cos^{-1}(x)}{\pi} - 3 \right) t \right] & (\frac{1}{2} \leq x \leq \frac{\sqrt{3}}{2}) \\ f_{0,+}(x) & (\frac{\sqrt{3}}{2} \leq x \leq 1) \\ f_0(-x) & (-1 \leq x \leq 0) \end{cases}$$

$$f_1(x) := \begin{cases} f_{1,-}(x) & (0 \leq x \leq \frac{1}{2}) \\ \sin \left[f \left(\frac{12 \cos^{-1}(x)}{\pi} - 3 \right) t \right] & (\frac{1}{2} \leq x \leq \frac{\sqrt{3}}{2}) \\ f_{1,+}(x) & (\frac{\sqrt{3}}{2} \leq x \leq 1) \\ f_1(-x) & (-1 \leq x \leq 0) \end{cases}, \quad (E2)$$

where $f_{0,-}, f_{0,+}, f_{1,-}, f_{1,+}$ are any functions that are infinitely differentiable on their domains and lead to f_0 and f_1 such that

1. $2 \sin(\frac{\pi}{10}) f_0(x)$ and $2 \sin(\frac{\pi}{10}) f_1(x)$ is bounded in $[-1, 1]$ for all $x \in [-1, 1]$. This ensures that they can be constructed using QSVT (in particular, using the technique presented in Theorem 10 of Ref. [37]).
2. $f_s^{(n)}(\frac{1}{2}^+) = f_s^{(n)}(\frac{1}{2}^-)$, $f_s^{(n)}(\frac{\sqrt{3}}{2}^+) = f_s^{(n)}(\frac{\sqrt{3}}{2}^-)$, and $f_s^{(n)}(0^+) = f_s^{(n)}(1^-) = 0$ for $s \in \{0, 1\}$ and $n \in \{0, 1, \dots, J-1\}$ for any integer $J \geq 4$.

The Hamiltonian H^Q in step 4 is defined as

$$H^Q := \frac{\pi(H_0 + 3I)}{12}. \quad (E3)$$

The functions f_0 and f_1 are defined in such a way that

$$f_0(\cos H^Q) - i f_1(\cos H^Q) = e^{-i f(H_0) t}.$$

Furthermore, as we discuss in more detail below, f_0 and f_1 are implementable via QSVT. Since the time complexity of QSVT scales polynomially on the cutoff number K_s^Q , the functions $f_0(x)$ and $f_1(x)$ are chosen to be class C^3 in $x \in [-1, 1]$ so that the sum in Eq. (E1) converges rapidly to $2 \sin(\frac{\pi}{10}) f_s(\cos(\pi x))$ and K_s^Q scales slowly with ϵ .

With respect to the above Hamiltonian, the unitary B_s in step 4 is defined as

$$B_s := |s\rangle \langle s| \otimes \begin{pmatrix} \cos(H^Q) & i \sin(H^Q) \\ i \sin(H^Q) & \cos(H^Q) \end{pmatrix} + |\bar{s}\rangle \langle \bar{s}| \otimes I \otimes I. \quad (E4)$$

See Fig. 14 for its circuit representation.

By defining the following function for $s_b, s_c \in \{0, 1\}$ and unitary U

$$\text{ctrl}_2[U, (s_b, s_c)] := [I - (|s_b s_c\rangle \langle s_b s_c|)] \otimes I + |s_b s_c\rangle \langle s_b s_c| \otimes U, \quad (E5)$$

the unitary B_s can be expressed as

$$B_s = (I \otimes \text{HAD} \otimes I) \text{ctrl}_2[e^{-iH^Q}, (s, 1)] \text{ctrl}_2[e^{iH^Q}, (s, 0)] (I \otimes \text{HAD} \otimes I). \quad (E6)$$

The operator $\text{ctrl}_2[e^{\pm iH^Q t}, (s_b, s_c)]$ can be constructed from $e^{\pm iHt}$ via double controlization [25], which makes use of qDRIFT. In this way, the unitary B_s can be approximated by the circuit shown in Fig. 15.

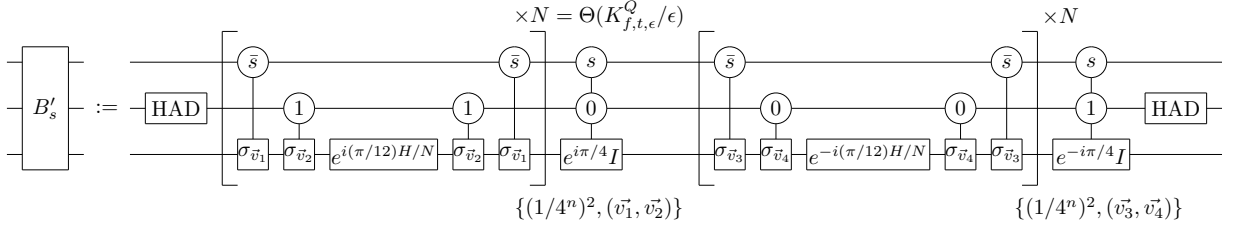


FIG. 15. *Definition of B'_s .*— $\text{ctrl}_2(e^{\pm iH^Q t}, (s_b, s_c))$ in Fig. 14 is replaced by its approximation by controlization.

In summary, the Algorithm 8 simulates the dynamics $e^{-if(H_0)t}$ by the following steps.

$$\begin{aligned}
 I \otimes I \otimes e^{\pm iHt} &\xrightarrow{\text{double controlization}} \text{ctrl}_2[e^{\pm iH^Q t}, (s_b, s_c)] \xrightarrow{\text{Eq. (E4)}} \\
 B_s = |s\rangle\langle s| \otimes \begin{pmatrix} \cos H^Q & i \sin H^Q \\ i \sin H^Q & \cos H^Q \end{pmatrix} + |\bar{s}\rangle\langle \bar{s}| \otimes I \otimes I &\xrightarrow{\text{QSVT \& post-application of } (S^{-s} \otimes I \otimes I)} \\
 \left(\begin{array}{c|c} \begin{matrix} 2 \sin(\frac{\pi}{10}) f_0(\cos H^Q) & 0 \\ \cdot & \cdot \\ 0 & -2i \sin(\frac{\pi}{10}) f_1(\cos H^Q) \\ \hline \sin(\frac{\pi}{10}) e^{-if(H_0)t} & \dots \\ \cdot & \dots \\ \cdot & \dots \\ \cdot & \dots \end{matrix} & \begin{matrix} 0 \\ \cdot \\ \cdot \\ \cdot \\ \cdot \\ \cdot \end{matrix} \end{array} \right) &\xrightarrow{\text{pre- and post-application of } \text{HAD} \otimes I \otimes I} \\
 &\xrightarrow{\text{robust oblivious amplitude amplification}} \begin{pmatrix} e^{-if(H_0)t} & 0 & 0 & 0 \\ 0 & \ddots & & \\ 0 & & \ddots & \\ 0 & & & \ddots \end{pmatrix}. \tag{E7}
 \end{aligned}$$

The leftmost column and the top row of the final matrix in Eq. (E7) is filled with 0 except for the top-left block because both $e^{if(H_0)t}$ and the entire matrix are unitary.

The procedure of Algorithm 8 ensures that the approximation error of simulating $e^{-if(H_0)t}$ is $O(\epsilon)$. There are two sources of errors in the overall procedure: the error due to the approximation in Eq. (E1) and that due to the approximation of B_s by the circuit given in Fig. 15. The former error is $O(\epsilon)$ by definition and the latter is upper bounded by (approximation error of B'_s) \times (number of queries to B'_s) $= \Theta(\epsilon/K_{f,t,\epsilon}^Q) \times K_{f,t,\epsilon}^Q = \Theta(\epsilon)$. Thus, the sum of these errors is $O(\epsilon)$.

The time complexity of the main process is asymptotically proportional to (time complexity of approximating B'_s) \times (number of queries to B'_s) $= \Theta(K_{f,t,\epsilon}^Q/\epsilon) \times K_{f,t,\epsilon}^Q = \Theta((K_{f,t,\epsilon}^Q)^2/\epsilon)$ (indeed, the total time complexity of gates other than B'_s grows slower than $(K_{f,t,\epsilon}^Q)^2/\epsilon$ and can thus be ignored). Moreover, the time complexity for the pre-processing step of Algorithm 8 is $O((K_{f,t,\epsilon}^Q)^3)$, which can be evaluated by noting that obtaining the gate sequence for QSVD implementing a function of polynomial of degree d requires a time complexity of $O(d^3)$ [47]. The total evolution time can be evaluated as (time evolution of approximating B'_s) \times (number of queries to B'_s) $= \Theta(1) \times K_{f,t,\epsilon}^Q = \Theta(K_{f,t,\epsilon}^Q)$.

2. Algorithm Comparison

We now compare the time complexities of the three algorithms: Algorithm 3 (uncompiled), Algorithm 4 (compiled), and Algorithm 8 (QSVD-based). Recall that for each algorithm here, the time complexity dominates the total evolution time regarding the scaling behavior, and thus we only focus on the former in this section. The time complexities of the pre-processing and the main processes are summarized in Table II.

Pre-processing: Rigorous comparison of pre-processing time complexities is difficult in general due to the difficulty in analyzing the quantities T_3 and T_4 . Nevertheless, the time complexity for Algorithm 4 increases more rapidly in terms of ϵ and n than that of Algorithm 8 because $K_{f,t,\epsilon}^Q$ does not depend on n and its ϵ dependence is given by $K_{f,t,\epsilon}^Q = O(1/\epsilon^{1/3})$ (this can be seen by considering that $f_s(x)$ defined in Eq. (E2) is 4-smooth and applying the result of Lemma 4, and subsequently noting that $K_{f,t,\epsilon}^Q = K_0^Q + K_1^Q$).

	Pre-processing Step	Main Process
Algorithm 3	T_3	$\Theta(C_{3,f}t^4n/\epsilon^3)$
Algorithm 4	$\Theta(\hat{K}^3t^3n/\epsilon^3) + T_4$	$\Theta(C_{4,f}t^2n/\epsilon)$
Algorithm 8	$O((K_{f,t,\epsilon}^Q)^3)$	$\Theta((K_{f,t,\epsilon}^Q)^2/\epsilon)$

TAB. II. *Comparison of time complexities of Algorithm 3 (uncompiled), Algorithm 4 (compiled), and Algorithm 8 (QSVT-based).*—The times T_3 and T_4 refer to the total classical computation time complexity for computing the Fourier coefficients and the values $N^{(F)}$ and $\hat{N}^{(F)}$ in Algorithms 3 and 4 respectively. $C_{3,f}$ and $C_{4,f}$ refer to function-dependent constants in Algorithms 3 and 4 respectively. The value $K_{f,t,\epsilon}^Q$ depends on the function f , the time t , and the allowed error ϵ .

Main Process: The main process scaling coefficients for Algorithms 3 and 4

$$C_{3,f} := \left(\sum_{k=-\infty}^{\infty} |\tilde{c}_k| \right)^3 \left(\sum_{k=-\infty}^{\infty} |\tilde{c}_k| k^2 \right) \quad \text{and} \quad C_{4,f} := \left(\sum_{k=-\infty}^{\infty} |\tilde{c}_k| \right) \left(\sum_{k=-\infty}^{\infty} |\tilde{c}_k| k^2 \right) \quad (\text{E8})$$

depend only on the function f and not on n , t , and ϵ . In terms of t and ϵ , the time complexity of Algorithm 4 scales slower than that of Algorithm 3. Furthermore, both algorithms are linear in terms of n . Therefore, it follows that compilation reduces the time complexity of the main process. For completeness, the explicit value of $C_{4,f}$ is calculated in the proof of Theorem 3. In contrast, the scaling coefficient for the main process of Algorithm 8, $K_{f,t,\epsilon}^Q$, depends on f , t , and ϵ , and its explicit expression is difficult to obtain in general. Nonetheless, below we show that for some class of functions, $K_{f,t,\epsilon}^Q$ depends on the allowed error ϵ as $\Omega(1/\epsilon^{2/9})$. Moreover, we show that a larger class of functions satisfies $K_{f,t,\epsilon}^Q = \Omega(1/\epsilon^q)$ for some $0 < q \leq 2/9$. Also, since K_s^Q are the cutoff numbers to used to approximate functions $2\sin(\frac{\pi}{10})f_s[\cos(\pi x)]$ via its Fourier series and $f_s(x)$ oscillates with frequency proportional to t in the range $x \in [1/2, \sqrt{3}/2]$ as can be seen from Eq. (E2), it is expected that $K_{f,t,\epsilon}^Q = K_0^Q + K_1^Q$ increases as t grows. The scaling of $K_{f,t,\epsilon}^Q$ can be obtained as an instance of the following lemma.

Lemma 8. *For a periodically 4-smooth function $g : [-1, 1] \rightarrow \mathbb{R}$, the following inequality is a necessary condition for $g_K(x) := \sum_{k=-K}^K c_k e^{-i\pi kx}$ (c_k are Fourier coefficients of g) to satisfy $|g(x) - g_K(x)| \leq \epsilon$ for all $x \in [-1, 1]$:*

$$\sum_{k=-\infty}^{-K-1} |c_k|^2 + \sum_{k=K+1}^{\infty} |c_k|^2 \leq \epsilon^2. \quad (\text{E9})$$

Proof: $\int_{-1}^1 dx |g(x) - g_K(x)|^2 \leq 2\epsilon^2$ is a necessary condition of $|g(x) - g_K(x)| \leq \epsilon$ for all $x \in [-1, 1]$. Due to Parseval's identity, $\int_{-1}^1 dx |g(x) - g_K(x)|^2 = 2[\sum_{k=-\infty}^{-K-1} |c_k|^2 + \sum_{k=K+1}^{\infty} |c_k|^2]$, thus Eq. (E9) is a necessary condition of $|g(x) - g_K(x)| \leq \epsilon$ for all $x \in [-1, 1]$. \square

Assuming that f is strictly periodically J -smooth, f_0 and f_1 in Eq. (E2) can also be defined to be strictly periodically J -smooth, thus $K_{f,t,\epsilon}^Q$ satisfies $K_{f,t,\epsilon}^Q = \Omega(1/\epsilon^{2/(2J+1)})$ by Lemma 4. In some cases, e.g., when $f^{(4)}$ has some jump (i.e., non-removable) discontinuities, f becomes strictly periodically 4-smooth, and thus for some class of function f , $K_{f,t,\epsilon}^Q = \Omega(1/\epsilon^{2/9})$ holds.

We can now compare the scaling of time complexities of all three algorithms in terms of ϵ . For any class of functions f such that $K_{f,t,\epsilon}^Q$ scales as $\Omega(1/\epsilon^q)$ ($0 < q \leq 2/9$), the time complexity scaling of Algorithms 3, 4, and 8 in terms of ϵ behaves as $\Theta(1/\epsilon^3)$, $\Theta(1/\epsilon)$, and $\Omega(1/\epsilon^{1+2q})$, respectively. By noting that the ϵ dependence of the time complexity of Algorithm 8 is $O(1/\epsilon^{5/3})$ due to the relation $K_{f,t,\epsilon}^Q = O(1/\epsilon^{1/3})$, the hierarchy presented in Eq. (21) follows.

Finally, we describe two technical factors that make Algorithm 4 more efficient than Algorithm 8 in terms of ϵ dependence.

Efficient inputting of high-frequency terms: QSVT requires d queries in total to the block-encoding unitary and its inverse when implementing a polynomial function of degree d . Consequently, the time complexity of the main process of Algorithm 8 increases proportionally to the total cutoff number $K_{f,t,\epsilon}^Q$, which gets larger as the precision increases. On the other hand, the time complexity of the main process of Algorithm 4 has no explicit dependence on the cutoff number \hat{K} . This feature is enabled because the information of Fourier coefficients \tilde{c}_k is input by random sampling according to the magnitude of \tilde{c}_k . As can be seen from the step 12 of Algorithm

4, applying unitaries corresponding to high frequency (i.e., large k) requires $\Theta(k^2)$ time complexity and is an obstacle in reducing the total time complexity in general. Fortunately, such high-frequency terms \tilde{c}_k for larger k typically have smaller magnitude $|\tilde{c}_k|$ than their low-frequency counterparts, and therefore costly unitaries (i.e., for large k) are rarely chosen. Moreover, the average time complexity of one iteration (steps 10 to 12 of Algorithm 4) given by $\Theta[(\sum_{k=-\hat{K}}^{\hat{K}} |\tilde{c}_k|k^2)/(\sum_{k=-\hat{K}}^{\hat{K}} |\tilde{c}_k|)]$ is tailored to converge in the limit $\hat{K} \rightarrow \infty$ by modifying input function f to a periodically smooth function \hat{f} with rapidly converging Fourier coefficients, and thus has no dependence on \hat{K} .

Iteration number in controlization procedure is independent of ϵ : In Algorithm 8, the allowed error of $\text{ctrl}(e^{-iHt})$ for making B'_s is proportional to $1/K_{f,t,\epsilon}^Q$ because B'_s and its inverse is called $K_{f,t,\epsilon}^Q$ times in total and the error accumulates with each query. Since the iteration number of controlization increases with increasing accuracy, the time complexity of main process of Algorithm 8 gains an additional dependence on $K_{f,t,\epsilon}^Q$, which in turn depends upon ϵ . This same logic holds for Algorithm 3. On the other hand, the iteration number $10k^2$ of controlization in Algorithm 4 is independent of $\hat{N}^{(F)}$ and consequently on ϵ due to compilation, and thus the controlization does not introduce any additional ϵ dependence.

Appendix F: Implementing Negative-time Hamiltonian Dynamics

Lemma 9. For a subset J of $\{0, 1, 2, 3\}^n$, a Hamiltonian $H \in \text{span}(\{\sigma_{\vec{v}}\}_{\vec{v} \in J})$, and a subgroup G of $\{\sigma_{\vec{v}}\}_{\vec{v} \in \{0,1,2,3\}^n}$ satisfying the condition in step 1 of Algorithm 5, the equality in Eq. (23), namely

$$\sum_{\sigma \in G'} \sigma H \sigma = \frac{\text{Ltr}(H)}{2^n} I \quad (\text{F1})$$

holds.

Proof: When $H = \alpha I + \sum_{\vec{v} \in J \setminus \{\vec{0}\}} c_{\vec{v}} \sigma_{\vec{v}}$, the r.h.s. of Eq. (F1) evaluates to $\alpha L I$. Since $\sum_{\sigma \in G'} \sigma (\alpha I) \sigma = \alpha \sum_{\sigma \in G'} I = \alpha L I$, it is sufficient to prove that for all $\vec{v} \in J$,

$$\sum_{\sigma \in G'} \sigma \sigma_{\vec{v}} \sigma = 0 \quad (\text{F2})$$

holds. From the condition on G in step 1 of Algorithm 5, for every $\vec{v} \in J$ there exists a Pauli operator $\tilde{\sigma} \in G'$ such that $\sigma_{\vec{v}}$ anti-commutes with $\tilde{\sigma}$. Therefore,

$$\sum_{\sigma \in G'} \sigma \sigma_{\vec{v}} \sigma = \sum_{\sigma \in G'} (\sigma \tilde{\sigma}) \sigma_{\vec{v}} (\tilde{\sigma} \sigma) = \sum_{\sigma \in G'} \sigma (-\sigma_{\vec{v}}) \sigma = - \sum_{\sigma \in G'} \sigma \sigma_{\vec{v}} \sigma, \quad (\text{F3})$$

as required. \square

Lemma 10. Let

$$G = \left\{ \pm \bigotimes_{i=1}^k \sigma_{v_i}^{(V_i)}, \pm i \bigotimes_{i=1}^k \sigma_{v_i}^{(V_i)} \right\}_{(v_1, \dots, v_k) \in \{0,1,2,3\}^k}, \quad (\text{F4})$$

with $\sigma_v^{(V)} := \bigotimes_{q \in V} \sigma_v^{(q)}$, where $\sigma_v^{(q)}$ refers to the Pauli operator σ_v applied on q -th qubit. Then G satisfies the condition in step 1 of Algorithm 5.

Proof: For all $\vec{v} \in J \setminus \{\vec{0}\}$, $\sigma_{\vec{v}}$ is either a single-qubit Pauli operator, namely $|\{j \in \{1, \dots, n\} \mid v_j \neq 0\}| = 1$, or a two-qubit Pauli operator such that $\{j \in \{1, \dots, n\} \mid v_j \neq 0\} \in E$. All single-qubit Pauli terms in $\{\sigma_{\vec{v}}\}_{\vec{v} \in J}$ can be written as $\sigma_v^{(q)} \otimes I^{\{\{1, \dots, n\} \setminus \{q\}\}}$ using $q \in \{1, \dots, n\}$ and $v \in \{1, 2, 3\}$. When σ_v anti-commutes with $\tilde{\sigma}$ and $q \in V_l$ (namely q is colored in c_l), then $\tilde{\sigma}^{(V_l)} \otimes \bigotimes_{i \in \{1, \dots, k\} \setminus \{l\}} I^{(V_i)} \in G$ anti-commutes with $\sigma_v^{(q)} \otimes I^{\{\{1, \dots, n\} \setminus \{q\}\}}$. Also, all two-qubit Pauli terms in $\{\sigma_{\vec{v}}\}_{\vec{v} \in J}$ can be written as $\sigma_{v_1}^{(q_1)} \otimes \sigma_{v_2}^{(q_2)} \otimes I^{\{\{1, \dots, n\} \setminus \{q_1, q_2\}\}}$ for $\{q_1, q_2\} \in E$ and $v_1, v_2 \in \{1, 2, 3\}$. When σ_{v_1} anti-commutes with $\tilde{\sigma}$ and $q_1 \in V_l$, (note that $q_2 \notin V_l$ from the definition of coloring), then $\tilde{\sigma}^{(V_l)} \otimes \bigotimes_{i \in \{1, \dots, k\} \setminus \{l\}} I^{(V_i)} \in G$ anti-commutes with $\sigma_{v_1}^{(q_1)} \otimes \sigma_{v_2}^{(q_2)} \otimes I^{\{\{1, \dots, n\} \setminus \{q_1, q_2\}\}}$. \square

The above logic holds for 2-local Hamiltonians, however, we now extend to the case of general Hamiltonians. To do so, we make use of a more general definition of a graph to encapsulate higher-order interaction terms.

Definition 3. (Graph for many-body Hamiltonians) A Hamiltonian containing many-body interactions (i.e. with J containing vectors with more than two nonzero elements) can be represented by a graph (V, E) where V is the set of qubits and E is the set of pairs $\{i, j\}$ ($i \neq j$) of qubits for which there exists a vector $\vec{v} \in J$ such that both v_i and v_j are not 0 (note that a given vector \vec{v} might contain more than two nonzero elements, therefore a single \vec{v} can corresponds to multiple edges).

Lemma 11. For a general J , G defined as

$$G = \left\{ \pm \bigotimes_{i=1}^k \sigma_{v_i}^{(V_i)}, \pm i \bigotimes_{i=1}^k \sigma_{v_i}^{(V_i)} \right\}_{(v_1, \dots, v_k) \in \{0,1,2,3\}^k}, \quad (\text{F5})$$

where $\{(c_i, V_i)\}_{i=1}^k$ is a valid coloring of a graph for the many-body Hamiltonian, satisfies the condition in step 1 of Algorithm 5.

Proof: For all $\vec{v} = (v_1, \dots, v_n) \in J \setminus \{\vec{0}\}$, all $q \in \{j \in \{1, \dots, n\} \mid v_j \neq 0\}$ are assigned different colors from the definition of the graph (V, E) . Therefore, for a $q \in \{j \in \{1, \dots, n\} \mid v_j \neq 0\}$, a Pauli operator $\tilde{\sigma}$ that anti-commutes with σ_{v_q} , and l such that $q \in V_l$, $\tilde{\sigma}^{(V_l)} \otimes \bigotimes_{i \in \{1, \dots, k\} \setminus \{l\}} I^{(V_i)} \in G$ anti-commutes with $\sigma_{\vec{v}}$ since $V_l \cap \{j \in \{1, \dots, n\} \mid v_j \neq 0\} = \{q\}$. \square

From Lemma 11, it follows that L can be taken smaller than or equal to 4^{k+1} , where k is the maximum number of qubits with which a single qubit interacts, namely $k = \max_{i \in \{1, \dots, n\}} m_i$ for $m_i := |\{j \in \{1, \dots, n\} \setminus \{i\} \mid \exists \vec{v} \in J, v_i \neq 0 \text{ and } v_j \neq 0\}|$. This can be shown from the fact that the chromatic number of a graph is upper-bounded by the maximum vertex degree plus one. As a consequence, L is upper-bounded by an n -independent constant and thus the time complexity is $\Theta(t^2/\epsilon)$ for a low-intersection Hamiltonian as defined in Ref. [36].